A NOVEL GLASS POLYALKENOATE CEMENT FOR FIXATION PURPOSES IN THE SKELETON

ADEL MOH'D FAWZI A.R. ALHALAWANI

DISSERTATION SUBMITTED IN FULFILMENT OF THE REQUIREMENTS FOR THE DEGREE OF MASTER OF ENGINEERING SCIENCE

DEPARTMENT OF BIOMEDICAL ENGINEERING
FACULTY OF ENGINEERING
UNIVERSITY OF MALAYA
KUALA LUMPUR

2014

UNIVERSITI MALAYA

ORIGINAL LITERARY WORK DECLARATION

Name of Candidate: **Adel Moh'd Fawzi A.R. Alhalawani**

Registration/Matric No: **KGA120068**

Name of Degree: **Master of Engineering Science**

Title of Project Paper/Research Report/Dissertation/Thesis ("this Work"): **A NOVEL GLASS POLYALKENOATE CEMENT FOR FIXATION PURPOSES IN THE SKELETON**

Field of Study: **Biomaterials and Tissue Engineering (Engineering and Engineering trades)**

I do solemnly and sincerely declare that:

(1) I am the sole author/writer of this Work;
(2) This Work is original;
(3) Any use of any work in which copyright exists was done by way of fair dealing and for permitted purposes and any excerpt or extract from, or reference to or reproduction of any copyright work has been disclosed expressly and sufficiently and the title of the Work and its authorship have been acknowledged in this Work;
(4) I do not have any actual knowledge nor do I ought reasonably to know that the making of this work constitutes an infringement of any copyright work;
(5) I hereby assign all and every rights in the copyright to this Work to the University of Malaya ("UM"), who henceforth shall be owner of the copyright in this Work and that any reproduction or use in any form or by any means whatsoever is prohibited without the written consent of UM having been first had and obtained;
(6) I am fully aware that if in the course of making this Work I have infringed any copyright whether intentionally or otherwise, I may be subject to legal action or any other action as may be determined by UM.

Candidate's Signature Date

Subscribed and solemnly declared before,

Witness's Signature Date

Name:
Designation:

Abstract

Healing complications following median sternotomy result from poor sternal fixation and contribute to mortality and morbidity. This study investigates the use of novel gallium (Ga) based glass polyalkenoate cements (GPCs) for improved sternal fixation post-sternotomy. The glass series consists of a Control (CaO-ZnO-SiO_2), and LGa-1 and LGa-2 which contain gallium (Ga) at the expense of zinc (Zn) in 0.08 mol% increments. X-ray diffraction (XRD) and particle size analysis (PSA) showed that all glasses were fully amorphous with a similar mean particle diameter. The glass series was formulated with E11 Poly(acrylic acid) (PAA) at 50 wt% addition. The additions of Ga result in both an increased working time (75 s to 137 s) and setting time (113 to 254 s). Fourier transform infrared spectroscopy (FTIR) analysis indicated that this was a direct result of increased unreacted poly(acrylic acid) (PAA) and the reduction of crosslink formation during working and setting times. The increasing presence of Ga resulted in an altered ion release profile with increased Ca, Zn, Si and Ga ions released into solution, with the 30 day solution displaying the largest content of all ions. Addition of Ga was also found to decrease the contact angle, representing more hydrophilicity and adhesive properties. Surface morphology and roughness (Ra) measurements made using Atomic Force Microscopy (AFM) showed that the addition of Ga increases Ra. Mechanical properties were reproducible and resulted in improved biaxial flexural strengths (σ_f) with the addition of Ga, with LGa-2 peaking at 29 MPa after 30 days, however, the additions of Ga had relatively no effect on the flexural strength with cement maturation. Compressive strength (σ_c) was decreased by the Ga addition, however, LGa-2 presented comparable values (17, 30 and 33 MPa) to the Control glasses (19, 31 and 33 MPa) after 1, 7 and 30 days, respectively. *Ex-vivo* tensile strengths proved that the LGa samples (0.16 wt% Ga) are

comparable to the Control samples. The strengths for Control cements were ~0.4, 0.6 and 0.5 MPa for 1, 7 and 30 days measurements, respectively. While LGa-2 strength values are ~0.3, 0.4, 0.4 MPa respectively, tested over the same periods. A scanning electron microscopy (SEM) survey revealed that all failures are adhesive, while energy dispersive x-ray analysis (EDX) presented high concentration values of all incorporated ions when compared with the ion release studies. Results show that LGa-2 can be used for sternal closure due to its novel characteristics in GPCs, including biocompatibility, improved handling properties, adhesion-ability, and chemotherapeutic properties, appropriate strength, and bone regeneration effects. Similar to any *ex-vivo* study, the main limitation of this project was the inability to consider the complications regularly encountered during sternotomy, such as bleeding and osteoporosis. Design limitations included testing of small bovine sterna, differing from the human sternum in dimension, and the inability to mimic the exact directions of physiological forces. Further, the use of formaldehyde is a potential complicating factor given its toxicity and unknown effect on the bioactive glass.

Abstrak

Proses pemulihan akibat daripada prosedur sternotomy median dari penetapan sternum yang lemah boleh menyumbang kepada kematian. Kajian ini adalah untuk menyiasat penggunaan novel galium (Ga) berasaskan simen polyalkenoate kaca (GPCs) untuk penetapan sternal yang lebih berkesan selepas sternotomy (post-sternotomy). Komponen kaca terdiri daripada kawalan (CaO-ZnO-SiO2), dan LGA-1 dan LGA-2 yang mengandungi galium (Ga) menggantikan zink (Zn) dalam 0.08 mol% kenaikan. Pembelauan sinar-X (XRD) dan analisis saiz zarah (PSA) menunjukkan bahawa semua komponen adalah amorfus sepenuhnya dengan diameter zarah min yang serupa. Komponen kaca tersebut dicampur dengan E11 Poli (asid akrilik) (PAA) pada kadar berat 50%. Penambahan kandungan Ga menyebabkan hasil dalam kedua-dua masa bekerja meningkat (75 s kepada 137 s) dan masa tetapan (113s kepada 254 s). Spektroskopi (FTIR) analisis menunjukkan bahawa ini adalah hasil langsung daripada peningkatan tindakbalas poli (asid akrilik) (PAA) dan pengurangan masa bagi pembentukan crosslink semasa bekerja. Kehadiran Ga yang semakin bertambah menyebabkan ion profil berubah dan ia menghasilkan sebatian yang mengandungi peningkatan dari segi Ca, Zn, Si dan ion Ga. Sebatian ini kemudian dilepaskan ke dalam air suling selama 30 hari dimana ia merebak dan menunjukkan kandungan terbesar bagi semua ion. Penambahan Ga juga didapati dapat mengurangkan sudut sentuhan, yang mewakili bahagian yang lebih hidrofilik. Pengukuran dari segi morfologi permukaan dan kekasaran (Ra) boleh dilakukan dengan menggunakan Microscopy Atomic Force (AFM) yang menunjukkan bahawa penambahan Ga meningkatkan Ra. Sifat-sifat mekanik dapat dihasilkan berulang-kali dan menyebabkan kekuatan lenturan dwipaksi (σf) bertambah dengan tambahan Ga, dengan LGA-2 memuncak pada 29 MPa selepas 30 hari. Bagaimanapun, penambahan Ga tidak memberi

kesan kepada kekuatan lenturan dengan kematangan simen. Kekuatan mampatan (σc) telah menurun dengan penambahan Ga, bagaimanapun, LGA-2 dimamaprkan nilai setanding (17, 30 dan 33 MPa) apabila dibandingkan dengan komponen kaca kawalan (19, 31 dan 33 MPa) selepas 1, 7 dan 30 hari. Kekuatan tegangan dalam *ex-vivo* membuktikan bahawa sampel LGA (0.16% berat Ga) boleh dibandingkan dengan sampel kawalan. Mikroskop imbasan elektron (SEM) mendedahkan bahawa semua kegagalan adalah pelekat, manakala tenaga serakan analisis x-ray (EDX) menyampaikan nilai-nilai kepekatan yang tinggi daripada semua ion yang diperbadankan berbanding dengan kajian pembebasan ion. Keputusan menunjukkan bahawa LGA-2 boleh digunakan untuk penutupan sternal kerana ciri-ciri baru dalam GPCs, termasuk kesesuaian dari segi biologi, keupayaan untuk melekat,dan sifat-sifat kemotherauputik, kekuatan yang sesuai, dan kesan pertumbuhan semula tulang. Batasan kajian utama bagi penyelidikan ini, termasuk ketidakupayaan untuk mempertimbangkan komplikasi kerap dihadapi semasa sternotomy, seperti pendarahan dan osteoporosis. Had reka bentuk termasuk ujian Accipiter terhadap lembu kecil yang berbeza dari tulang dada manusia dari segi dimensi, dan ketidakupayaan untuk meniru arahan yang serupa seperti impakdari segi fisiologi. Di samping itu, penggunaan formaldehid adalah faktor yang merumitkan disebabkan oleh bahan ketoksikannya dan kesan yang tidak diketahui terhadap bioaktif kaca.

Acknowledgements

I would like to thank the Atlantic Innovation Fund, Canada (Grant No. 57-02-03-1035) for the complete financial support during the project.

I would take this opportunity to acknowledge with much appreciation the crucial rule of the principal investigator of the project, Prof. Mark Robert Towler who has invested his full effort in guiding me to achieve the goals of the project. I appreciate his keen interest and support during his presence in Malaysia and his endless support from overseas. I would also like to acknowledge with much appreciation the support and supervision of Dr. Belinda Pingguan-Murphy. Special thanks go to our head of department, Dr. Nahrizul Adib Kadri for his continuous support and encouragement. His position as a co-principal investigator was significant in getting the permission to use different research facilities in the University of Malaya. Further, I would like to express my deepest appreciation to all those who provided me the possibility to complete this dissertation report, to the management, lecturers, and staff in the University of Malaya, particularly, in the Faculty of Engineering.

Furthermore I would like to thank my parents, brothers and sister for their endless love and support.

Thanks to the people who have been instrumental in the successful completion of this project, especially Dr. Declan Curran, Dr. Daniel Boyd, Dr. Anthony Wren, Dr. Yasir Al-Saffar, Mr. Ali Moradi, and Mr. Eraj Mirza.

Table of Contents

List of Figures

List of Tables

List of symbols and abbreviations

Abbreviation/symbol	Full term of the abbreviation/symbol
3D	Three-dimensional
DSWI	Deep Sternal Wound Infection
HVR	Heart Valve Replacement
USA	United States of America
Ca	Calcium
Zn	Zinc
Ga	Gallium
Si	Silicon
GPC	Glass Polyalkenoate Cement
PAA	poly(acrylic acid)
CT	Computed Tomography
MRI	Magnetic Resonance Imaging
SS	Stainless Steel
CBC	Cabled Butterfly Closure
SSD	Sternal Synthesis Device
STD	Sternal Talon Device
CAD	Computer Aided Design
PMMA	Poly(methyl methacrylate)
THR	Total Hip Replacement
HA	Hydroxyapatite
TCP	Tri-Calcium Phosphate
CPC	Calcium Phosphate Cement
FDA	Food and Drug Administration

CC	Cubic Centimeter
SPECT	Single Photon Emission Computed Tomography
GCS	Gentamicin Collagen Sponge
ICU	Intensive Care Unit
VAC	Vacuum Assisted Closure
GIC	Glass Ionomer Cement
Ag	Silver
Al	Aluminium
ENT	Ear-Nose-Throat
Sr	Strontium
CSP	Cerebral Spinal Fluid
DNA	Deoxyribonucleic acid
TSC	Tri-Sodium Citrate
NBO	Non-Bridging Oxygen
UV	Ultra Violet
PET	Positron Emission Tomography
FDG	F-fluorodeoxy glucose
DTA	Differential Thermal Analysis
Tg	Transition temperature
XRD	X-Ray Diffraction
PSA	Particle Size Analysis
SEM	Scanning Electron Microscopy
EDS	Energy Dispersive X-ray Analysis
P:L	Powder: Liquid
T_s	Net setting time
T_w	Working time

FTIR	Fourier Transform Infrared
MP-AES	Microwave Plasma-Atomic Emission Spectrometer
PPM	Part Per Million
d_w	Distilled water
AFM	Atomic Force Microscopy
σ_c	Compressive strength
σ_f	Biaxial flexural strength
PBS	Phosphate Buffered Saline
ANOVA	One way analysis of variance
RA	Roughness

CHAPTER ONE

INTRODUCTION

1. Introduction

1.1 Background

1.1.1 Anatomy of the bone

"The adult human skeleton has a total of 213 bones, excluding the sesamoid bones" (Clarke B., 2008). Bones are categorized into long, irregular, flat and short bones. Mainly, bones of the skeleton system provide the structural support, protection of internal structures and organs, locomotion and movement (Marieb E. N. and Hoehn K., 2013).

Long bones have growth plates (epiphysis) at the ends, long shaft (diaphysis), strong outer surface composed of compact (cortical) bone and spongy inner trabecular (cancellous) bone containing the bone marrow. In addition, growth plates of long bones are covered with hyaline cartilage for bone protection and shock absorption. Long bones include the humeri, tibiae, femurs, phalanges, clavicles, radii, metacarpals, ulnae, fibulae, and metatarsals (Clarke B., 2008; Marieb E. N. and Hoehn K., 2013).

Flat bones are strong bones that provide the base for the muscle attachment and the necessary protection to vital organs. Cortical bone forms the anterior and posterior surfaces whereas the center consists of cancellous bone and bone marrow; this is necessary to provide more strength and protection. Flat bones include the sternum, scapulae, ribs, mandible, and skull (Marieb E. N. and Hoehn K., 2013).

Short bones include the sesamoid bones, patellae, tarsal and carpal bones. Whereas irregular bones include the hyoid, coccyx, sacrum, and vertebrae bones (Marieb E. N. and Hoehn K., 2013).

Compact and cancellous bones differ in the unit microstructure and porosity. Cancellous bones are composed of a network (honeycomb-like) of cancellous rods and plates within the bone marrow, whereas compact bones are much denser and surround the marrow space (Clarke B., 2008), however, both bones are made of the same matrix elements and cells (Nazarian A., 2008). Additionally, compact bones form 80% of the adult human skeleton while cancellous bones form 20% only (Clarke B., 2008). Hence, the protective and mechanical functions are fulfilled by the cortical bone while the metabolic functions are fulfilled by the more metabolically active cancellous bones; this will result in faster remodeling of cancellous bone. On the other hand, the heterogeneity characteristics and anisotropic nature of the cancellous bones makes it more sensitive, weak and easily affected by the osteoporosis, bone cancer and osteoarthritis (Keaveny T. M., et al., 2002). In terms of mechanical properties, the cortical bone provides better compression strength than tension strength while trabecular bone depends on the loading direction, health, age and anatomic site, for example its strength decreases with the increase in age (Keaveny T. M., et al., 2002).

In general, bone strength is preserved by undergoing modeling-remodeling process (growth) through the human life. Bone modeling helps the bone to adapt the changes in the biomechanical forces while remodeling replaces the micro-damaged, old bone with a new stronger bone (Clarke B., 2008).

1.1.2 Anatomy of the sternum

The sternum is a flat, anteriorly convex bone and is also called breast-bone (Stark P. and Jaramillo D., 1986). The sternum's thickness is 8 to 14.5 mm and connects with the first 7 pairs of thoracic cage ribs through the costal cartilage. The costal cartilage provides the elasticity and dynamic behavior for the sternum during inhalation (respiration) and exhalation (expiration) respiration cycles (Stark P. and Jaramillo D., 1986; Dieselman J. C. 2011; Korff A., et al., 2011). The normal length of the sternum for males is 208.6±14.6 mm and 182.9±17.4 mm for females (Korff A., et al., 2011).

Three-dimensional (3D) multiple forces (cyclic tension) are imposed on the sternum during respiration cycles due to the pull and push muscle forces in different directions. Inhalation muscles are external intercostals, scalenes, diaphragm, parasternal intercostals, and sternocleidomastoid (Figure 1.1). During exhalation, the pressure of the gas in lungs is higher than that of the atmosphere and hence requires no additional muscle contraction. However, during forced exhalation, different muscles contract including rectus abdominis, transversusabdominis, internal and external abdominal oblique, and internal intercostals (Dieselman J. C., 2011).

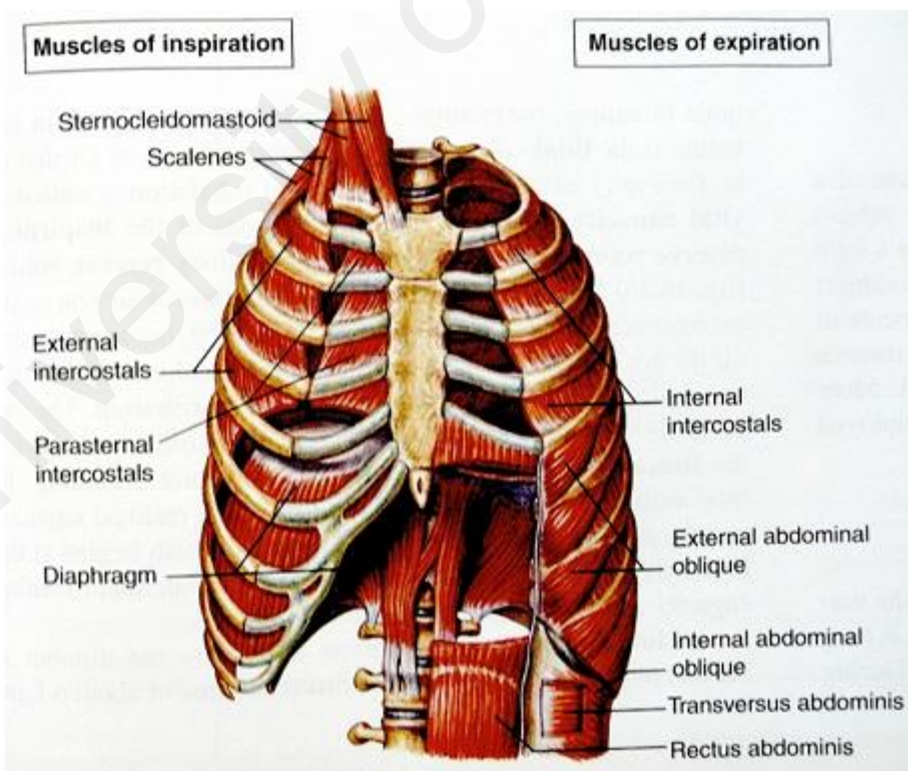

Figure 1.1: Inhalation and forced exhalation muscles [Reproduced from (Dieselman J. C., 2011)]

The sternum consists of three main parts: the manubrium, corpus (body), and xiphoid (Figure 1.2). The manubrium is the densest region of the sternum. The corpus is fused directly below the manubrium; it is the part that connects the seven intercostal ribs with the sternum and is longer, but narrower, than the manubrium. The xiphoid process is fused below the corpus and is not connected to any of the thoracic ribs (Stark P. and Jaramillo D., 1986; Marieb E.N. and Hoehn K., 2013). Xipho-sternal junction is the junction between the sternal body and the xiphoid process (Stark P. and Jaramillo D., 1986; Dieselman J. C., 2011).

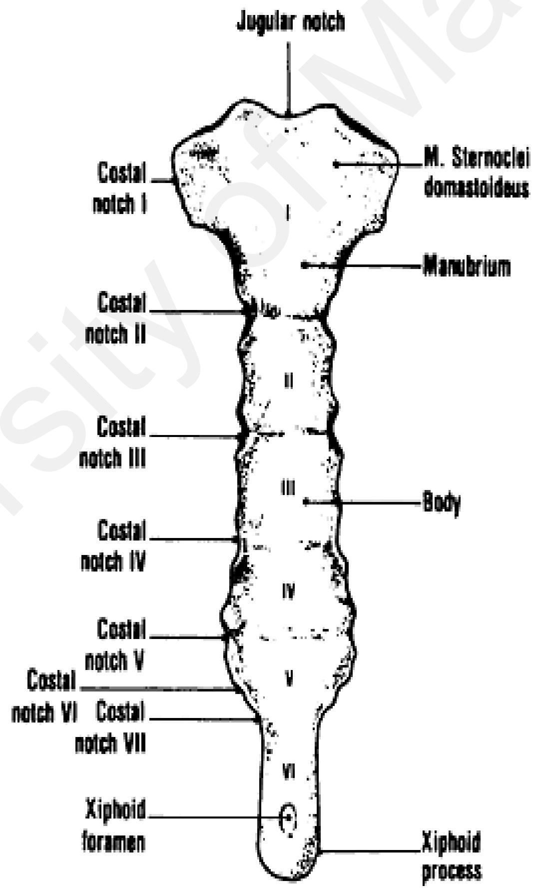

Figure 1.2: Normal gross anatomy of sternum [Reproduced from (Stark P. and Jaramillo D., 1986)]

The sternum was also defined as "a sandwich bone having an interior core of trabecular bone encapsulated by a thin cortical shell" (Decoteau D.M. et al., 2006). It consists mainly of two forms of bones, namely the compact and spongy cancellous bones. The compact is denser and forms the thin anterior and posterior surfaces (Figure 1.3), while the cancellous bone is made of bone marrow and involves a higher ratio of spongy cells; the thin denser compact bone and higher porous cancellous bone marrow serve for the required flexibility and elasticity during respiration cycles (Stark P. and Jaramillo D., 1986; Dieselman J. C., 2011).

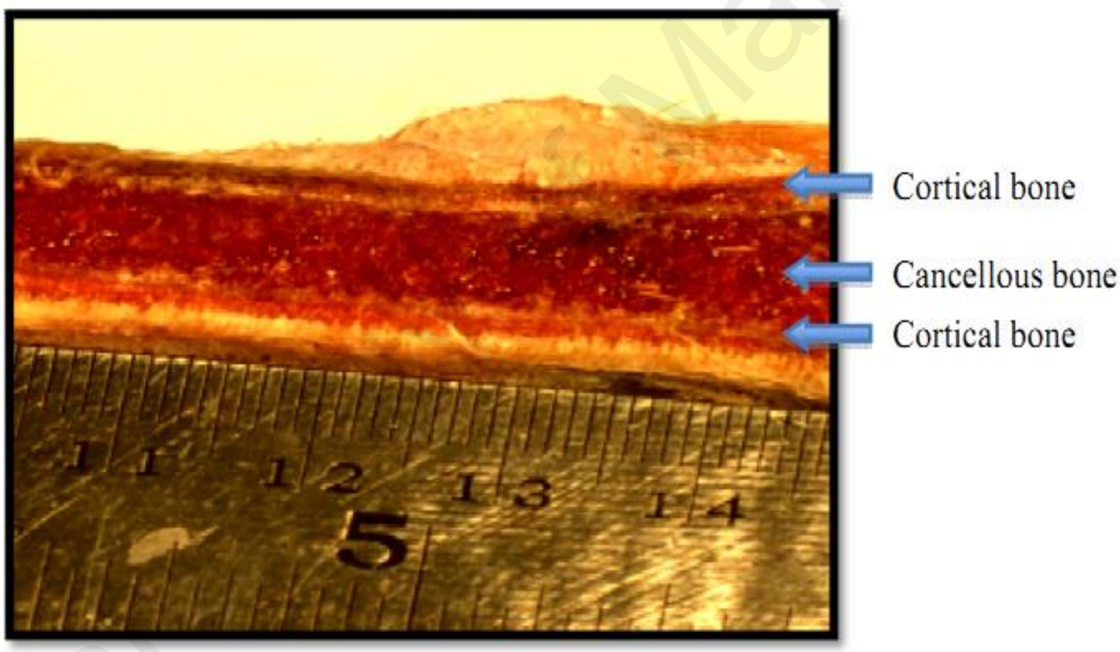

Figure 1.3: Cross section of human sternum bone [Reproduced from (Dieselman J. C., 2011)]

1.1.3 Biomechanics of the sternum

The efficiency of various sternal fixation techniques is tested using biomechanical analysis techniques (Pai S., 2005). Various researchers are interested in testing the unity and stability of the closure technique through stiffness analysis; stiffness is the slope of displacement over load (Cheng W. et al., 1993). Hence, the stiffer and stable fixation is characterized by the lesser displacement at each corresponding load.

Generally, two main techniques are used for testing sternal closure techniques, namely static and dynamic testing (Dieselman J. C., 2011). Both techniques are typically conducted *ex-vivo* because it is less variable, controlled, rapid and inexpensive alternative when compared with the use of animal and cadaver models (Pai S., 2005).

Static testing measures the force at which the fixation technique fails due to a steadily increasing load, while dynamic testing mimics the tension forces applied on the sternum due to lateral direction forces during breathing and coughing (Dieselman J. C., 2011). Depending on the applied load and its relative direction, these testing techniques can be used to demonstrate different failure mechanisms of closure devices (Dieselman J. C., 2011). Majority of studies (Wangsgard C. G., 2008; Cohen G., 2002; Casha A. R.., 1999c; Hatcher B., 2011; Pai S., 2008) analyzed the biomechanics of sternal fixation techniques from three loading perspectives which are transverse shear, lateral distraction and longitudinal shear (Figure 1.4). The transverse shear mimics the use of arm's assistance to pull the body upright, lateral distraction mimics the forces imposed due to coughing or breathing and longitudinal shear mimics the use of one extended arm to support the body (also called lateral flexion stretching) (Dieselman J. C., 2011).

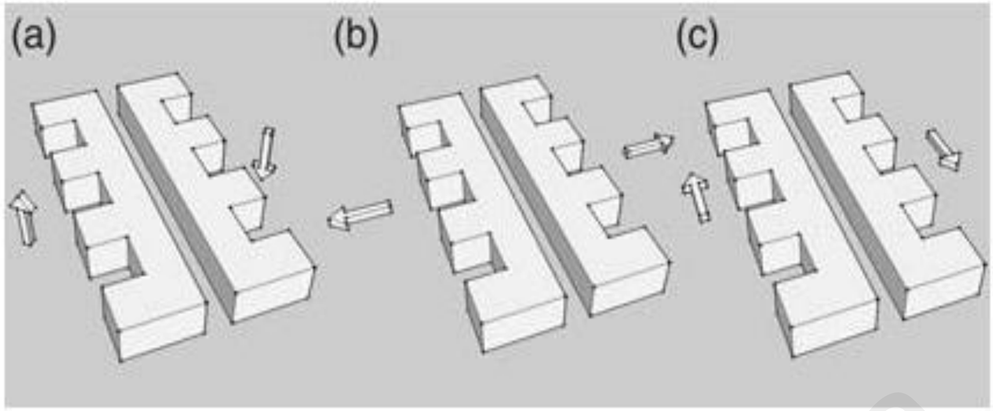

Figure 1.4: Different sternal loading conditions - a) transverse shear b) lateral distraction c) longitudinal shear [Adapted from (Dieselman J. C., 2011)]

In 1999c, it was presented by Casha et al. that as a safety margin for any closure technique, it must be able to resist twice the maximum potential stresses imposed on the sternum. Also, their study presented that indirect measurements resulted in a force of 260 N (~26 Kg) imposed on the sternum during a 42 mm Hg (~5.6 kPa) pressure generating cough, while their developed mathematical model called as Laplace law (Equation 1.1) showed that a pressure of 5.6 kPa results in a force of 24 Kg in comparison with the 26 Kg indirect measurement (Casha A. R. et al., 1999c).

$$T = RLP = 0.17 * 0.25 * 5.6 = 238\ N\ (\sim 24\ Kg) \ldots\ldots\ldots\ldots\ldots\ldots\ldots\ldots\ldots\ldots\ldots\ldots\ldots\ldots Eq.1.1$$

Where T is the tension (N), R is the cadaver's sternal radius (m), L is the chest's height (m) and P is the distending pressure (kPa) (Figure 1.5). Additionally, they demonstrated that the distending pressure of normal cough is 100 mm Hg (~13.3 kPa); imposing a force of 56 Kg (555.3 N), whereas the distending pressure of maximal cough reaches to 300 mm Hg (39.9 kPa); imposing a force of 168 Kg (1666 N) (Casha A. R. et al., 1999c).

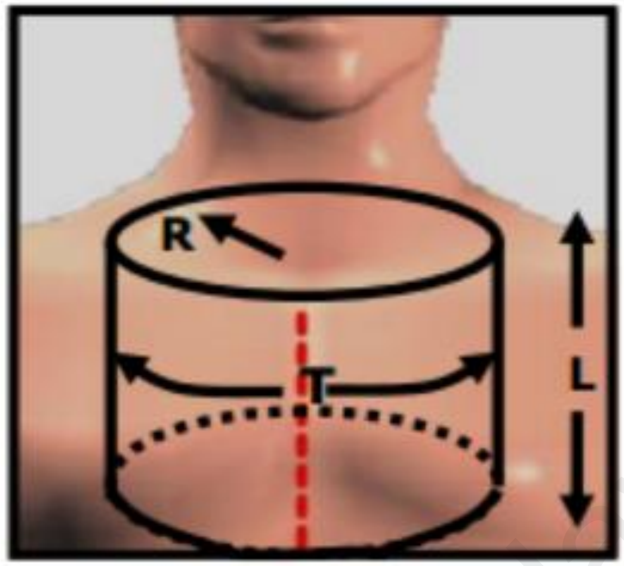

Figure 1.5: Estimation of tension forces imposed on midline sternum *in vivo* [Reproduced from (Pai S., 2008)]

Other studies (Trumble, et al., 2002; Dasika, et al., 2003) presented that according to the Laplace low; forces ranging between 160 N to 400 N and 550 N to 1650 N are imposed on the sternal midline during breathing and coughing respectively (Pai S., 2008). These results match with the results presented by Casha et al., (1999c).

1.1.4 Median sternotomy

Sternotomy was first introduced in 1950s (Dalton M.L., et al., 1992). It is also called median sternotomy and is one of the most significant surgical operations for easier access to the heart preceding surgery (Gunja, N., et al., 2004). It precedes a vast majority of thoracic/cardiac surgeries such as coronary bypass surgery, cardiac valve replacement and open-heart surgery (Gunja, N., et al., 2004; Korff A., et al., 2011). Surgeons use special devices (saw) to make a midline incision through the sternum bone which provides the ability to perform different thoracic surgeries and reach for most of the thoracic organs, hence, sternotomy has revolutionized the area of cardiothoracic surgery (Grevious, 2009; Choukairi F., et al., 2011). Sternotomy remains the mostly preferred choice for sternum incision; although, other approaches such as lateral thoracotomy (approaching the chest cavity by intercostal incision) were developed and are minimally invasive. Sternotomy is more appropriate for access to the thoracic structures due to its lower incidence of respiratory complications and lesser pain (Choukairi F., et al., 2011).

Median sternotomy procedure starts with the separation of superficial sternal tissues. Then, along the centre of the sternum; a longitudinal bisection/incision is performed using a high frequency saw. The linear and proper bisection of the sternum results in reduced complications during recovery including fracture and bleeding. Surgeons will have the ability to have the required size of opening while the bisected halves of the sternum are hold by a sternal retractor. Then the sternal closure plays a significant role in minimizing the complications after any thoracic operation. It was indicated that 2% of the cardiac post-operative complications occur due to improper and poor sternal fixation (Dieselman J. C., 2011).

“Major sternal complications are infrequent after cardiac surgery. However, when they occur, sternal complications such as nonunion/displacement, dehiscence, or Deep Sternal Wound Infection (DSWI) result in considerable morbidity, mortality, and resource utilization” (Fedak P.W. et al. 2010).

1.2 Research problem and significance

In Europe, 6000 children are born annually with the heart valvular defect requiring immediate Heart Valve Replacement (HVR) (Cox, M. A.J., 2009). Moreover, in United States of America (USA), more than 60,000 patients undergo surgery operations for HVR every year (Boestan, I. N. and Sarvasti, D., 2005).

There is a need for a transformative, new technology for robust sternal closure in the event of sternotomy where the closure itself provides robust fixation that can withstand the maximum forces applied on sternum.

1.3 Aim and objectives

The research aims to develop a Ga containing Glass Polyalkenoate Cements (GPCs) for fixation and stabilization of the sternum, post sternotomy surgery. This project has the following interrelated objectives:

- It should be possible to synthesize the glasses using melt/quench fabrication.
- The role of Ga incorporation, on the expense of zinc, in the glass series should be identified.
- When mixed with aqueous poly(acrylic acid) (PAA), the glasses should form pastes with handling properties in line with industry standards (ISO-9917).
- Resultant GPCs should possess mechanical properties comparable or better than the bone that they are replacing to minimize stress shielding effects that reduce bone density.
- Investigate the influence of Ga-containing GPCs for fixation and stabilization of the ribcage, post sternotomy surgery through an *ex-vivo* study.

1.4 Research hypothesis

The hypothesis behind this research is that Ga containing GPCs can be used for fixation and stabilization of the rib cage, post sternotomy surgery.

1.5 Outline of the research approach

The dissertation consists of the following chapters:

- Introduction: this chapter introduces the main concepts in which the research is concerned, the research problem and significance, aim and objectives, research hypothesis and the outline of the research approach.
- Literature review: this chapter surveys previous studies relevant to the field of research.
- Methodology: this chapter describes and explains the research procedures adopted. All methods used to collect the data and generate the findings are reported in this chapter.
- Results and discussion: this chapter presents the tables, figures and text relevant to the complete data analysis. It also interprets the results along with a comprehensive discussion of the research findings. Limitations of the study are also discussed in this chapter.
- Conclusion: this chapter summarizes the findings and discusses their implications.

CHAPTER TWO

LITERATURE

REVIEW

2. Literature review

2.1 Post sternotomy complications

Major sternal complications such as dehiscence, mediastinitis, osteomyelitis, SWI and/or nonunion/displacement are infrequent after cardiac surgery (Fedak P. W. et al., 2010; Mossad S. B. et al., 1997). However, such complications, when they do occur, result in considerable morbidity, mortality, and resource utilization (Fedak P. W. et al., 2010). Casha et al. (1999a) showed that major sternal complications occur due to osteoporosis in 2% of the sternal closure procedures. Osteoporosis is defined as the imbalance in bone remodelling, characterized by the imbalance between cell formation and cell resorption; particularly in older patients (Sambrook P., 2001; Blanche C., and Shaux A., 1988). It also refers to the loss of bone minerals due to the complete or partial resorption of cancellous bone struts. This will markedly lead to loss of connectivity and simply less density of bone plates (Figure 2.1), hence contributing to the risk of fracture due to the lesser strength. Bone modeling imbalance occurs with aging, but are also associated with other circumstances, including: the reduction of mechanical loading due to immobilization, bed rest, presence of large amounts of corticosteroids (treatment for asthma or arthritis) and the reduction of sex hormone concentrations (most probably in females after menopause). Clinically, the loss of bone minerals has no effect, unless a fracture occurs (Sambrook P., 2001).

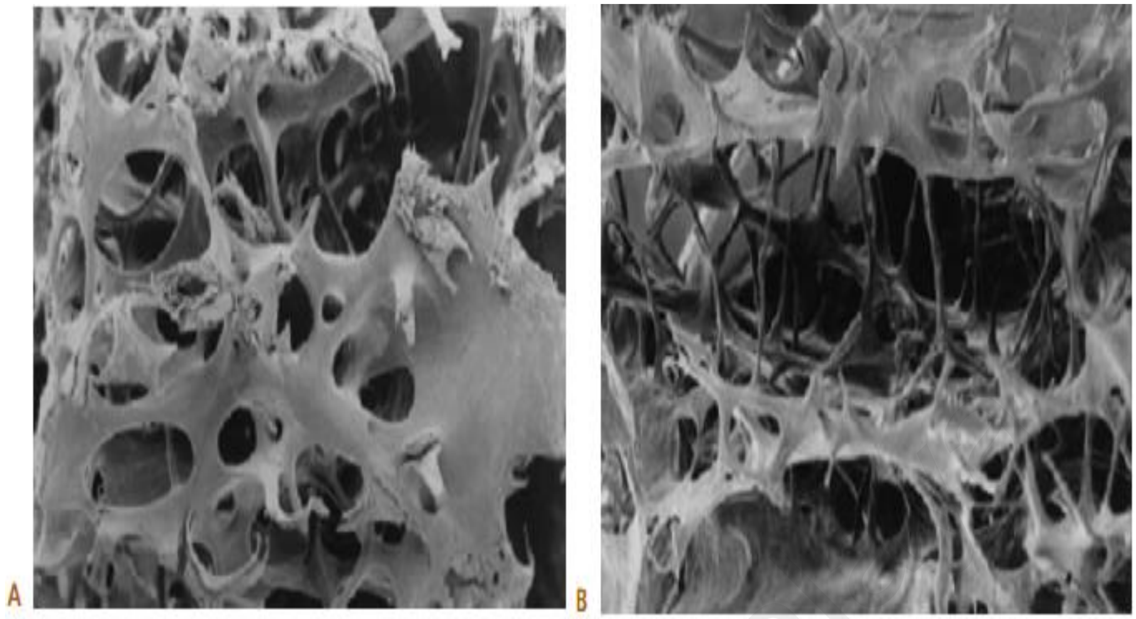

Figure 2.1: Scanning Electron Micrographs of (a) Normal bone-higher density and unity (b) Osteoporotic bone-higher porosity and non-unity (Sambrook P., 2011)

Furthermore, osteoporotic sternums prevent clotting and platelet surface contact and hence contribute to bleeding issues during sternotomy due to the loss of the sternal table surface and were mostly realized in old patients (Blanche C., and Shaux A., 1988).

Both parts of the sternum are affected by the osteoporosis, but the cancellous is more affected due to its heterogeneity, porous and isotropic structure and higher metabolic activity.

Various methods were proposed to control bleeding of osteoporotic sternum. Some studies proposed the use of foreign body agents except Vivostat (Kjaergard H.K., and Trumbull H.R., 2000; Sherman R., et al. 2001; Sabel M., and Stummer W. 2004; Mair H., et al. 2005), while other proposed the use of bone wax (Harjula A, and Jarvinen A., 1983). The detailed methods will be reviewed in the section of sternal fixation techniques.

2.1.1 Deep Sternal Wound Infection (DSWI)

2.1.1.1 Overview and statistics

López Almodóvar et al. (2008) and Mavros et al. (2012) had identified DSWI as one of the sternal fixation complications that contributes to high mortality and morbidity despite the strategies for wound healing and antibiotic advances. It was reported by Schimmer et al., (2012) that DSWI contributes to 14-47% of the total mortality rates. It occurs in 1-4% of the total cases of those patients undergoing median Sternotomy (Lee T.Y. et al., 2007; Porter, K. et al., 2012), whereas Schimmer et al. (2012) reported in their study that it occurs in 0.5-8% of the total number of patients undergoing median Sternotomy. Table 2.1 presents the SWI rate at the Cleveland clinical foundation (Ohio, USA) during 1988 to 1994 (Mossad S.B. et al., 1997).

Table 2.1: SWI rates at the Cleveland Clinic Foundation, USA [Reproduced from (Mossad S. B. et al., 1997)]

Year	No. of operations	SWI rate	
		No.	%
1988	2,981	48	1.62
1989	2,985	53	1.78
1990	3,010	66	2.19
1991	3,218	52	1.62
1992	3,391	80	2.36
1993	3,148	63	2.01
1994	3,447	74	2.1
Total	22,180	436	1.9

SWIs are considered rare but a major post-sternotomy complication after open heart surgery. They may lead to osteomyelitis, mediastinitis or dehiscence. Despite the management and prevention advances of infectious diseases, mediastinitis contributes to morbidity and life-threatening events (Barthelemy A., 2006).

2.1.1.2 Causes and complications

2.1.1.2.1 Dehiscence

Sternal dehiscence is one of the major causes of 10-40% mortality and morbidity after median sternotomy with an incidence rate of 0.3-8% (Jolly, S. et al., 2012; Schimmer C., et al., 2008). Sternal dehiscence occurs due to sternal fracture, sternal de-vascularization, osteoporosis, coughing, obstructive pulmonary disease and other force imposing activities. The advances in dehiscence with no treatment either using antibiotics or surgical operations leads to further life-threatening events requiring surgical procedures; this involves the association of mediastinitis or osteomyelitis. Sternal dehiscence is directly related to the SWI. The best practice in preventing the SWI and sternal dehiscence is the proper stable sternal approximation (Schimmer C., et al., 2008).

2.1.1.2.2 Mediastinitis

The region between the right and left pleural cavities is known as mediastinum (Figure 2.2). It covers mainly the trachea, great vessels, heart, and esophagus. The mediastinum consists of four main parts, namely the middle, superior, anterior and posterior mediastinum. The middle mediastinum involves the pericardium and heart, while the superior mediastinum joins the lower border of T4 vertebra to the sternal angle. The anterior and posterior mediastinums lie in front and behind the middle mediastinum respectively (Figure 2.3).

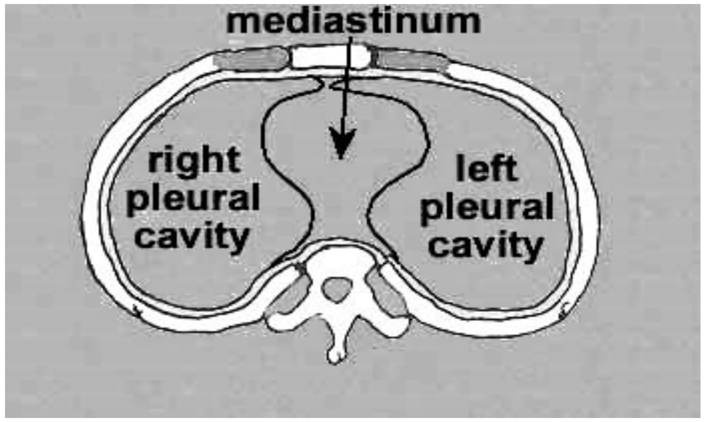

Figure 2.2: Cross section of thorax subdivision [Reproduced from (Norman W., 1999)]

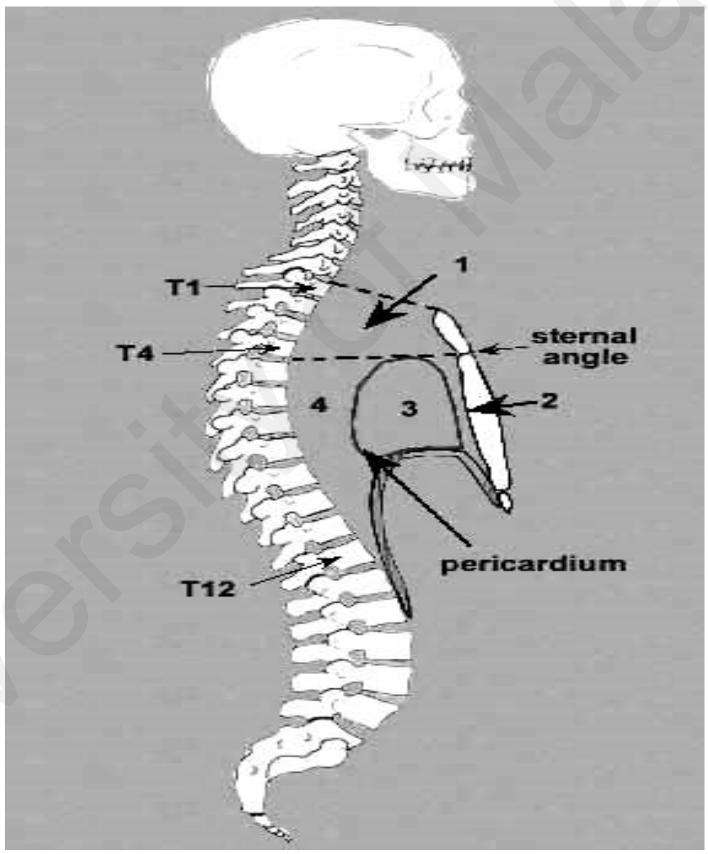

Figure 2.3: Sagittal section for subdivisions of mediastinum: (1) Superior mediastinum (2) Anterior mediastinum (3) Medial mediastinum (4) Posterior mediastinum [Reproduced from (Norman W., 1999)]

Mediastinitis is the invasion of the anterior mediastinum (Barthelemy A., 2006) as can be seen in Figure 2.4. It occurs due to the SWI and is characterized by the deeper travel of the superficial wound infection, this will in-turn affect the structure of mediastinum. It is one of the post-sternotomy complications which occur with an incidence rate of 1-5% (Choukairi F., et al., 2011). Major consequences of the mediastinitis are chronic infection and inflammatory state on both the mediastinum structures and the surface of the sternum (Choukairi F., et al., 2011). Infections that occur at the surface of the sternum are also called sternal wound and might be chronic as seen in Figure 2.5.

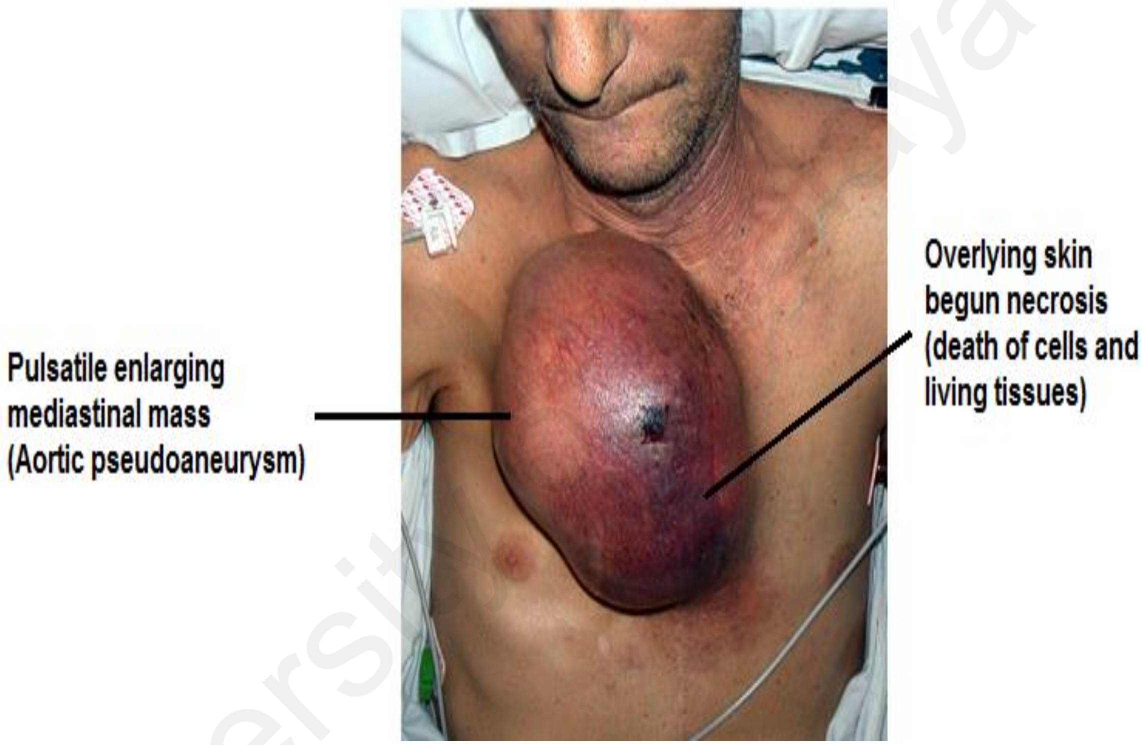

Figure 2.4: Progressively pulsatile, enlarging mediastinal mass with dry, attenuated and thin skin and soft tissue presented in a 58 years old male who was previously subjected to aortic grafting, renal failure due to polycystic kidney disease and was also treated for the developed sternal infection with antibiotics and radical sternal debridement [Adapted from (Shifrin D.A., et al., 2008)]

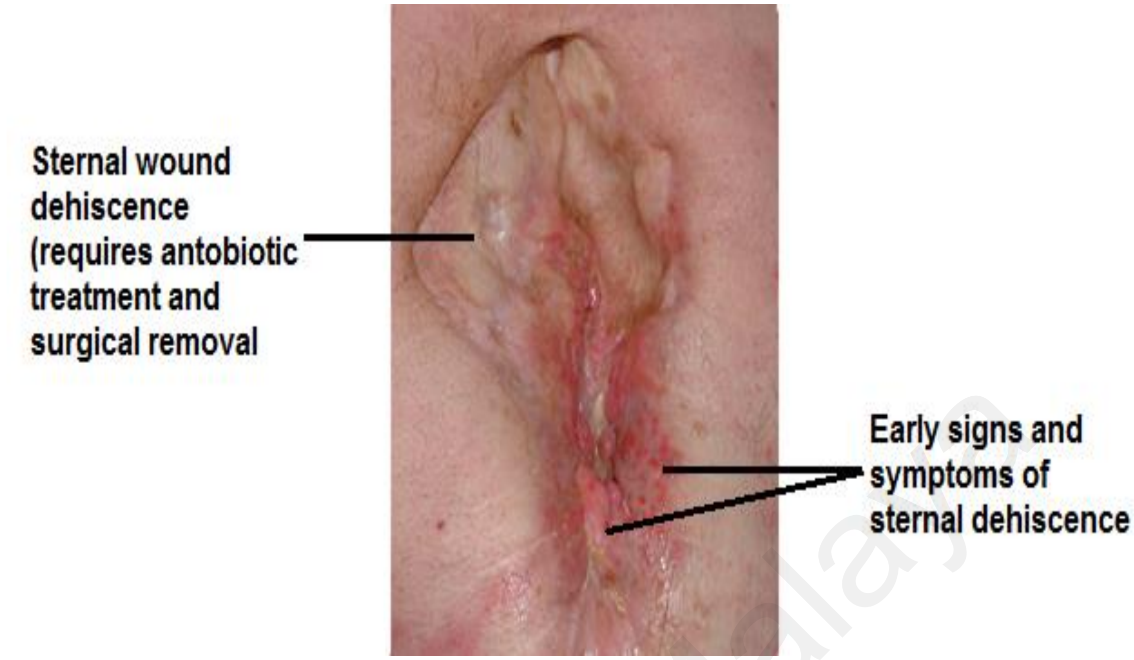

Figure 2.5: Chronic sternal wound in unidentified subject [Adapted from (Choukairi F., et al., 2011)]

Pairolero and Arnold (1984) presented a system for classifying Mediastinitis (Table 2.2).

Table 2.2: Mediastinitis classification system [Adapted from (Pairolero P.C., and Arnold P.G., 1984)]

TYPE 1	➢ Is realized within few days from the initial surgery. ➢ No evidence of osteomyelitis, although dehiscence is realized. ➢ No signs of instability ➢ No treatment is indicated.
TYPE 2	➢ Is realized within few weeks from the initial surgery. ➢ There is evidence of positive cultures and drainage such as osteomyelitis. ➢ Requires surgical operation/reconstruction
TYPE 3	➢ Is realized within months or sometimes years after the initial surgery. ➢ There is evidence of chronic wound infections. ➢ Requires surgical reconstruction.

In cases of initial infection, appropriate cultures, swabs and samples are to be collected. The treatment starts with antibiotics even in the cases of overwhelming infection; nevertheless, it is preferred to withhold antibiotics until results are obtained from the microbiological analysis of the collected samples. Surgeons then can perform surgical debridement for effective removal of non-viable tissue as a healing management approach; although, more surgical reconstruction is required if there is evidence of extensive sternum disruption (Choukairi F., et al., 2011). Prior to the surgery, investigations should be considered such as full blood count, serum albumin levels, electrolytes and inflammation markers for ensuring the patient's fitness for general anesthesia (Choukairi F., et al., 2011). Imaging techniques such as Ultrasound, Computed Tomography (CT) and Magnetic Resonance Imaging (MRI) are useful. Ultrasound provides information relative to the collection of fluids, CT scan provides useful detection of fluid location and sternal disruption while MRI is useful in cases that it is suspected the infection reached bones; however, it should be noted that any metal work during previous sternotomy will limit the effectiveness of MRI imaging (Choukairi F., et al., 2011).

2.1.1.2.3 Osteomyelitis

Following the sternotomy operation, the integration between the sternum and its surrounding tissues and structures is compromised. The area overlaying the sternum will have little soft tissue or muscle and hence poor blood supply. The tissue loss between the skin and the sternum will probably cause the complication of superficial wound infection which leads to osteomyelitis (Figure 2.6). Additionally, this could be due to the high stresses imposed on the area during coughing, sneezing and other shoulder activities (Choukairi F., et al., 2011). Sternal Osteomyelitis is infection in the sternum caused by germs or most probably by bacteria (Dugdale D.C., 2012) while the untreated osteomyelitis will undergo chronic infection and lead to mediastinitis. From Table 2.2, it is evident that osteomyelitis is characterized in type II of the three main types of sternal wound infection. It occurs within 2 to 3 weeks after the initial surgery (Scholl L., et al., 2004).

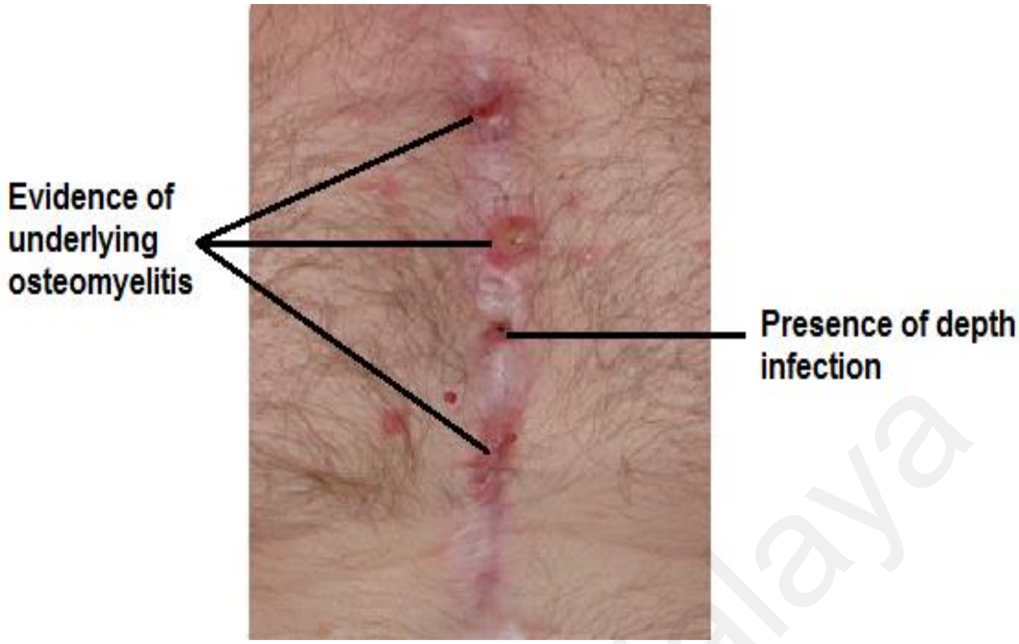

Figure 2.6: Sternal non-healing osteomyelitis in unidentified subject [Adapted from (Choukairi F., et al., 2011)]

The treatment of osteomyelitis might start with antibiotics, but in most cases, the surgical operation is significantly deemed. During the surgical operation, the necrotic tissues are removed, so that the wound can granulate, then irrigation with antiseptic and/or antibiotic takes place (Mittapalli M.R., 1979).

2.1.2 Sternal displacement

The abnormal or non-physiologic motion of the sternum in known as sternal instability; it occurs after the disruption of reuniting wires or bone fracture of the surgically fixed sternum. It was shown that instability is more associated with the old patients, osteoporotic bones and in the cases of mediastinitis development while the prevention is achieved through the excellent sternal approximation (Cahalin L.P., et al., 2011).

The sternal instability might result in excessive sternal movement, sternal fracture, pain, and difficulty or inability to perform various activities (Choukairi F., et al., 2011).

2.2 Sternal fixation techniques

The traditional techniques for sternal closure may not always contribute to the optimal fixation and in fact, no single technique is widely adopted for the robust sternal fixation (Fedak P.W., et al., 2010). This gives an evidence for the need of a robust technique for rigid sternal fixation and further reduction in DSWIs rate.

2.2.1 Wiring

Wiring using Stainless Steel (SS) has been the standard technique for sternal closure since 1957 due to its simplicity, strength, short healing time and rigidity (Julian O.C., et al., 1957). Casha et al. (1999c) investigated 6 different sternal wiring/suturing techniques using Ethicon no. 5 SS wire (Ethicon, UK), Ethibond no. 5 suture (Ethicon, UK) and Sternaband (StonyBrook Surgical Innovations, Stony Brook, NY) and produced force-displacement curves. Wire closure types involved straight, Ethibond, repair, figure of eight, multi-twist and sternaband SS wires. They used a "steel jig" as a sternal model. Computerized material testing equipment (Autograph ASG-10 KN, Shimadzu, Japan) was used to pre-tension the wires around the model up to 10 N. A data capture card (Amplicon PC20G, Amplicon, UK) was used to record the displacement data every quarter-second based on the separation of the two halves of the jig model at a velocity of 2 mm/min. Table 2.3 summarizes the comparison between the 6 wiring techniques, whereas Figure 2.7 shows the force-displacement curves for the compared techniques.

Table 2.3: The summary and comparison of the six tested wiring techniques [Adapted from (Casha A.R. et al., 1999c)]

<table>
<tr><th colspan="2">Closure technique</th><th>Displacement (mm) at 20 Kg force</th><th>Maximum force (Kg)</th><th>Comment</th></tr>
<tr><td>Straight</td><td>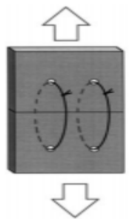</td><td>0.78±0.19</td><td>98.0±4.8</td><td rowspan="3">Testing showed that the straight technique provided less displacement than the Ethibond and repair techniques; all three techniques were tested using two wires.</td></tr>
<tr><td>Ethibond</td><td>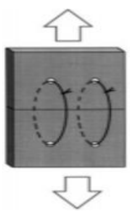</td><td>9.37±1.01</td><td>58.8±1.8</td></tr>
<tr><td>Repair</td><td>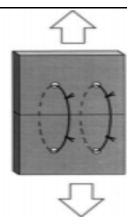</td><td>5.08±0.12</td><td>46.0±2.0</td></tr>
<tr><td>Figure of eight</td><td>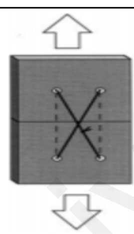</td><td>1.20±0.20</td><td>92.8±1.3</td><td rowspan="3">One wire of each was used during testing because of the double strands of each technique in comparison with the single wire of straight, ethibond and “repair” of straight techniques. The Multi-twist technique was the most stable in comparison to the other techniques because four wires are twisted with each other instead of two.</td></tr>
<tr><td>Sterna-band</td><td>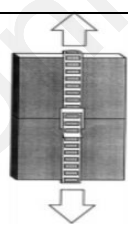</td><td>1.37±0.49</td><td>73.3±1.5</td></tr>
<tr><td>Multi-twist</td><td>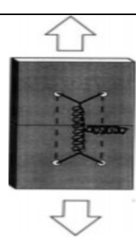</td><td>0.37 ±0.06</td><td>77.1±3.4</td></tr>
</table>

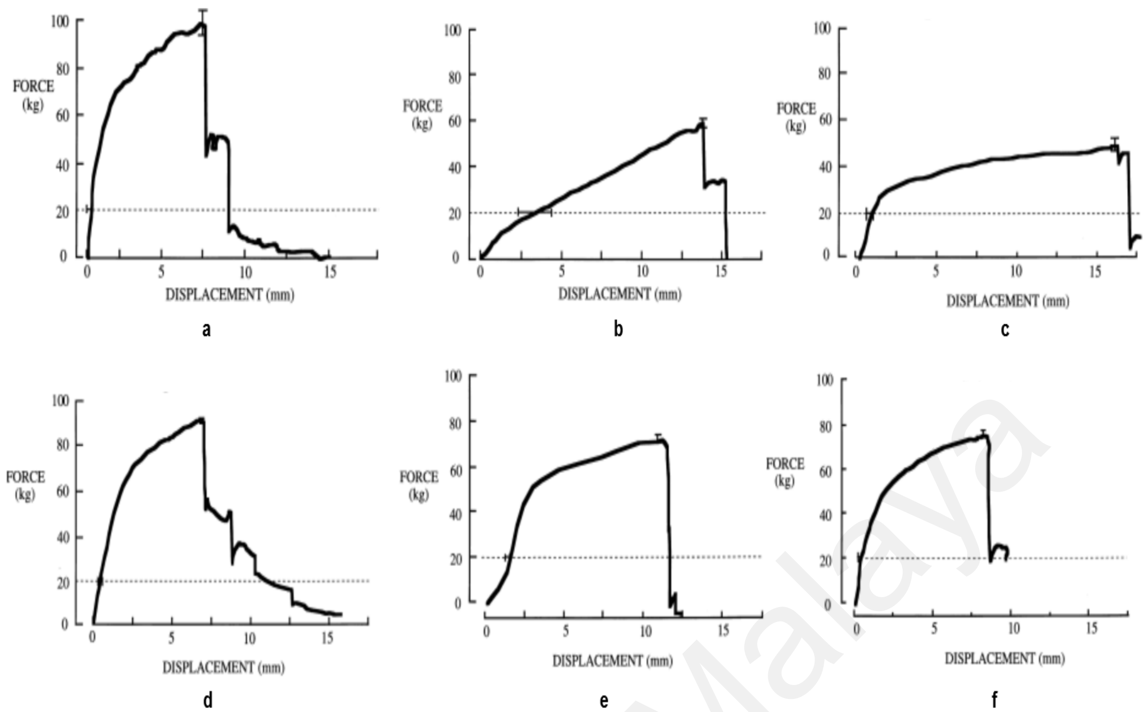

Figure 2.7: Force-displacement curves for various sternal wiring techniques as tested using computerized materials testing machine - a) Straignt b) Ethibond c) Repair d) Figure of eight e) Sterna-band f) Multi-twist [Reproduced from (Casha A.R. et al., 1999c)]

For the six wiring techniques, the maximum force applied was 20 Kg because the no.5 SS untwists at the range of 20 to 22 Kg, hence the displacement was measured at the starting-point of material deformation (Casha A.R. et al., 1999c). The Laplace law was employed to measure the maximum coughing force on the sternum after median sternotomy as results indicated that all wires may untwist under severe coughing forces; usually considered 150 Kg, although they may reach 168 Kg (Casha A.R. et al., 1999b). Thus, Casha et al. (1999c) demonstrated that the closure device is expected to have a safety margin able to withstand double the maximum force applied. This study also recommended the use of at least eight straight wires; four figure-of-eight wires or four multi-twist wires (Casha A.R. et al., 1999c). Limitations involved the analysis of wire fracture only and the use of a steel sternal model which differs from the biological or cadaver sternum. Despite these shortcomings, they demonstrated that the multi-twisted technique is useful in bleeding-fractured sternums as it appears to be able to stop the bleed by the lateral part of the closure. Also, the Ethibond technique was determined as the best technique for patients with a small chest who do not generate high forces on the sternum through coughing and those having high risk of dehiscence and osteoporosis; pediatric and elderly patients, respectively. The advantageous use of interlocking multi-twisted wires over conventional or figure-of-eight sternal closures was also evident from a further study performed by the same group (Casha A.R. et al., 1999a). The same group also performed fatigue testing on various closure techniques (polyester, figure-of-eight, steel wire, sternal bands, peristernal) using sheep sternums (Casha A.R. et al., 2001) to assess the rates of wire cutting through the bone. The sheep sternal samples were used because bovine bone was not allowed in England at that time and the porcine sternum differs from the human sternum in being keel shaped (Casha A.R. et al., 2001). They tested peristernal, figure-of-eight, sternal bands and polyester closure techniques against standard SS closure (control group) eight times using adjacent paired samples. Additionally, fatigue cycles between 1 and 10 Kg were applied on all models and displacements measured at minimum and maximum loads (Table 2.4). They further calculated the percentage cut-through of each closure as the displacement at the maximum load between the 1st and 150th cycles (Table 2.5).

Table 2.4: Displacement at 10 Kg load (150th cycle) comparing 4 closure techniques with standard SS technique (values are expressed in mean ± standard deviation) [Reproduced from (Casha A.R. et al., 2001)]

Closure type	Displacement (mm)	
	Test closure technique	Control technique
Polyester	1.01 ± 0.17	0.22 ± 0.11
Figure-of-eight	0.52 ± 0.36	0.22 ± 0.17
Sternal band	0.66 ± 0.26	3.27 ± 2.84
Peristernal	0.72 ± 0.51	2.14 ± 1.46

Table 2.5: Percentage cut-through the bone comparing 4 closure techniques with standard SS technique (values are expressed in mean ± standard deviation) [Reproduced from (Casha A.R. et al., 2001)]

Closure type	**Number of cycles**		
	25	**75**	**150**
Steel wire	100	100	100
Polyester	427±157	454±109	453±137
Figure-of-eight	234±72	196±37	232±35
Sternal band	51±29	34±14	23±8
Peristernal	43±22	40±14	34±7

Tables 2.4 and 2.5 show that the sternal band and peristernal techniques are superior to the SS control (Casha A.R. et al., 2001). Additionally, the use of figure-of-eight or polyester technique requires caution since they were associated with faster cut-through in comparison with the control model (Casha A.R. et al., 2001). The results also showed different rates of cutting through the sternum for the five types of technique (Casha A.R. et al., 2001). The superiority of sternal bands over the SS wires was contradicted by Cheng et al. (1993) who compared the biomechanical stability of No. 5 SS wire closure with 3 types of band closure techniques (5 mm Mersilene ribbon, 5 mm plastic band, 5 mm SS band) and concluded that SS wire closure is superior to sternal band techniques on cadaver sternums.

Dogan et al. (2004) reported that the use of standard steel wires is associated with osteomyelitis, dehiscence, prolonged hospitalization and increased morbidity and mortality. They proposed the use of sternal approximation using suture anchor device (made of titanium) that can overcome major complications associated with steel wires and wire-cut through the sternal bone. Based on the tests performed on a cadaver model, they indicated that the suture device is recommended for patients with metabolic bone disease as it was associated with less post-operative complications and facilitated MRI due to the compatibility of titanium with MRI (Dogan O.F. et al., 2004). Major limitations of their study were the small sample size, no biomechanical analysis of the proposed device and lack of clinical trials. The outcome of this study succeeded previous work by Kalush and Bonchek (1976) who reported the success of SS bands by peristernal closure especially for obese patients.

Many other studies (Losanoff J.E. et al., 2007; Losanoff J.E. et al., 2004; Marco R.F. Di. Et al., 1989; McGregor W.E. et al., 1999; Murray K.D. and Pasque M.K., 1997; Shih C-C. et al., 2004; Shih C-M. et al., 2005; Tavilla G. et al., 1991; Timmes J.J. et al., 1973; Zurbrugg H.R. et al., 2000 and Grapow T.R. et al., 2012) considered different wiring and cabling techniques for sternal fixation. However, this was contradicted by Gunja et al. (2004) who reported complications from SS sutures including poor sternal healing, dehiscence, SWI and sternal separation in 0.5-2.5% of cases (Gunja N. et al., 2004). Schulz et al. (2005) also indicated that the wiring techniques usually fail to achieve the required level of rigidity. It has been suggested that rigid sternal fixation using more than 6 wires would reduce the incidence of SWI (Friberg Ö. et al., 2006b). Jolly, et al. (2012) developed a new technique called “Cabled Butterfly Closure (CBC)” which consists of 12 equally spaced wires made from SS (no. 6) and are conjoined together in order to hold both halves of the sternum (Figure 2.8). The wires are then twisted together in the middle of the sternum, so forming the final cabled bond. The procedure starts from the xiphoid and continues upward as can be seen in Figure 2.9.

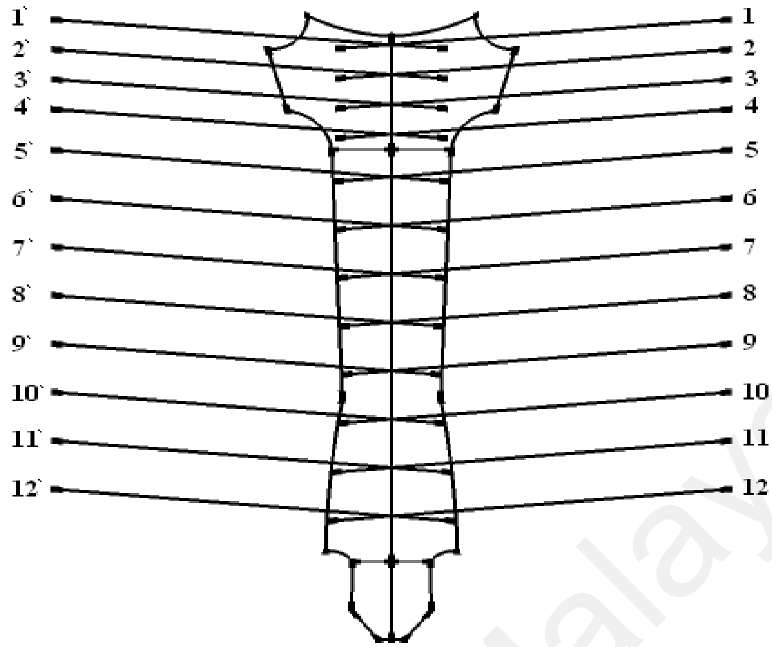

Figure 2.8: CBC by pulling and twisting conjoined wires [Adapted from (Jolly, S. et al., 2012)]

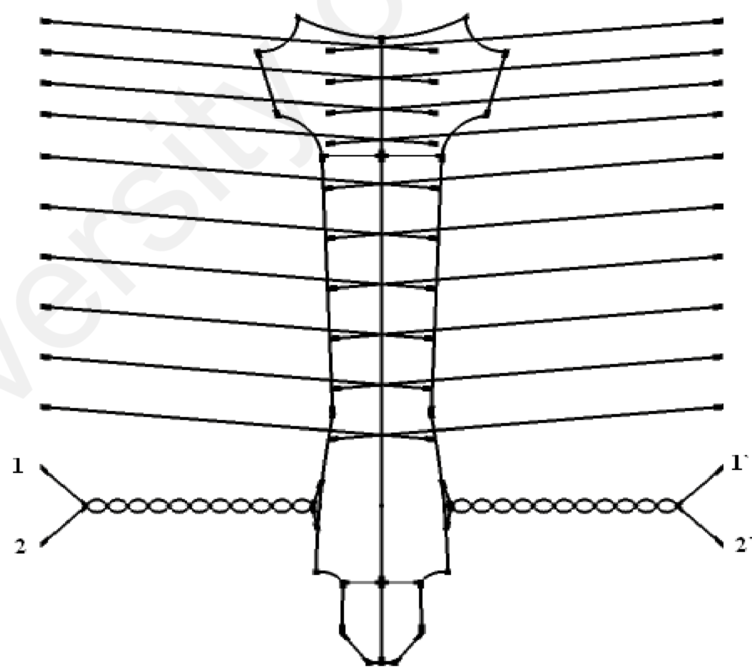

Figure 2.9: The process starts from the xiphoid and continues upward [Adapted from (Jolly, S. et al., 2012)]

This technique was reported to be superior to simple wiring as it provides the required stability against coughing and other imposed forces by dissipating them over a broader area. Additionally, this cabling design minimises dehiscence in contrast to the 8 wires closure technique. The effectiveness of this technique was confirmed when four of six cables (butterflies) failed due to coughing while the sternum remained stable. Other advantages include cost effectiveness and suitability for osteoporosis sufferers and for both light and heavy patients (Jolly, S. et al., 2012).

2.2.2 Interlocking systems

Zeitani et al. (2008) and Levin et al. (2010) studied the biomechanical properties of two sternal reinforcement devices. Zeitani et al. proposed the use of a Sternal Synthesis Device (SSD) (Mikai SpA, Vicenza, Italy) whereas Levin et al. proposed the use of a Sternal Talon Device (STD) (KLS Martin Group, Jacksonville, FL).

2.2.2.1 Sternal Synthesis Device

The device consists of two clips made of 0.7 mm titanium sheet and can slide into each other and then placed on either side of the sternum. The significant advantage of SSD is that the 5 mm wide horizontal segments can interlock at different lengths, permitting the surgeon to fit the device according to the size of the sternum (Figure 2.10). SSD is available in two sizes to better adapt different sizes of sternum; standard (1.6 g weight, 32.2 mm vertical length, 40 mm horizontal length) and large (2.0 g weight, 40.2 mm vertical length, 48 mm horizontal length) devices.

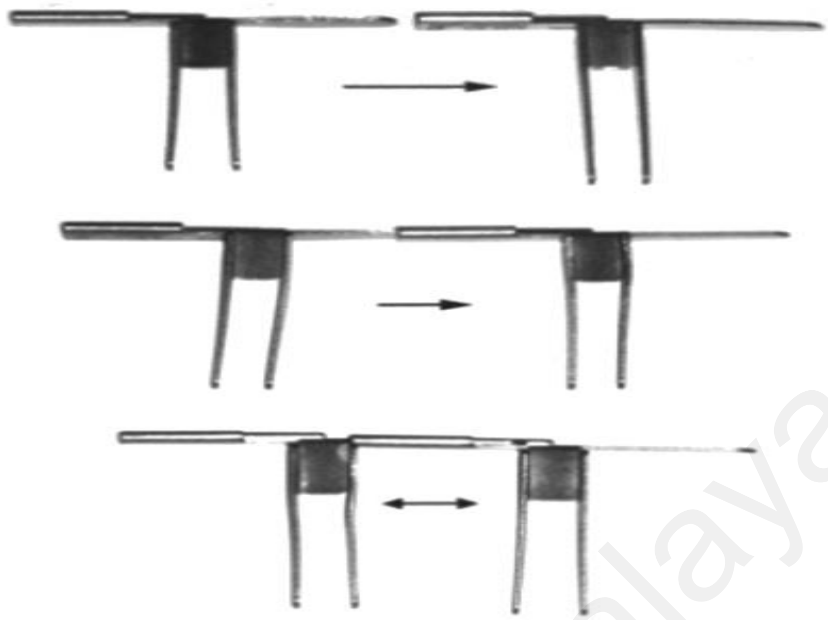

Figure 2.10: Assembly of clips in SSD [Reproduced from (Zeitani J. et al., 2008)]

The study was subdivided into two sections; mechanically testing 22 artificial polyurethane sternums (formed from 20 lbs/ft^3 dense polyurethane foam) to determine the forces that cause implant failure and, subsequently, a clinical trial to test the SSD on 45 patients. For further support during the first stage of testing, wiring (2-3 No. 5 SS wires) was also applied around the sternum. The clinical trial involved 45 patients who were submitted to median sternotomy for valve replacement (n=4) or coronary artery bypass grafting (n=41); all patients had at least three preoperative risk factors of SW complications (diabetes mellitus, depressed left ventricular function, chronic obstructive pulmonary disease, obesity, peripheral vascular disease) and a faulty paramedian sternotomy. The trial aimed to test sternal reinforcement with the SSD. The maximum forces (1,200 N) at which the artificial models failed during mechanical testing are below the maximum severe coughing force (~1600 N) (Casha A.R. et al., 1999b; Trumble D. R. et al., 2002; Dasika U. K. et al., 2003). Although displacement was seen in all models, the displacement was less for the SSD when compared with the wired control (Zeitani J. et al., 2008; McGregor W.E. et al., 2003). The device implantation (Figure 2.11) for each sternal half took approximately 4 to 6 min and patients were followed-up during the first three post-operative months (Zeitani J. et al., 2008). Results from the clinical trials showed no interoperative complications associated with implantation. However, post-operative respiratory failure was realized in 3 patients requiring prolonged mechanical ventilation and, of those, 1 patient experienced superficial dehiscence. It was determined that reinforced SSD is a promising technique in terms of preventing the sternal wound instability especially for patients who are at high risk of dehiscence (Zeitani J. et al., 2008).

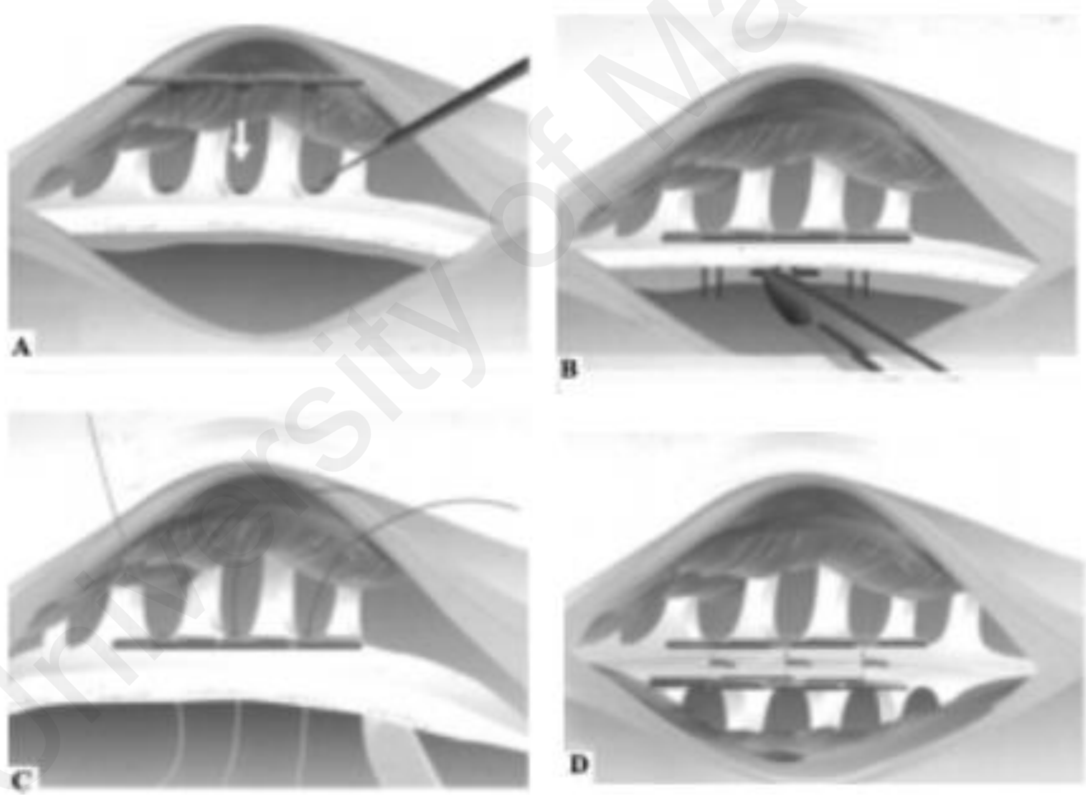

Figure 2.11: SSD implantation technique- A) Dissection of the muscle fascia using electrocautery to facilitate the device insertion B) clips insertion and fixation into the intercostals spaces and then the vertical fingers of the device are bent outward so that the clips are held firmly with the sternum C) Support for the fixation using 2-3 steel wires around the implanted clips D) the reinforced closure of the sternum after tightening the wires [Reproduced from (Zeitani J. et al., 2008)]

2.2.2.2 The Sternal Talon Device

The STD is made of titanium and is available in both single legged and double legged form (Figure 2.12) which increases flexibility for placement. The study on the STD is similar to that performed on the SSD, with the distinction that it considers the use of the device as an alternative to the wiring technique. The procedure of Talon sternal fixation is shown in Figure 2.13 (Levin L.S. et al., 2010).

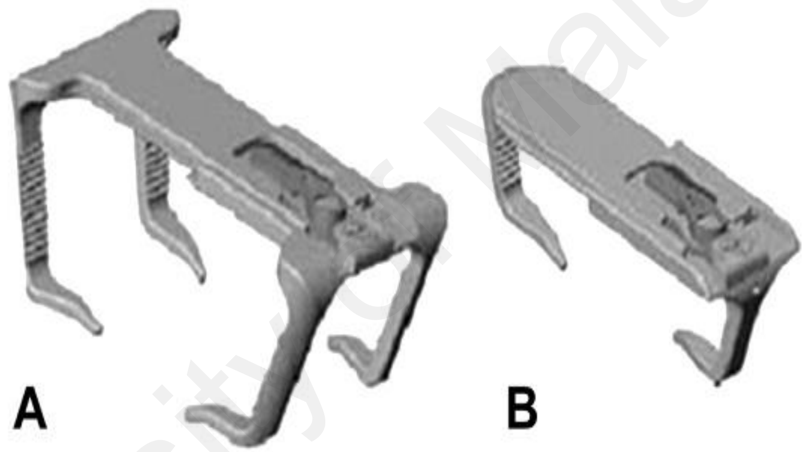

Figure 2.12: Talon sternal fixation devices- a) double legged and b) single legged [Reproduced from (Levin L.S. et al., 2010)]

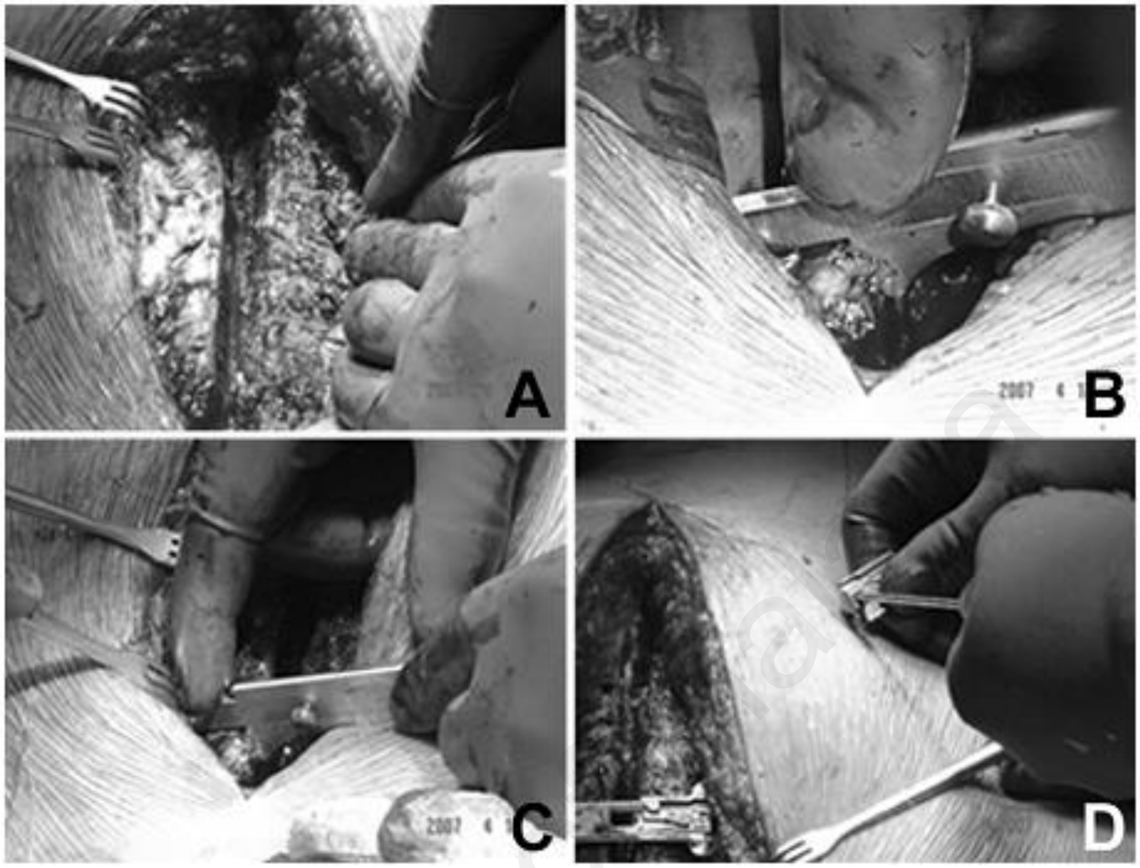

Figure 2.13: Talon implantation technique- A) Preparation for sternal width measurements B,C) Use of calipers to perform sternal measurements to facilitate the length and depth of the fixation device D) Placement of 3 Talon devices [Reproduced from (Levin L.S. et al., 2010)]

Clinical trials of the Talon involved 42 patients (26 male and 16 female; aged 34 to 84 years) who underwent sternal stabilization after median sternotomy (Levin L.S. et al., 2010). Similar to the study performed by Zeitani et al. (2008), Levin et al. (2010) performed the procedure only on patients with three or more risk factors in order to determine safety and efficacy of the Talon device. Their study reported a reduced placement time, from 30 min to between 8 to 10 min; longer than the 4 to 6 min required placing the SSD (Zeitani J. et al., 2008). The trial resulted in successful placement of the Talon in all cases with no reports of death, dehiscence or instability. However, superficial postoperative infection was reported in a single patient and was treated using oral antibiotics (Levin L.S. et al., 2010). Interlocking sternal fixation devices provided better sternal fixation in comparison with wiring techniques. Further studies performed by Baskett (1999) and Gandy and Moulton (2008) revealed that interlocking fixation techniques reduce the major post-sternotomy complications, especially for patients with high risk factors such as diabetes, pulmonary diseases, obesity and wound dehiscence.

2.2.3 Plate-screw systems

The introduction of the plate-screw system was mainly based on the need for a new sternal fixation technique to provide more stability than that of the wiring or interlocking closure systems, particularly with high-risk patients (Gunja, N., et al., 2004), facilitating faster sternal healing and decreasing the incidence rate of post-operative complications associated with median sternotomy (Gunja, N., et al., 2004). Plate-screw systems provide huge advantages when compared with other techniques due to their physical ability to hold all bone fragments during the sternal healing process; this would effectively limit the sternal disruption and movement (Dieselman J. C. 2011). Hence, satisfying the knowledge demonstrated by Robert Danis in 1949 that if the movement of the fractured bone is minimized and held firmly with compression, then it would heal without formation of a fibrous tissue (Dieselman J. C. 2011). Most of the plating techniques for sternal fixation had not been evaluated mechanically (Gunja, N., et al., 2004; Schulz A. P., et al., 2005; Huh K. et al., 2008), thus there is little data directly comparing plating and wiring techniques (Gunja, N., et al., 2004). Gunja et al. (2004) conducted a study to determine the optimal configuration for an X-shaped sternal plate system in terms of the number, type and location of the metal plates. They used a commercial sternum model made of Polyurethane (Sawbones, Pacific Research Laboratories, Vashon, WA), and a midline sternotomy was treated with 3 X-shaped plates (Walter Lorenz Surgical, Jacksonville, FL).

Uniaxial lateral loading was applied to both halves of the sternum to measure the relative distraction. (Gunja, N., et al., 2004). The model was tested such that each side of the sternum is loaded at 8 locations with equal forces (Figure 2.14) to maximize the loading uniformity along the overall length of the sternum.

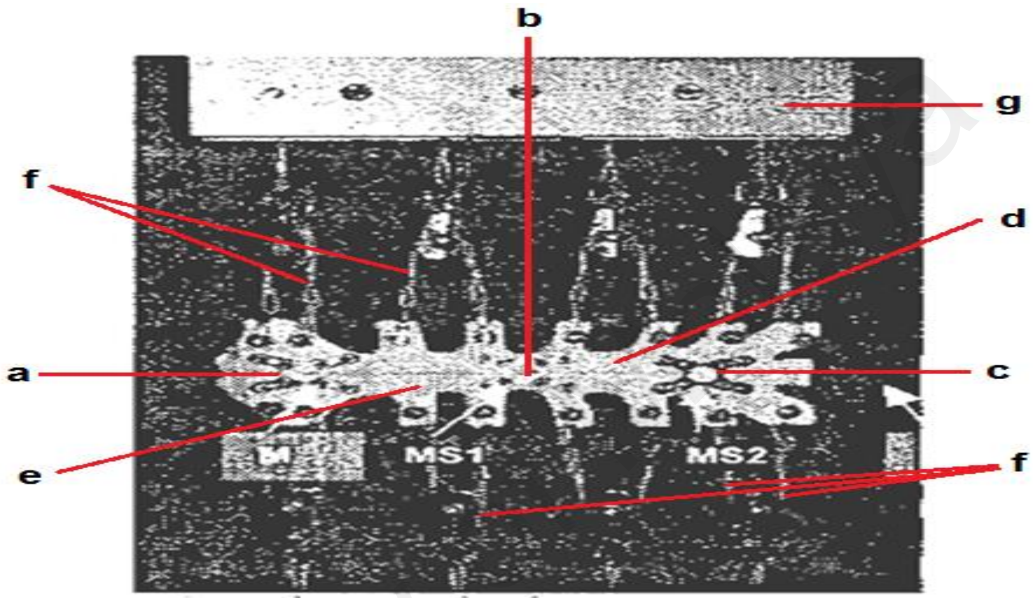

Figure 2.14: Experimental setup of the sternal fixation model- a) x-plate placed on Manubrium b) x-plate placed on midsternum 1 c) x-plate placed on the midsternum 2 and xiphoid d,e) both halves of sternum f) uniaxial 8 equal forces applied on each side of the sternum in increments of 44.5N to maximum load of 400N g) Clamping system to perform uniaxial lateral pull tensile tests [Adapted from (Gunja, N., et al., 2004)]

During the test, ten distraction measurements were taken by the four 5mm calibration markers (placed on different sternal regions) at each incremental trial and the average distraction was calculated at each location. Figure 2.15 shows the displacement versus load (distraction) at the Xiphoid, 2 mid-sternum locations and the manubrium locations (Gunja, N., et al., 2004).

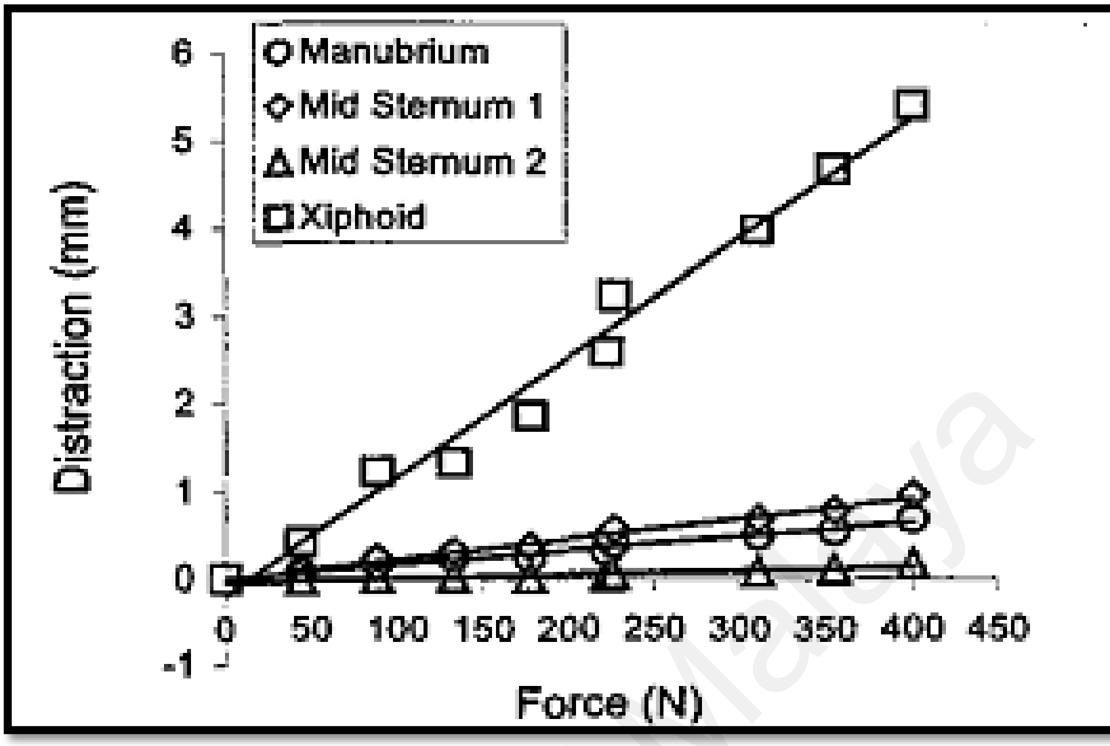

Figure 2.15: Distractions versus load force for 4 places of the sternum model fixed with 3 X-shaped plates [Reproduced from (Gunja, N., et al. 2004)]

Results showed that the use of polyurethane is valid for sternum model while it was shown that the stability of the fixation depends heavily on the location of the plates and the subsequent load. Additionally, the results showed about 5 mm distraction in xiphoid and <1 mm distraction in the other 3 locations; hence the study didn't provide rigid fixation in all parts but helped the surgeons to identify the best sites for plate fixation. The test was performed on a model sternum that didn't allow for dehiscence, bleeding and other complications which could be encountered during the clinical situation (Gunja, N., et al. 2004).

Decoteau et al. (2006) performed a screw pullout and cyclic loading tests using screws for both cortical and cancellous bones. They indicated that there are different successful methods for rigid fixation but most of them are considering the polyurethane model which differs from the cadaveric model in having significant difference in the properties when compared with the properties of the native or cadaver sternum. Hence, the tests were performed on porcine sternal samples to determine the superiority of either screw type for rigid sternal fixation. Their results showed that the mean screw pullout force for screws for cortical bone were significantly lower (28.9±11.74 N) than the screw pullout force for those for cancellous bone (67.2±10.23 N). They demonstrated that the distraction in the screw-plate technique occurs mainly due to screw loosening (Decoteau DM. et al., 2006) and further suggested that attention should be directed towards the geometrics of the screw threading which is directly related to the fatigue resistance of the sternal fixation technique. Ford et al. (2011) considered various associated complications and deficiencies such as wobbling and loosening of the screw within the plate. They reported that there is no fixation device capable of supplying locking and subsequently withstanding compressive forces for fixation of the two halves of the sternum. In response to this, they presented a new device consisting of one screw in another screw (an "anti-wobble" device) to reduce post-operative displacement (Ford M. et al., 2011). The inner screw is a flat head screw made of SS which penetrates the bone plate, while the outer screw, also made of SS is tightened into the inner screw (Figure 2.16). The authors stated that the device was capable of providing both locking and withstanding forces that cause screw loosening or pullout (Ford M. et al., 2011).

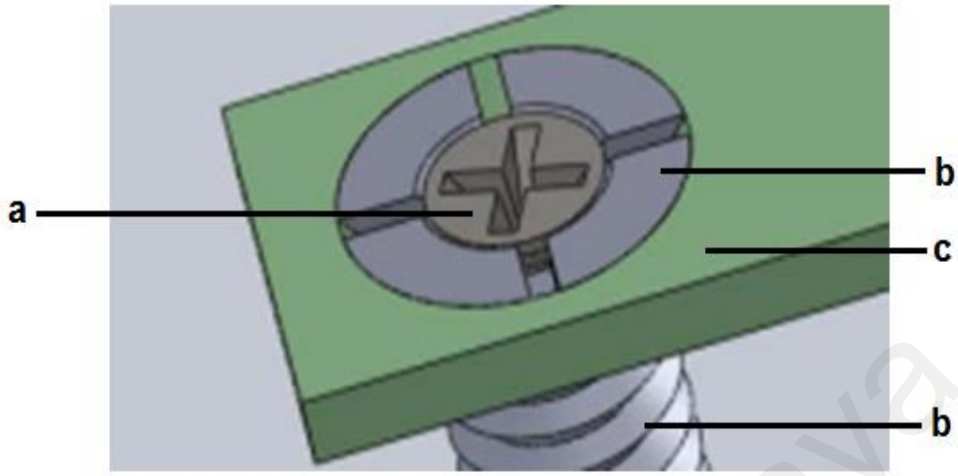

Figure 2.16: Computer Aided Design (CAD) model of anti-wobble plate screw system- a) Outer screw, b) inner screw c) fixation plate [Adapted from (Ford M. et al., 2011)]

Schulz et al. (2005) tested the application of pure titanium H-shaped 8 holes plates (Figure 2.17) on a 28 year old male (Figure 2.18-a) who underwent a horizontal fracture in the sternum (Figure 2.18-b) during a motorbike accident. The procedure started with an 8 cm incision (longitudinal) over the non-union sternum, then removal of fibrous tissue and grafting of the cancellous bone. The device was then placed and locked by screwing into the sternum (Figure 2.19). Results showed a positive performance of the fixation technique; however, the authors reported the need for a thinner plate (<5 mm) to allow for smaller screws (Schulz A. P., et al., 2005). Moreover, they indicated that the wiring techniques are not appropriate and usually fails to achieve the required sternal fixation being evident from the conducted CT scan that shows the fracture along the horizontal direction of the sternum. CT scan was useful in performing the required measurements of the proper fixation device (Schulz A. P., et al., 2005).

Figure 2.17: H-shaped plate for sternal fixation- a) holes with different angels of direction to counter-balance the multidirectional forces imposed on the sternum b) standard stable angular cortical screws [Adapted from (Schulz A. P., et al., 2005)]

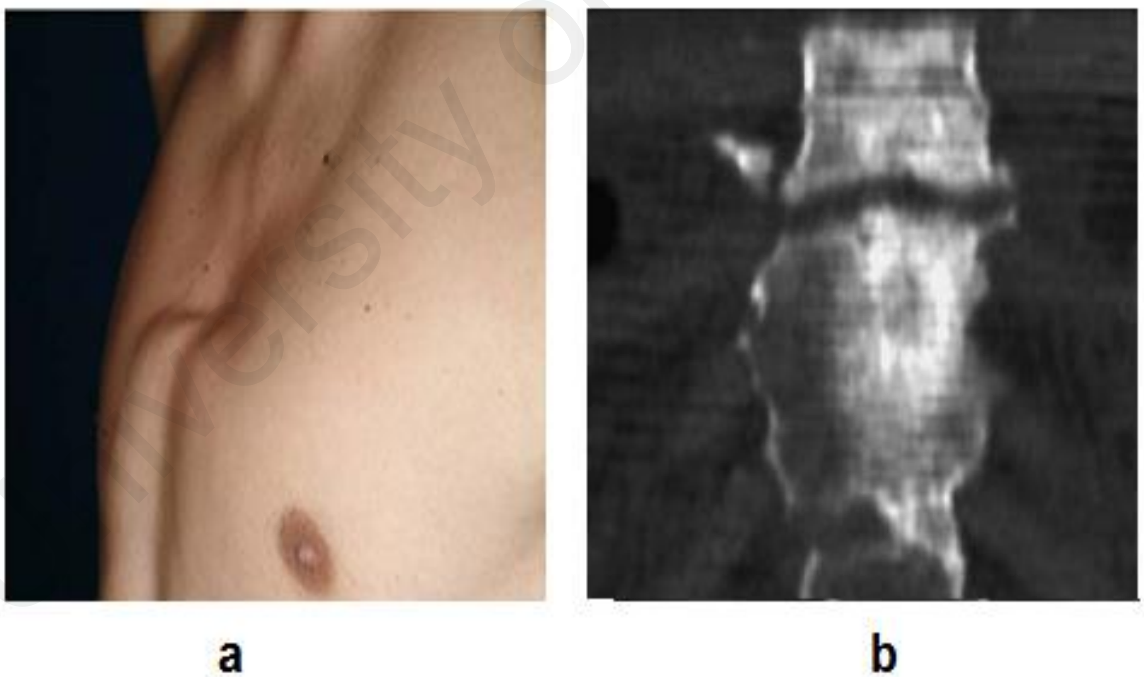

Figure 2.18: Case report- a) Luxation (dislocation) of sterum b) CT scan for implant measurements [Reproduced from (Schulz A. P., et al., 2005)]

Figure 2.19: Placement of H shaped sternal fixation device [Reproduced from (Schulz A. P., et al., 2005)]

Shifrin et al. (2008) applied a sternal-lock (Lorenze) plate fixation to a 58 year old man who had a pulsatile, enlarging mediastinal mass (16 x 14 x 14 cm) following a massive aortic pseudoaneurysm surgical operation (Figure 2.20). The technique involved the use of 2 X-shaped plates in the centre of the sternum and 3 curved plates in the caudal (inferior) and cephalad (superior) bones (Figure 2.21). Thoracic surgery aimed to reconstruct the aortic arch, and involved direct approximation of the sternal edges using forceps. Subsequently, Lorenze plate fixation was used; by applying two X-shaped plates to the centre of the sternum and 3 curved plates in the caudal (inferior) and cephalad (superior) bones. The construct remained stable with no signs of sternal infection at the 3 month follow up (Shifrin D. A., et al. 2008). Consequently, it was concluded that for sternal reconstruction; plating is considered as the ideal option (Shifrin D. A., et al. 2008). Other studies (Cohen D. and Griffin L., 2002; Ozaki W. et al., 1998) demonstrated that plating systems such as H-shaped system are preferred over the wiring techniques by providing more stability, lesser disruption of the underlying vasculature, decreased infections and lesser pain; nevertheless, more investigation is required for robust sternal fixation techniques in critical cases such as osteoporotic sternums, and DSWI.

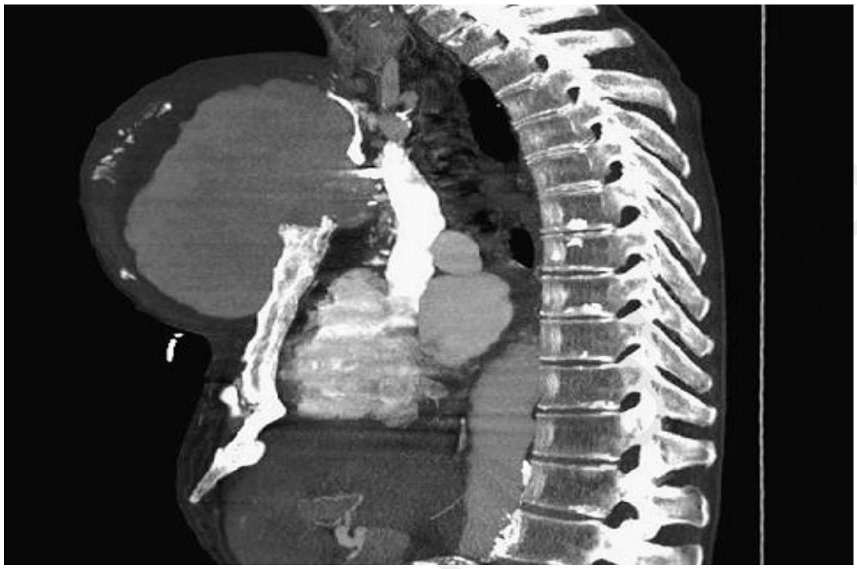

Figure 2.20: CT scan for the massive aortic pseudoaneurysm for a 58 years old man [Reproduced from (Shifrin D. A., et al. 2008)]

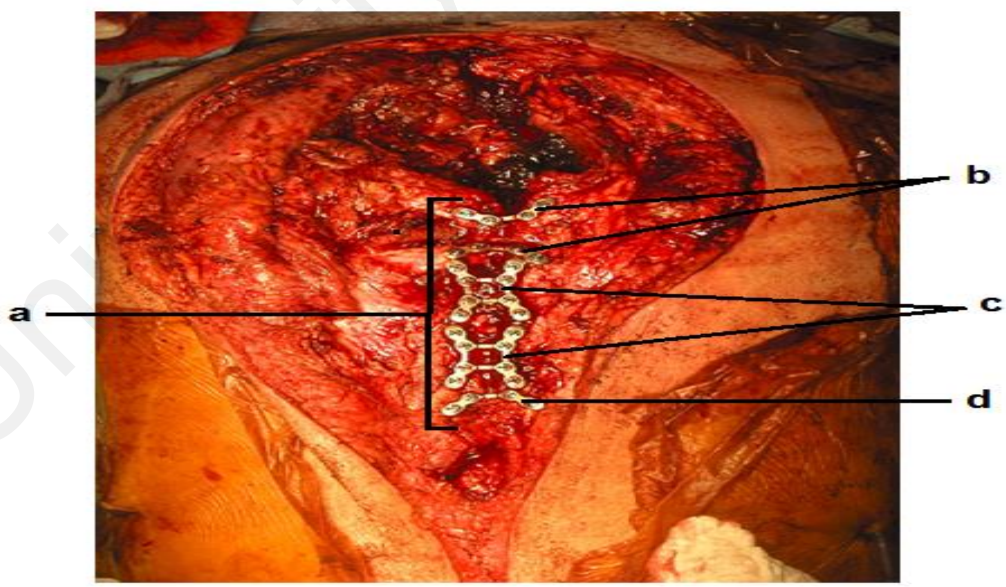

Figure 2.21: a) Lorenze sternal-plate fixation device including b) 2 curved plates placed above the centre of the sternum, c) 2 X-shaped plates placed in the centre of the sternum and d) 1 curved plate placed directly below the centre of the sternum [Adapted from (Shifrin D. A., et al. 2008)]

López Almodóvar, et al. (2008) and Huh, et al. (2008) discussed transverse plate sternal fixation technique known as "Sternal Sparing". The design of López Almodóvar, et al. consisted of two titanium plates (2.4 mm thick) connected using emergency release pin and titanium unilock screws (Synthes GmbH, Solothurn, Switzerland). The length of screws was measured directly using depth gauge. Their studies reported that the wound infection following the cardiac surgery/Sternotomy is one of the most associated complications while solutions are still limited. López Almodóvar, et al. (2008) proposed the rigid fixation by placing 3 plates on 3 thoracic ribs (rib-to-rib fixation [Synthes CMF, Paoli, Pa]) and single star plate on manubrium (Figure 2.22) in 2 patient cases with DSWI while Huh, et al. (2008) employed 3 to 5 plates along the sternum with a single star plate on the manubrium (Figure 2.23) in 14 patient cases with major post-sternotomy complication including chronic dehiscence (9 cases), acute dehiscence (3 cases), previous mediastinitis (2 cases).

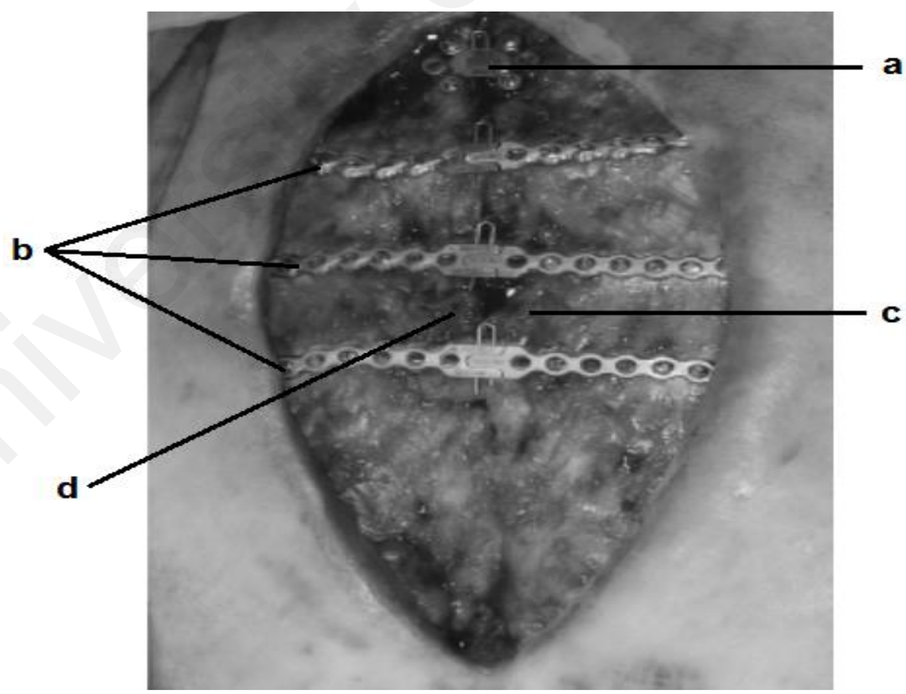

Figure 2.22: Sternal sparing technique- a) Star plate placed on the manubrium b) 3 "rib to rib" hole plates c) left half of the sternum d) right half of the sternum [Adapted from (López Almodóvar L.F., et al. 2008)]

Figure 2.23: Sternal sparing technique consisting of 4 "rib to rib" hole plates and a single star plate placed on the manubrium [Reproduced from (Huh, J. et al. 2008)]

Other studies (Elahi M.M. et al., 2004; Song D.H. et al., 2004; Cicilioni O.J. et al., 2005; Raman J. et al., 2006; Plass A. et al., 2007; Voss B. et al., 2008; Chou S.S. et al., 2011 and Fawzy H. et al., 2011) have considered different plating techniques for rigid sternal fixation and reduced incidence rate of SWIs. Table 2.6 compares some of the clinical plating techniques performed between 2004 and 2011.

Table 2.6: Comparison of some plating fixation techniques published from 2002 through 2011

Authors	Fixation technique	Clinical cases	Postoperative complications	Comment
Elahi, et al.	2.4 mm fixation plates (Synthes Mandibular Trauma Set; Synthes, Paoli, PA), with SS wires.	6 with complicated sternal closure.	None reported.	The wire/plate fixation provides more stability resulting in no complications.
Song, et al.	Combination of plates secured by bi-cortical screws.	45 (26 males/19 females); high risk for sternal dehiscence.	Post-operative deaths unrelated to the sternal fixation technique (n=4). Associated with fixation (n=18).	Plate fixation resulted in no incidence of mediastinitis compared with incidence due to the wire closure in 28 cases of the same study group.
Cicilioni, et al.	3 (minimum) Synthes 2.4 mm locking Titanium plates.	50	Seroma formation (n=5 patients). Bleeding (n=2). Pectoral muscle dehiscence (n=1). Incomplete bony union (n=1). Late recurrent infection (=1).	Complete healing in 98% of patients.
Raman, et al.	Sternalock system (Jacksonville,	320 with 3 or more risk	12 death cases (3.75%) in group	Technique suitable for high risk

	Florida) with mono-cortical, self-tapping screws.	factors of DSWI, divided into group S (n=105, rigid plate fixation) and control group (n=215).	S and 18 death mediastinitis reported in 13% of controls ($p<0.05$). No mediastinitis in group S.	patients.
Plass, et al.	Transverse plating technique (Synthes™, Switzerland).	3 cases suffering from sternal infection and instability.	-	Technique resulted in stable sternal fixation.
Voss, et al.	Transverse plating technique (Synthes™, Switzerland); self-tapping unilock screws with 2.4 mm titanium plates.	15 with sternal non-union	Plate removal in 3 patients due to post-operative pain; one death (not related to the fixation).	Technique provides stable fixation with complicated sternal dehiscence.
Chou, et al.	SternaLock (Biomet Microfixation Inc, Jacksonville, FL).	2 cases with unstable sternal fixation.	No complications reported.	System can provide rigid sternal fixation following median sternotomy.
Fawzy, et al.	3 rib-plates with a single manubrial plate (Titanium Sternal Fixation System®, Synthes).	40 cases.	2 cases developed SWI.	Technique can be used effectively in cases with sternal instability.

‘Table 2.6, Continued’

2.2.4 Cementing

“Acrylic” was the first developed cement in the 1930s for dental filling applications (DiMaio F.R., 2002). In the 1950s, poly(methyl methacrylate) (PMMA) was utilised in cranioplasty and in the 1960s, it was used in a Total Hip Replacement (THR) surgery (DiMaio F.R., 2002; Saha S. and Pal S., 1984; Kenny S.M and Buggy M., 2003; Provenzano M.J. et al., 2004). Recent developments of calcium-phosphate cements such as Hydroxyapatite (HA) and Tri-Calcium Phosphate (TCP) have facilitated the integration of cements with bone (Kenny S.M and Buggy M., 2003). From 1970s to the present day, the development of new cements such as GPCs with a wide variety of biomechanical and physiochemical properties was based mainly on the increasing number of potential surgical challenges.

Muehrcke, et al. (2007) studied the effective use of Calcium Phosphate Cement (CPC) called as “Callos” to control bleeding in severely osteoporotic, fragile sternums. Callos is approved by the Food and Drug Administration (FDA) for bone void filler applications in non-load bearing applications (Schildhauer T.A. et al., 2000; Lobenhoffer P. et al., 2002). The study identified 11 subjects who have osteoporotic sternums out of 246 patients and selected them for median Sternotomy. CPC was applied after wire closure. Patients were followed up for 6 months using CT scans. There was no evidence of infection, dehiscence, or non-union. Callos did not dissolve at blood pH and is the only CPC capable of accepting pins and screws directly after setting. Limitations of the study were small sample size, lack of a control group and an inability to identify the rate of sternal remodelling. Muehrcke, et al. (2009) Performed a follow-up study with seven patients. They applied the cement directly onto osteoporotic sternums (Figure 2.24) using a spatula (Figure 2.25). The comparison of preoperative and postoperative CT scans for the majority of patients (15 out of 18) revealed that the application of CPC to the osteoporotic sternums resulted in greater bone mineral density. It was also evident that the cement partially reabsorbs. Moreover, the follow up showed no evidence of dehiscence. Limitations of the study were the inability to obtain a preoperative scan for all patients and the absence of a control group.

Figure 2.24: Severely osteoporotic sternum associated with loss of lateral sternal table (>35%) in a 72.28±5.96 old patient who underwent open heart surgery through median sternotomy incision [Reproduced from (Muehrcke D.D., et al., 2009)]

Figure 2.25: Applying CPC with spatula and digit after the preparation of cerclage wires for sternal fixation [Reproduced from (Muehrcke D.D., et al., 2009)]

Recent developments by Doctors Research Group, Inc. (Southbury, CT) resulted in the first use of Kryptonite cements; "a polymer comprised of castor oil based polyols, a reactive isocyanate and calcium carbonate powder that cures In Situ" (Doctors Research Group, Inc., 2009). The viscous liquid form is formed by interoperative mixing of three components parts, which then polymerizes to transform the material from its liquid injectable form to an adhesive taffy-like paste (in approximately 20 min) and then to a moldable putty (over the next 24 h) as can be seen in Figure 2.26 (Doctors Research Group, Inc., 2009).

Figure 2.26: Kryptonite cement polymerization (transition from liquid injectable form to a sticky taffy-like shape and then to moldable putty) [Reproduced from (Doctors Research Group, Inc., 2009)]

Fedak, et al. (2010) applied Kryptonite bone cement to fresh cadaveric sternal models (part A) and to a selected clinical case series (part B). In part A, four samples were fixed using a conventional wiring technique (seven SS wires) whereas five samples were fixed using wire closure with the addition of 6 Cubic Centimeter (cc) of Kryptonite as a thin (1-2 mm) coating on each half of the sternum (Figure 2.27-a). Constructs were stored at 37 °C and after 24 h, were mounted in an accelerated cyclic biomechanical testing machine at loads 10-100 N (lateral distracting force). Micro-displacement sensors were placed at the midsternal region and about 1 inch from the superior and inferior ends of the sternum (Manubrium and Xiphoid, respectively). 24 h post cementation; the adhesive solidified forming a contiguous core along the interior portion of the cancellous bone (Figure 2.27-b). Additionally, Figure 2.27-c shows the adhesive cement expanding outside of the compact bone after fixation for biomechanical testing. Results on the wire closed construct showed measurable displacement (≥ 2 mm) in all segments of the sternum at load forces ≥ 400 N, while the cemented constructs showed no displacement at load forces ≤ 600 N (Figure 2.28). In part B, the wire and cement closure techniques were compared on a selected clinical case series (University of Calgary and Calgary health region, Canada). Clinical comparison results showed that the adhesive closure was not associated with infection or cement migration. Additionally, Single Photon Emission Computed Tomography (SPECT) results indicated that the adhesive, along with the use of conventional wires, can rapidly augment bone strength without compromising the perfusion of the sternum; this is considered as an advantage as successful sternal closure should improve stability without decreasing sternal perfusion, which would limit the healing process (Spotnitz W.D., 2008). The limitations of their study included the lack of animal model testing and the only force studied on the stability of the sternum was lateral stress; other forces were not considered (Fedak P.W. et al., 2010).

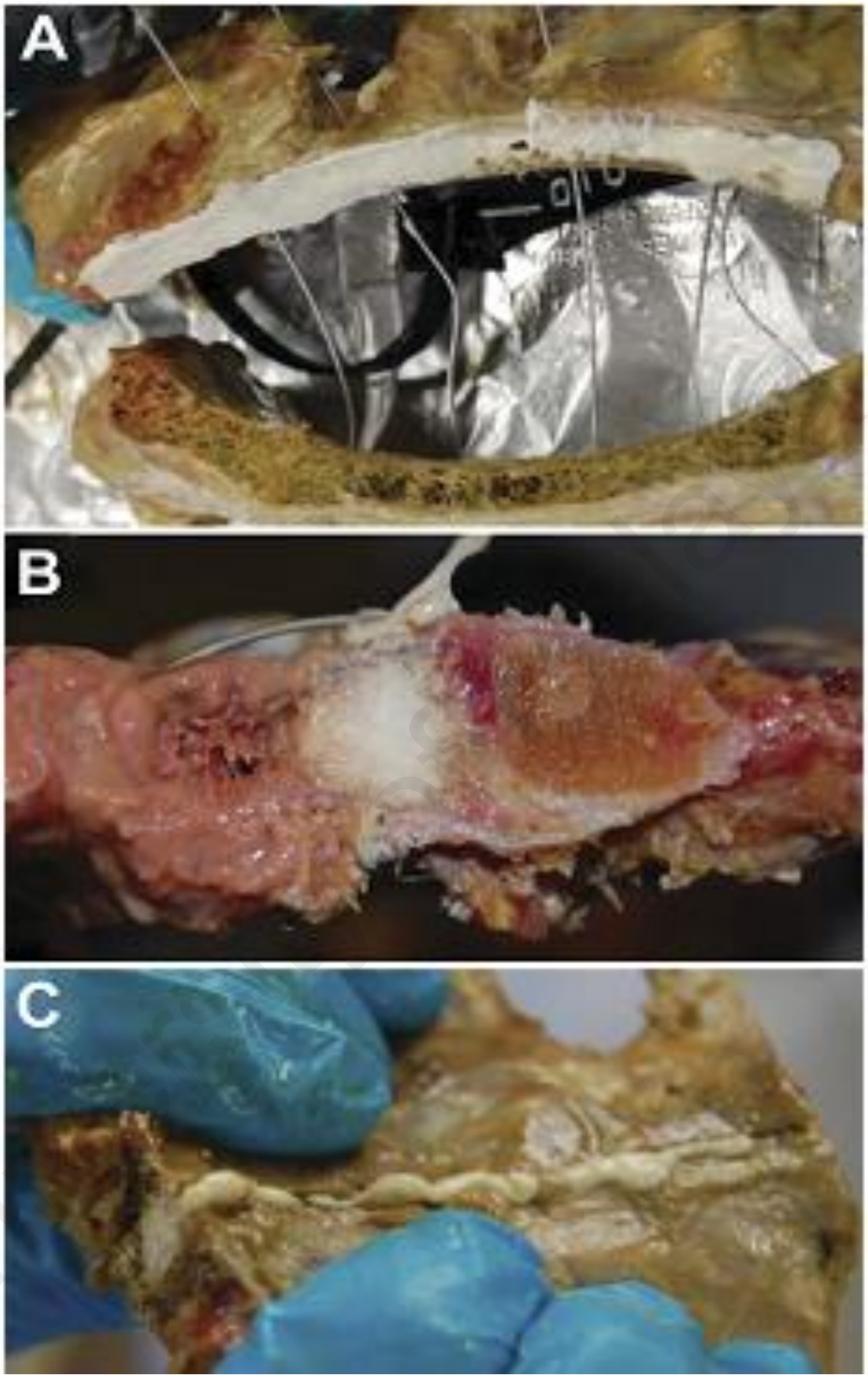

Figure 2.27: Sternum morphology- A) Kryptonite is applied on both halves of the cadaveric sternum after midline sternotomy, B) The Kryptonite adhesive became solid (bonelike) forming a contiguous core along the interior portion of the cancellous bone after 24 hours of application, C) Long section of the cadaveric sternum showing the adhesive expanding outside the compact bone and edges of both halves are approximated [Reproduced from (Fedak P.W. et al., 2010)]

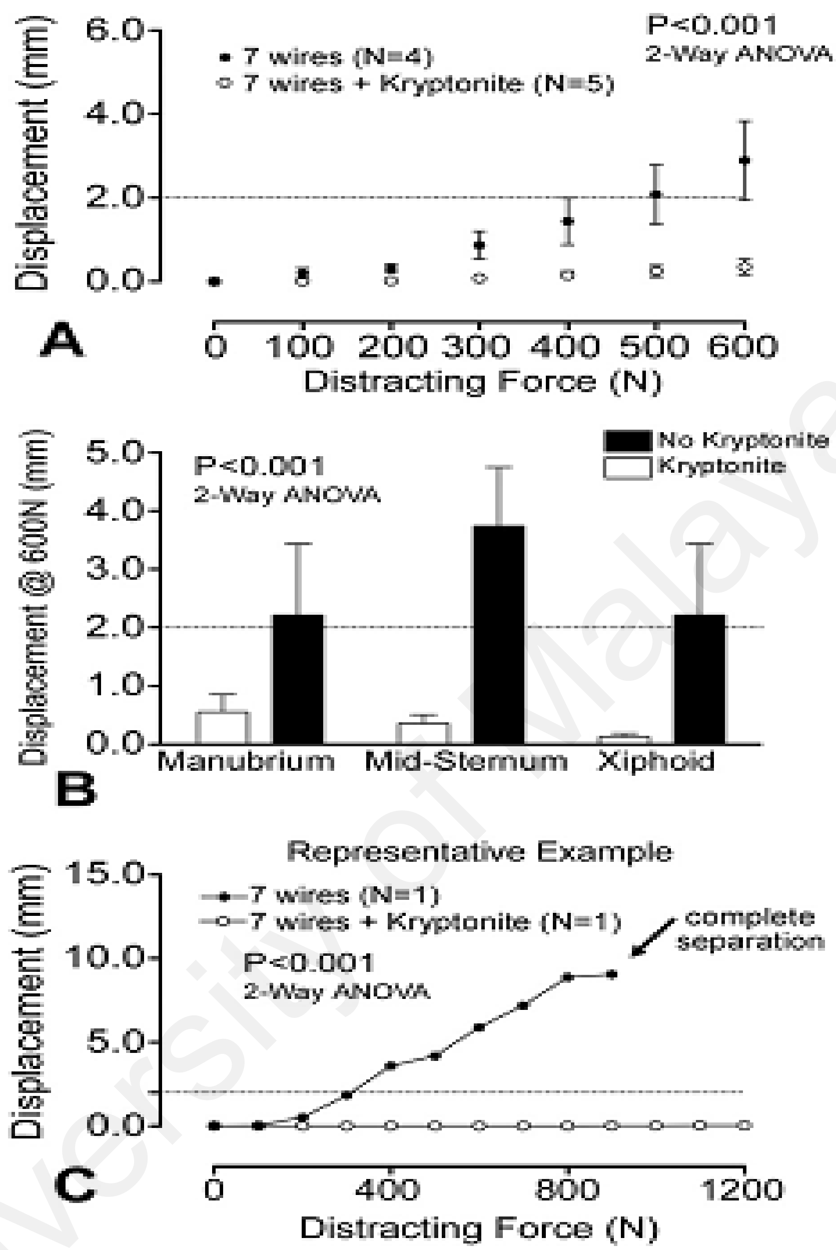

Figure 2.28: Statistical analysis of mechanical testing results- A) Grouped mean data showing the significant displacement observed with increasing the lateral stress (load) in the conventional wire celcrage group compared to the modified adhesive closure using Kryptonite where pathologic displacement was not observed despite the significant increments of lateral force (up to 600 N), B) Grouped mean data comparing the displacement observed in all sternal regions (Manubrium, Midsternum and Xiphoid) for conventional wire cerclage closure and modified adhesive closure when 600 N lateral stress force is applied C) Representative example showing minimal displacement observed in all regions when modified adhesive closure is used despite the high loading force (1200 N) and also compared to the conventional wire cerclage closure [Reproduced from (Fedak P.W. et al., 2010)]

2.2.5 Antibiotic incorporation

Diefenbeck, et al. (2006) reported that infection rates range from 0.8-1.2% in total hip arthroplasty (orthopaedic surgery) and 3.6-8.1% in closed fracture to 17.5-21.2% in open fractures (trauma surgery). Infections might necessitate revision surgery and long term hospitalization and can cause mortality (Wren A.W. et al., 2010). Antibiotics are used to treat bacterial infections. They have the ability to penetrate the soft tissue and bone for healing purposes (Barthelemy A., 2006). The efficacy of antibiotics is limited due to the increased resistance of bacterial agents against their specific targeting drugs (Kohanski M.A. et al., 2010). Gentamicin is an aminoglycoside antibiotic used in the treatment of bacterial attack such as that in urinary tract and chest infections, burns and wounds (Ailakis J., 2011).

Schimmer et al. (2012) performed the first controlled, double blind, single centre and prospectively randomized study for investigating the effective benefit of using Gentamicin Collagen Sponges (GCS) to reduce the complications associated with the DSWIs. Figure 2.29 shows the trial profile for the cases involved in the study in the duration between June 2009 and June 2010 in the Wurzburg University Hospital (Würzburg, Germany).

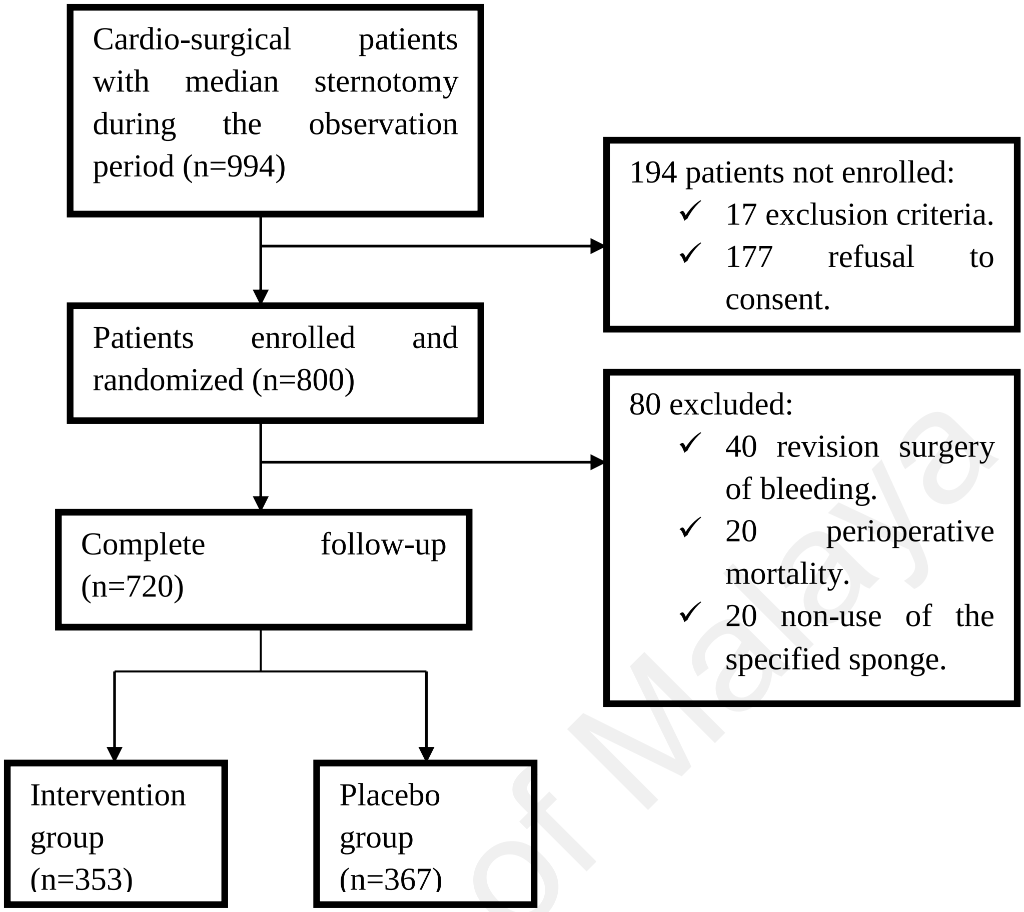

Figure 2.29: Cases profile in the duration between June 2009 and June 2010 in the Würzburg University Hospital (Würzburg, Germany) [Adapted from (Schimmer, C. et al. 2012)]

The method involved the randomization of 400 GCSs (intervention group) and 400 placebo sponges (control group). All patients were subjected to continuous check-up preoperatively and postoperatively on days 1,2,4,7 and on the day before discharge (Schimmer, C. et al. 2012). DSWI was realized in 13 of 367 cases (3.52%) for the control group and 2 of 353 cases (0.56%) for the intervention group. This shows significant effect of using GCSs in reducing DSWI for patients undergoing median sternotomy. The conclusions of Friberg et al. (2006a) supported Schimmer et al. (2012). Friberg and colleagues investigated into the use of GCS (intervention group) and intravenous prophylaxis (control group) in 398 and 967 patients, respectively. The rate of SWI was 9% in the control group and 4.3% in the intervention group. A further study (Reser D. et al., 2012) confirmed the benefits of GCS in reducing SWI for patients who underwent median sternotomy. 4,863 patients suffered from postoperative bleeding after cardiac surgery due to the sterility issues in the Intensive Care Unit (ICU). They analyzed the data in order to investigate the occurrence of SWI for the cases after re-exploration in the ICU. The use of GCS (after reoperation for bleeding) was effective in reducing the incidence of SWI by placing the sponge between both halves of the sternum. Limitations were that this study was single-institution, it did not consider large randomized populations and there was no control group. A further study (Mavros et al., 2012) investigated the suitability of GCS to prevent wound infection after median sternotomy. Meta analysis of the results suggested GCSs helped the prevention of postoperative SWIs for patients who underwent cardiac surgery (Mavros et al., 2012).

2.2.6 Vacuum Assisted Closure (VAC)

Sternal osteomyelitis is a common consequence of cardiac surgery which requires flap coverage and debridement (Scholl L. et al., 2004). A VAC device (KCI Inc, San Antonio, TX) has applicability in situations including wound stabilization (prior to the reconstructive surgery), wound infection management (after the reconstructive surgery) and wound closure. In cases of severe sternal infection, sternal debridement and total sternotomy are suitable for the effective removal of all contaminated bone; this process involves crushing of the pectoralis muscle flaps between both edges of the sternum. The VAC sponge/device is placed on the mediastinum and between both sternal edges (Figure 2.30).

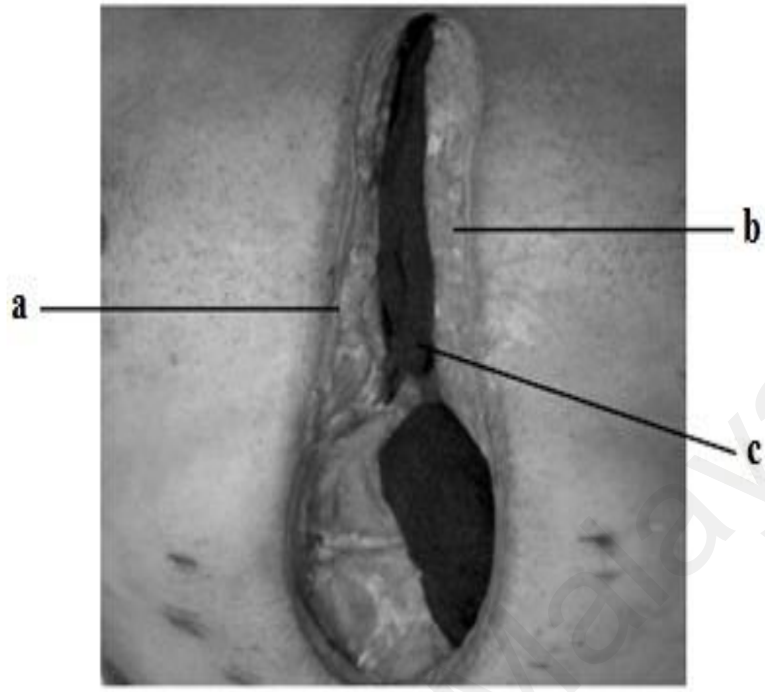

Figure 2.30: Placement of VAC sponge on the mediastinum. (a) right edge of the sternum (b) Left edge of the sternum (c) VAC sponge [Adapted from (Scholl L. et al., 2004)]

The VAC sponge resulted in no erosion or bleeding in the underlying cardiovascular structures (Scholl L. et al., 2004). The device was associated with a decreased number of soft tissue flaps and dressing changes required for closure (Song et al., 2003). Moreover, it helps in achieving complete wound healing without extensive flap reconstruction and sternal debridement (Song et al., 2003). Additionally, it is useful when infections appear after muscle flap reconstruction (Scholl L. et al., 2004). Postoperative infection occurred in one out of 13 patients (Figure 2.31). Other studies (López Almodóvar L.F., et al., 2008; Huh, J. et al., 2008) reported some advantages of using the VAC system including shorter hospital stay and reduced number of complications. Re-debridement using VAC avoided the necessity of second flap reconstruction (Figure 2.32).

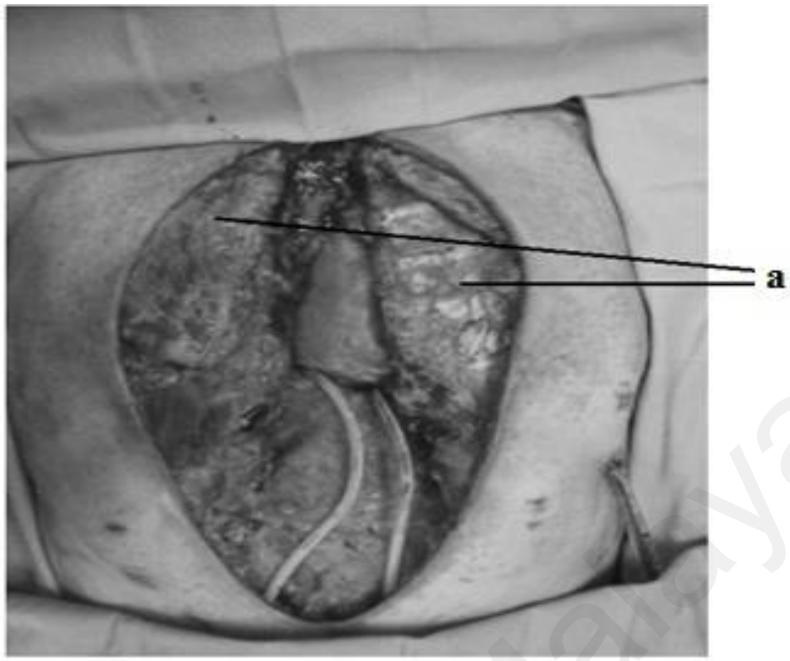

Figure 2.31: Elevation of bilateral pectoralis major flap muscles for sternal wound coverage. (a) bilateral pectoralis major flaps [Adapted from (Scholl L. et al., 2004)]

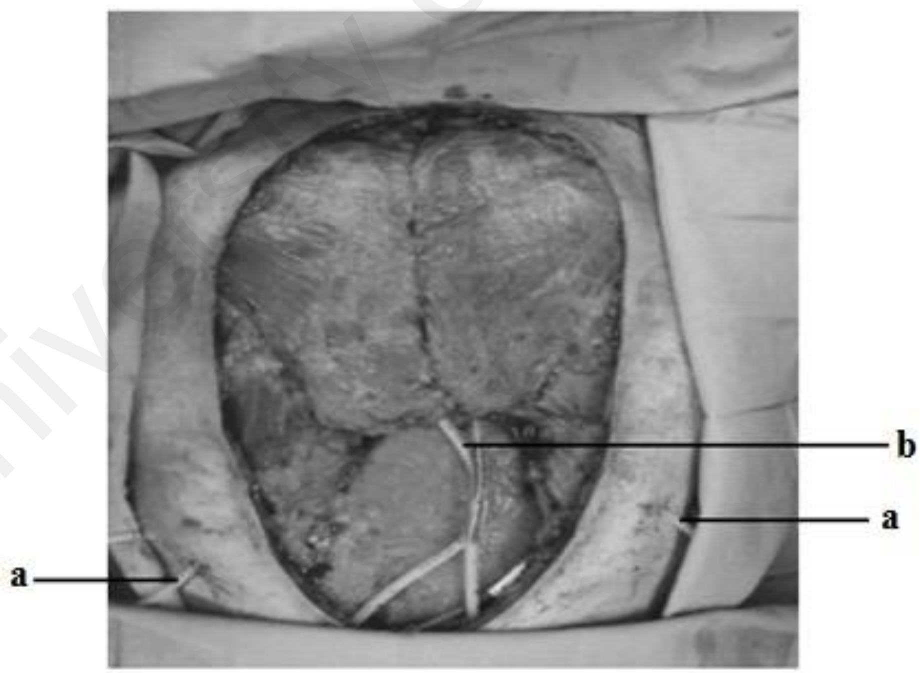

Figure 2.32: Advanced and sutured bilateral pectoralis flaps. (a) skin closure sutures(b) pectoralis midline sutures [Adapted from (Scholl L. et al., 2004)]

2.3 Critical discussion

Major sternal complications including non-union, DSWI, or dehiscence are infrequent after open heart surgery; however, they contribute to a considerable mortality and morbidity when they occur. More than 1 million sternotomy operations are performed yearly worldwide through which the risk factors (old age, diabetes, obesity and/or osteoporosis) are common and can result in various complications (Fedak P.W. et al., 2010). Researchers showed many innovations and high efforts to improve the sternal closure technique, but the ideal characteristics of sternal closure have not yet been met. Patients always seek the therapeutic option with less invasive procedures, pain and recovery period, nevertheless, sternotomy remains as the most preferred surgery after thoracic surgeries, especially cardiac surgeries. Hence, innovation is required not only to develop a sternal closure technique which eliminates sternal displacement, but also to provide chemotherapeutic effect and hence reducing the mortality and morbidity caused by postoperative complications. This section will discuss the pros and cons of the current techniques for sternal fixation as well as the characteristics of perfect adhesive cement for robust sternal fixation and reduced postoperative complications.

2.3.1 Pros and Cons of current techniques

Several closure devices and techniques were proposed; many of them were tested *ex-vivo* and *in-vivo* for the purpose of mechanical testing with forces that mimic the physiologic sternal forces and to develop more rigid sternal fixation devices capable of withstanding large forces with major risk factors such as osteoporosis, old age, obesity and/or diabetes patients.

The common technique that causes the instability of the sternum, postoperative pain and other complications is wiring technique which may result in various fractures in both halves of the fixed sternum, especially in cases of osteoporotic sternums. Studies (Grapow M. T.R. et al., 2012; Jolly S. et al., 2012) indicated the advantageous use of wiring techniques over the plating systems due to their practicality and cost effectiveness. Other techniques such as titanium plates were suggested and tested to reinforce the sternal stability; these techniques depend on the screws for anchoring the device into the bone. Other studies (Levin L.S. et al., 2010; Zeitani J. et al., 2008) suggested the use of Titanium Talon plates for further and improved sternal closure; however, their size, postoperative pain and long-term follow up contributes to major disadvantages of such fixation devices. Even though, all the proposed methods are useful whereas improvements in the sternal closure and its stability were clearly achieved, it should be considered that the use of wiring, Talon and/or plate-screw systems for the sternal closure in patients with acute or narrow osteoporotic bone might result in major complications. On the other hand, light techniques including bands, staples or wires are easy to use and cost effective but were not able to provide the sufficient support especially for patients with major risk factors.

Different cementing techniques were also considered. PMMA cements have been used due to their excellent mechanical strength. But, these cements are non-chemically adhesive, not conductive to bone regeneration, impose thermal and chemical challenges to host tissue during implantation and not resorbable (Kenny S.M and Buggy M., 2003; Provenzano M.J. et al., 2004). On the other hand, HA and TCP cements have received high concern because of their biocompatibility, isothermic properties and bioabsorption; however, they have poor mechanical strength and cannot withstand similar to the natural bone in different loading configurations, hence are not applicable for load bearing application (Doctors Research Group, Inc., 2009). The kryptonite cement has excellent *in-vivo* and *ex-vivo* (cadaveric) biocompatibility proved by the chemical analysis that demonstrated no potential or unexpected harmful chemical particles in the material (Doctors Research Group, Inc., 2009); this was also evident from the literature which studied the castor oil derived implantable polymers and demonstrated their relevant biocompatibility (Ohara G.H. et al., 1995); however, due to the poor adhesion ability of the cement for the soft tissue or cartilage, they cannot be tested on animal samples and may contribute to adhesive migration.

In order to facilitate wound healing post closure, GCS or vancomycin incorporation reduced incidence of SWI by approximately 50%, which could minimise patient discomfort, reduce the need for revision surgeries and increase savings for healthcare providers (Friberg et al., 2006b).

2.3.2 Perfect adhesive cement

The perfect adhesive cement for sternal fixation should have excellent mechanical, chemical and physical properties, including:

- **Suitable tensile strength**

In the first 24 h after median sternotomy; patients would be subjected to several stress forces causing sternal displacement and instability (Fedak P.W. et al., 2010). It is significant to develop an adhesive which provides the suitable tensile strength and withstand the maximum forces that might be imposed during coughing, sneezing or daily activities. Additionally, the repetitive cyclic mechanical tests must mimic the physiologic forces applied on all regions of the sternum whereas results must show no significant displacement or non-union.

- **Radiopacity**

After sternotomy, follow-up using imaging techniques such as X-Ray, MRI, SPECT or CT scans is necessary through which the sternal displacement, perfusion of adhesive in the host bone, proof of effectiveness of the adhesive in the long-term and delayed healing can be observed and investigated (Khaled Z., 2009). On the other hand, imaging techniques provide the ability to compare the proposed adhesive with the control group. Hence, it is significant for the adhesive to be radio-opaque and visible without exposing the patient to high dosages of radiation energy.

- **Injectability**

Ideal adhesive must be injectable into the site of the host bone and set rapidly to provide high strength and support for the surrounding bone by the process of successful degradation while causing no adverse effects (Young A., O.J, 2012).

- **Biocompatibility**

Biocompatibility is considered as the main biological property of all adhesive closures; the adhesive should release no toxic substances. Additionally, it should not cause infection, rejection or inflammatory reactions (Khaled Z., 2009).

- **Suitable viscosity**

Cement's viscosity represents the capacity of the material to flow into the porous network within the trabecular bone and as a result enabling effective interlock at the interface between the cement and bone. Typically, ideal cements represent lowest viscosity at the early time periods for injection and as the reaction starts, viscosity increases so that reducing the flow ability of the cement (Khaled Z., 2009).

- **Excellent working and setting times**

The ideal transition of the cement from the low viscosity state (injectable mixture) to rigid fixation cement is associated with excellent working and setting times. Both working and setting times can be evaluated from the cement's viscosity along with the healing time (Khaled Z., 2009). Typically, the setting time for sternotomy should be quick (10-15 min) in order to reduce the operation time, avoid cement migration and achieve the proper rigid fixation of both sternal halves.

- **Removable when necessary**

After sternal approximation, removal of excess cement that may expand out of the cortical bones is significant. Moreover, at some instances such as re-operation or infectious cases, removal of adhesive might be required as well. Hence, the ideal cement should be able to be removed easily while still providing the ideal physical and mechanical properties.

- **Cost effectiveness**

Other than the reproducibility (ability to produce large number of same cement), the ideal sternal adhesive must be affordable for all patients so that its use is not limited due to its high cost; this also requires unlimited supply of the cement source.

2.4 Glass Polyalkenoate/Ionomer Cements

2.4.1 Overview

GPCs or Glass Ionomer Cements (GICs) were first developed by Wilson and Kent in 1972 and were traditionally used in dental applications. Several studies (Jonck L.M. et al., 1989; Jonck L.M., and Grobbelaar C.J., 1990; Brook I.M. et al., 1992; Jonck L.M., and Grobbelaar C.J., 1992; Geyer G., and Helms J., 1997) noted various beneficial features for

GPCs. Additionally, their use in dental applications resulted in no significant adverse reactions in over 20 years (Hatton P.V. et al., 2006). Their main advantages in the field of dental applications included excellent biocompatibility, chemical adhesion to the mineral phase of the bone and tooth, lack of exothermic polymerization which is significant in avoiding overheat or damage of surrounding tissue, stability in the aqueous environment, osteoconductive activity due to the ability to exchange ions with the biological environment, lack of shrinkage, and release of clinically beneficial fluoride ions resulting in the prevention of dental caries/cavities (Wren A.W. et al., 2010; Hatton P.V. et al., 2006; Bertolini M.J et al., 2008); these advantages had resulted in the development of GPCs for various biomedical applications (Brook I.M and Hatton P.V, 1998). Despite these features, the use of conventional GPCs had been limited due to some disadvantages such as poor strength, brittleness (due to reduced wear resistance) and water sensitivity (Bertolini M.J et al., 2008). Researchers showed large efforts in order to enhance the properties of conventional GPCs using other methods of preparation to obtain modified glass formulations resulting in better mechanical properties (Knobloch L.A. et al., 2000). Also, the investigation into the addition of antimicrobial compounds and antibacterial ions had resulted in improved antibacterial properties and were significant due to the reported toxicity of released Aluminum ions (Wren A.W. et al., 2010; Polizzi S, et al., 2002; Reusche E. et al., 2001). Antimicrobial compounds such as chlorhexidine (Takahashi Y. et al., 2006) and tri-sodium citrate (Wren A.W. et al., 2009) and antibacterial ions such as silver (Ag) and Zn (Wren A.W. et al., 2009; Boyd D. et al., 2006; Coughlan A., et al., 2008) were investigated in the literature.

2.4.2 Synthesis

GPCs are formed when an acid/base setting reaction takes place between a polyalkenoic acid such as PAA and ion leachable glass powder in aqueous solution (Figure 2.33). The organic acid causes degradation of the glass particle surface resulting in release of ions such as Calcium (Ca^{2+}) and Aluminum (Al^{3+}). After that, the carboxylate groups of the polymer chelate with the released cations in order to crosslink the polyacid chains, so that the set cement has polysalt matrix within the glass particles (Bertolini M.J et al., 2008).

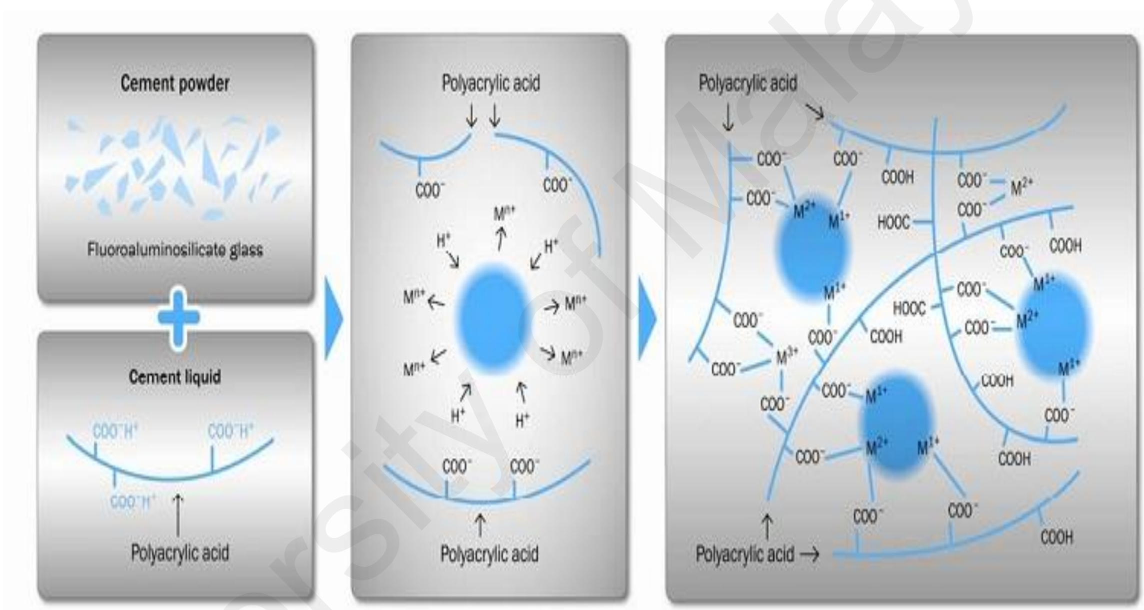

Figure 2.33: Setting reaction of conventional GPCs [Reproduced from (Lohbauer U., 2010)]

Basically, GPCs are derived from calcium silicate-alumino-fluoro glasses. These glasses are formed using the diffusion method, and depending on the required composition, the processing temperature ranges from 1200-1550 °C. Through this formation process, the fluorine is lost from the melt resulting in variable composition between batches. Alternatively, deficiencies in the use of conventional fusion method encouraged the use of soft chemistry, which resulted in the production of more homogeneous materials processed at lower temperatures. Besides, glasses with high melting points; that cannot be prepared using conventional melting methods are prepared using sol-gel process (Bertolini M.J et al., 2008) through which the chemical process converts the solution gradually into gel-like material containing both solid and liquid phases.

It can be generalized that many efforts and researches have been done to improve the chemical, mechanical and physical properties of GPCs using other types of glass powders; this shows that the modification of glass formulations may directly affect the properties of the cement.

2.4.3 Applications

2.4.3.1 Dentistry

Dental restorative materials have been subjected to different researches in the last decades. Until late 1970s, amalgam was mainly used for direct restorations while ceramics and gold were used as standard materials for indirect restorations. However, the use of amalgam was then limited due to its toxic and allergic potential caused by the release of mercury. Moreover, other limitations involved high need for biocompatible and tooth-colored restorations. As a result, further developments were stimulated to find dental cements as lining and luting materials whereas the aesthetic appearance is considered. In 20^{th} century, establishment of different cements, including zinc oxide eugenol in 1875, zinc phosphate in 1879 and silicate cement in 1908, was successful for the bonding of bridges, crowns, orthodontic bands, inlays and posts as filling and cavity lining materials (Lohbauer U., 2010).

In the early 1960s, hydrophilic materials showed evidence of being capable to wet and react with dentin and HA, resulting in durable bond with the structure of the tooth, and because HA is present in both dentin and enamel, calcium chelating reactants were most promising. Besides, researchers were investigating into water soluble polyelectrolyte systems containing polycarboxylic and citric acids. In 1963, researchers investigated, for the first time, into the potential use of polyacrylic acid through which a high quality adhesive is achieved with the dental tissue. The interest of using polyacrylic acid was due to its ability to chelate with calcium resulting in hydrogen bonds with organic polymers instead of collagen. Consequently, materials such as poly carboxylic acid (containing fluorides, fillers and copolymers) became available. Besides the main advantages of polycarboxylic acid including biocompatibility and high compressive strength; they have potential ion-binding to the HA phase of enamel and dentin. Silicate cements had resulted from the work done by Wilson and Kent through which they modified the ratios of Al_2O_3/SiO_2 in the silicate glass (Lohbauer U., 2010).

GPCs were first developed in 1972 for dental applications to serve as restorative and luting cements (Wren A.W. et al., 2010); the development was based on modifications of the setting properties of the cement by employing the effect of tartaric acid. Later, various developments were evolved in GPCs which resulted in various formulations of GPCs through changes in both the polycarboxylic acid and glass powder. In general, GPCs have led to various reproducable techniques with different improved formulations. In 2005, it was presented by Nagaraja and Kishore, that restorative material should have same characteristics as the natural tooth in all respects; it must possess the ideal properties and adhere perseveringly to the surrounding dentin and enamel. GPCs can satisfy these requirements. Even though, their major problem is weak toughness and strength for long-term filling and load-bearing applications (Lohbauer U., 2010), but, because both solid and liquid phase components are materials of variant chemical diversity (Nagaraja Upadhya P.

and Kishore G., 2005); GPCs has a significant potential for orthodontic and other medical applications resulting in potential need for further development.

2.4.3.2 Ear-Nose-Throat (ENT) surgery

Various diseases of middle ear require eradication operations. The ontological surgeons usually perform auditory canal and middle ear reconstruction operations using materials or tissues due to bone destruction (Geyer, G. et al., 1997). Ionocem was the first GPC developed to be used in bone surgery in 1989, specifically in the middle ear (Hurrell-Gillingham K. et al., 2006). Early *in-vivo* and *in-vitro* studies provided sufficient evidence for the biocompatibility and stability of GPCs in various ear reconstruction operations (Driscoll C. et al., 1998). In the study held by (Geyer G., and Helms J., 1997), their investigation involved patients undergoing middle ear reconstruction surgeries and generalized that GPCs behave as bone replacement materials and are well handled and tolerated by the body. Consequently, GPCs were employed in otorhinolaryngology (ENT) as low load bearing applications. However, variant concerns raised at the same time due to the toxicity of the GPC during *in-vivo* setting (Hurrell-Gillingham K. et al., 2006). Researchers had subdivided the effective use of GPCs in ENT operations into two major fields, namely, artificial ear ossicles and fixation cochlear implants. Hehl et al. used GPCs to bridge over the damaged incudo-stapedial joint, fix pistons to the longer process of the incus during stapedotomy operation and fix columellas to the head of the stapes (Hurrell-Gillingham K. et al., 2006). Geyer and helms, on the other hand, used GPCs to reconstruct the posterior wall of the external auditory canal and obliterate the mastoid cavity as well (Hurrell-Gillingham K. et al., 2006). GPCs are used for repairing ossicular chains, and for reconstruction of total or partial defect of the long process of the incus, body of the incus, head of the malleus and/or malleus handle. Successful reconstruction of defects in the long process of the incus was reported in other studies; however, it was reported that the use of GPCs for replacing external auditory canal was unsuccessful due to lack or extremely prolonged epithelialization of the GPCs' surface (Hurrell-Gillingham K. et al., 2006).

2.4.3.3 Orthopedics

As discussed earlier, GPCs were first introduced for dental applications. Then, due to their advantages including biocompatibility and adhesion to the mineral phase of the bone without shrinkage or heat up of the surrounding tissues as compared to acrylic based cements, researchers have been interested in developing this material as bone cement. Developments resulted in improvements of the mechanical properties such as biaxial flexural strength (50 MPa), compressive strength (200 MPa) and setting time (6 min); all of these enhancements were found significant and encouraged the use of GPCs in orthopedic procedures (Boyd D. et al., 2008). "The first study to evaluate the use of GPCs in orthopedics was done by Jonck et al. in 1989, in which a GPC was implanted in the tibia of baboons (Papio ursinus)" (Brook I.M and Hatton P.V, 1998). However, the biological response resulted from their study led to limitation of using GPCs in load bearing orthopedic applications. Hence, it was noted that GPCs perform better in the situations where the clinical success do not depend on the strength of the cement, however it provided better biological properties compared to acrylic based cements. Additionally, GPCs have various advantages over acrylic based cement such as adhesion and stability, so that it was used for reinforcement of osteoporotic femoral heads in order to enhance the stability of the implanted dynamic hip screws (Brook I.M and Hatton P.V, 1998).

Other studies demonstrated that the presence of Al^{3+} in the glass phase of GPCs have restricted their use in orthopedics due to their influence on bone mineralization (Wakayama I., et al., 1997; Polizzi S. et al., 2002) upon release. Besides, it has been involved in pathogenesis of degenerative brain diseases (Exley C., 1999; Guo G.-W., and Liang Y.-X., 2001; Boyd D. et al., 2008). Hence, various researches investigated into changes in the composition of the glass phase for possible use in orthopedic applications; they investigated into the incorporation of Strontium (Sr^{2+}), Zinc (Zn^{2+}) and Calcium (Ca^{2+}) that all showed positive therapeutic effect on bone, and also investigated into the necessity of Al^{3+} removal due to its disadvantages (Placek, L. et al., 2012). Additionally, Placek et al. investigated into the effective use of Gallium (Ga^{2+}) due to its therapeutic effect especially in treating bone cancer. Gallium also has immunosuppressive and anti-inflammatory effects as resulted from the animal models of human disease.

On the other hand, serious reverse events such as death were reported following skull base surgery through which large volumes of GPCs were applied in-direct contact with brain tissue or Cerebral Spinal Fluid (CSP). However, doubts have been regarded to the followed surgical approach and glass composition. Carter et al. reported that the influence of ions' release is not limited to the surrounding tissue but may far cause other consequences in the body (Hurrell-Gillingham K. et al., 2006). This demonstration provides evidence for the promising incorporation of Gallium in GPCs which would release during Sternotomy and provide therapeutic effect, hence are expected to reduce the DSWI complications and improve postoperative healing time.

2.4.4 Drawbacks of current iterations of GPCs

As compared to acrylic based cements, the strength of GPCs is a drawback in load bearing applications. However, the adhesion and physical properties mitigate this drawback (Brook I.M and Hatton P.V, 1998). Additionally, GPCs have limitations due to poor resorption, mechanical, and wear-resistance properties. But yet, various efforts have been made to improve these properties by applying different filler materials (Goenka S. et al., 2011).

Another drawback is that the composition is tissue and site dependent due to the fact that GPCs are bioactive materials, but not inert. The inappropriate application of GPCs to the biological system might result in adverse events; however, it is biocompatible bone cement and showed osteoconductive activity eliciting favorable clinical outcomes (Brook I.M and Hatton P.V, 1998). Furthermore, GPCs are sensitive to water during initial stage of cement setting, for example, the mechanical strength of GPCs decreases upon exposure to saliva; however, research presented that this drawback can be overcome by modifying the conventional GPCs using water soluble resin (Ana I.D. et al., 2003).

2.4.5 Role of Zinc (Zn^{2+}) in GPCs

The conventional GPCs have weak mechanical strength while their use in orthopedic applications is limited (Boyd D. et al., 2008). It was reported that Zn-GPCs have superior biaxial flexural strength over many commercial materials, hence are considered suitable for load bearing applications (Boyd D. et al., 2008). On the other hand, Zn^{2+} can result in increased bone mass due to its ability to increase deoxyribonucleic acid (DNA) of osteoblasts (Boyd D. et al., 2008). The mechanism of action for Zn-GPCs –bactericidal drug that induces bacterial cell death- starts with interaction with DNA's phosphorous moieties resulting in inactivation of DNA growth/multiplication (Ravishankar R.V. and Jamuna B.A., 2011). For example, Zinc oxide inhibits E.coli (food-borne bacteria). Authors investigated into the use of TriSodium Citrate (TSC) as an additive of CPCs to improve the strength of Zn-GPCs and their setting and working properties. However, specific concentration of TSC should be considered to avoid decreasing the biaxial flexural strength so that with 10 wt% TSC, better mechanical and handling properties are achieved (Boyd D. et al., 2008). Indeed, Zn^{2+} was considered for GPCs due to the disadvantages of Al^{3+} and its ability to function as both an intermediate and network modifying oxide in a similar way to Al^{3+}. (Boyd D. et al., 2008).

2.4.6 Role of Silver (Ag^{+}) in GPCs

Studies reported the effect of using Ag+ on physical and antimicrobial perspectives of GPCs; while explanations for their effect on mechanical properties were not elucidated efficiently. Silver ions within the Zn-GPCs cause disruption on the structure of the cement. Moreover, it was indicated that their release from the cement is not completely biocidal; however, they result in better release of zinc ions due to the structure disruption (Coughlan A. et al., 2008). Silver ions behave as antimicrobial agents by preventing the initial attachment between the bacterial cell and constructing materials; they bind to the negatively charged components in nucleic acids and proteins causing changes in the structure of the bacterial cell wall, nucleic acid and membranes so that affecting the viability of the bacterial cell (Coughlan A. et al., 2008). For example, they inhibit the activity of various types of bacteria such as E.coli, S. auerus, and B. subtilis (Ravishankar R.V. and Jamuna B.A., 2011). Coughlan A. et al. (2008) elucidated that by increasing the silver and decreasing the zinc ions within the GPC cement; the capability of antibacterial activity is improved significantly.

2.4.7 Role of Titanium (Ti) in GPCs

Titanium and its alloys are of wide interest in many medical applications due to their biocompatibility, corrosion resistance and high mechanical strength when compared with other metals (Wren A.W. et al., 2010). It also showed bioactive behavior and osteointegration with the bone under specific conditions such as heat and medium solution. The addition of Titanium to the glass phase of Zn-GPCs (Wren A.W. et al., 2010, 2011, 2011) was significant in improving the compressive and biaxial flexural strengths and hence facilitating its use for vertebral restoration/stabilization and other load bearing applications such as supporting hip implants.

On the other hand, its addition to Zn-GPCs has resulted in disruption and increment of the non-bridging oxygen (NBO) within the glass; this has resulted in significant reduction in Sr release, little change in Ca and Zn release and increased release of Si after 30 days (Wren A.W. et al., 2011). Moreover, authors (Wren A.W. et al., 2010, 2011) elucidated that Ti within Zn-GPCs increases both setting and working times when mixed with different molecular weights of PAA (E9 and E11). Specifically, it was reported that increasing the concentration of titanium in the glass phase results in higher degree of ion integration and particle dissolution; this results by the setting action of the Ti-Si-Sr-Zn-Ca glass through which Titanium reduces the availability of the zinc ion and hence longer setting and working times. However, the NC decreases (1.83-1.35) with addition of TiO_2 (Wren A.W. et al., 2010). Titanium particles (TiO_2) are involved in antimicrobial activities based on their stimulation by the near Ultra Violet (UV) light; this results in generation of strong oxidizing power when illuminated. Moreover, the photo-catalyzed TiO_2 particles generate active free hydroxyl radicals (-OH) that are responsible for the bactericidal activity (Ravishankar R.V. and Jamuna B.A., 2011). Different studies (Pham H.N. et al., 1995; Kim B. et al., 2003; Chawengkijwanich C. and Hayata Y., 2008) discussed the effective use of TiO_2 particles against bacteria and fungi such as Escherichia coli.

2.4.8 Role of Strontium (Sr^{2+}) in GPCs

Strontium ion replaces Ca ions (both are ionic radii) due to its radiopacific nature, antibacterial properties and its ability to assist in formation of healthy bones (Boyd D. et al., 2008; Curran D.J. et al., 2011). Boyd and Towler (2006) investigated into the effects of Strontium on the mechanical properties of Zn-GPCs and indicated that the addition of Sr on the expense of Ca increases the compressive and biaxial flexural strengths and give the opportunities for the cement to be used in load bearing applications.

Strontium –with low doses- is effective in inhibiting bone resorption and stimulating bone formation in both animals and humans. Sr has affinity to bones and is integrated into it by ionic substitution and surface exchange (Boyd D. et al., 2008). Furthermore, it was reported that Sr increases the activity of osteoblasts and decreases the activity of osteoclasts within the bone (Curran D.J. et al., 2011); osteoblasts are responsible for bone growth while osteoclasts are responsible for bone resorption. However, it was reported by Boyd and Towler (2006) that adding Sr on the expense of Ca would increase the setting time. Reports by researchers have highlighted that the inclusion of SrO into GPCs improves the antibacterial activity and also improves the therapeutic properties *in-vivo*. The study done by Guida et al. (2003) indicated that Sr is more associated to antimicrobial activity than fluoride, so that the antibacterial activity is improved with the addition of Sr. Additionally, it was reported that Sr reduces post-operative complications resulting from contamination or residual bacteria. For example, significant bacteriocidal activity was realized against A. Viscous type of bacteria only in the presence of Sr.

2.4.9 Role of Gallium (Ga^{3+}) in GPCs

In the studies done by Placek, et al. and Wren, et al., they formulated and tested a series of GPCs with E11 PAA at 50 wt% addition due to its suitability for orthopedic applications (resulted from the physical analysis of the E9 and E11 at 50, 55 and 60 wt% addition of PAA). The results were derived after 1, 7 and 30 days investigations and showed that the addition of Ga plays a significant role in increasing both compressive and biaxial flexural strengths when compared with the free-Ga control cements; however, results showed that no significant difference was obtained to analyze the effect of different Ga contents on the compressive and biaxial flexural strengths at 1, 7 and 30 days. Investigations by other authors (Warrell R.P. et al., 1984; Warrell R.P. and Bockman, 1989; Bernstein L.R., 1998) resulted in that Ga has antiresoptive activity that is significant in lowering the excessive loss of Ca and inhibiting bone resorption, hence avoiding osteoporosis and hypocalcaemia. Additionally, it was reported that Ga ions has an increasing effect on osteoblasts -without cytotoxic effect on bone cells- and inhibitory effect on osteoclasts. The effective use of stable Ga nitrate and radioactive Gallium for scanning various low growth rate tumors was also investigated due to its superior radioopaque nature when compared with Positron Emission Tomography (PET) scanning through which the uptake of F-fluorodeoxyglucose (FDG) by tumors resulted in limitations; low growth rate tumors include prostate cancer, hepatocellular carcinoma, indolent lymphomas and neuroendocrine tumors. The study done by Placek, et al. showed that the glass powder mixed with E11 (50 wt%) PAA provides better setting and working times than the E9 (50, 55 and 60 wt%) or E11 (55, 60 wt%) and elucidated its suitability for orthopedic applications. It can be concluded that the molecular weight of PAA (E9 and E11) plays a significant role in improving the handling properties of the cement while the addition of Ga showed insignificant impact on the handling properties. On the other hand, it was elucidated that the role of Ga in GPC's formation is unknown but is expected to perform a similar structural role as Al due to the same valence state (Wren A.W. et al., 2012).

The *in-vitro* efficiency of Ga as an antibacterial agent was reported (Valappil S. et al., 2008) along with various records elucidating its efficiency in clinical treatment including osteoporosis, hypocalcaemia of malignancy (Warrell R.P. and Bockman, 1989) and suppressing bone pain and ostolysis that are associated with bone metastases and multiple myeloma (Warrell, R.P. et al., 1987). Ga, in addition, has a therapeutic effect for bone cancer treatment (Ortega R. et al., 2003; Chitambar C.R., 2010). Moreover, it has immunosuppressive and anti-inflammatory activity in animal models of human disease (Chitambar C.R., 2010); in the study done by Collery, et al., it was reported that Ga was successful in inhibiting tumor growth by more than 90% in 6 out of 8 mice that had a solid tumor. Specifically, they reported the use of 30 to 60 mg/kg/24 hour of Gallium over 10 days of experiments (Wren A.W. et al., 2012).

Research by Placek, et al. and Wren, et al. supported the development of Ga-GPCs to be injected into bone cavities formed by removal of a tumorous/cancerous growth. They reported that the use of Ga in GPCs for orthopedic applications has the potential due to its chemotherapeutic effect upon release from the cement while the cement fills the cavity created by the surgical procedure. On the other hand, their study elucidated that Ga acts as a network modifier in similar pattern to Zn it is replacing within the glass; this was evident from the Differential Thermal Analysis (DTA) that yielded insignificant changes (6 °C) in transition temperature (Tg) between the mixed glass compositions (Table 2.7).

Table 2.7: Glass compositions (Placek L. et al., 2012)

	Lcon. (Control)	**LGa-1**	**LGa-2**
SiO_2	0.48	0.48	0.48
Ga_2O_3	0.00	0.08	0.16
ZnO	0.40	0.32	0.24
CaO	0.12	0.12	0.12

It can be concluded that the addition of Ga to the glass powder of GPCs would have the potential and particular interest for various orthopedic applications such as sternotomy to serve as a chemotherapeutic effect and improve the mechanical, chemical and handling properties of the GPC cement.

2.4.10 Critical discussion

Recently, high interest was granted to bioactive glasses in the development of novel biomaterials for different clinical applications such as bone tissue engineering. Bioactive glass materials were successfully used *in-vitro* and *in-vivo* and it was shown that particular ion dissolution from these materials provides chemotherapeutic effect. On the other hand, the composition of the bioactive glasses and the ability to change it resulted in numerous forms of composite materials or bone augmenting materials due to their advantages over other materials. They were added to PMMA based cements to improve the bioactive response. They were also used as coating material on the surface of hip stems (as an example of metallic implants) to form a more stable bond between the implant and the host tissue so that reducing the issues related to metallic implants such as corrosion and release of toxic ions.

Indeed, the use of conventional GPCs was directly related to dental applications; however, recent researches by authors have led to the development of these cements for orthopedic applications. Investigations have been mainly relevant to changes in the composition of the glass powder or the use of different molecular weights and concentrations of PAA. Additionally, authors have been also interested in improving the mechanical, handling and biological properties of those cements. Titanium was introduced in the glass phase of GPCs to replace silica and improve the cement's mechanical and biological properties. Furthermore, Zinc and silver ions were added to the glass phase due to their positive antimicrobial activity. Particularly, Zinc resulted in improved bone mass and bioactivity showing significant potential to be used in orthopedic applications as skeletal cement. However, the mechanical properties of Zinc have limited their use in load bearing applications. Consequently, Strontium was added to replace Calcium within the glass phase in order to enhance both therapeutic action and radiopacity. Strontium also has excellent antimicrobial activity *in-vitro*. However, the addition of Strontium must be monitored in order to avoid the negative impact on the mechanical and handling properties.

Various studies introduced the importance of Gallium ion and its compounds in medical field. Focus was given to the development and characterization of Ga-GPCs; however, cell culture and ion release studies are missing and need to be considered to identify the therapeutic effect and suitable concentrations. Ga-GPCs has an effective potential for various orthopedic applications due to the excellent properties of Gallium including therapeutic effect, immunosuppressive and anti-inflammatory effects, radioactivity and ability to enhance the mechanical and handling properties of GPC cements.

Ga-GPCs has the potential to be used as a coating that adheres to the material implant and releases Ga ions which can provide proper antibacterial and radioopaque properties. On the other hand, Gallium can be used as a coating for radiopharmaceuticals in order to obtain molecular tumor imaging due to its advantageous short half-life of about 68 min (Chitambar C.R., 2010) and its ability to overcome PET's associated limitations.

The objective of this study is to perform further required investigations for the suitability of using Ga-GPCs for sternotomy application.

CHAPTER THREE

METHODOLOGY

3. Methodology

3.1 Glass synthesis

Three Ga containing glass compositions (Control, LGa-1, LGa-2) were formulated. The Control was a Ga-free CaO-ZnO-SiO2 glass, LGa-1 and LGa-2 contain incremental concentrations of Ga at the expense of Zn (Table 3.1). Glasses were prepared by weighing out appropriate amounts of analytical grade reagents and ball milling (1 h). The mixture was then oven dried (100 ºC, 1 h) and sintered at 1500 ºC for 1 h in a platinum crucible and shock quenched into water. The resulting frit was dried, ground and sieved to retrieve a glass powder with a maximum particle size of <45 μm (Figure 3.1).

Table 3.1: Glass compositions (mol%)

	Control	LGa-1	LGa-2
SiO_2	0.48	0.48	0.48
Ga_2O_3	0.00	0.08	0.16
ZnO	0.40	0.32	0.24
CaO	0.12	0.12	0.12

3.2 Glass characterization

3.2.1 X-Ray Diffraction (XRD)

Diffraction patterns were collected using a Siemens D5000 X-ray Diffraction Unit (Bruker AXS Inc., WI, USA). Glass powder samples were packed into standard stainless steel sample holders. A generator voltage of 40 kV and a tube current of 30 mA were employed. Diffractograms were collected in the range $10^{\circ} < 2\theta < 70^{\circ}$, at a scan step size 0.02˚ and a step time of 10 s.

3.2.2 Particle Size Analysis (PSA)

Particle size analysis was achieved using a Beckman Coulter Multisizer 4 Particle size analyzer (BeckmanCoulter, Fullerton, CA, USA). Glass powder samples were evaluated in the range of 0.4 μm - 100.0 μm with a run length of 60 seconds. The fluid used was de-ionized water at a temperature range between 10-37 °C. The relevant volume statistics were calculated on each glass.

3.2.3 Scanning Electron Microscopy (SEM) & Energy Dispersive X-ray Analysis (EDS)

Backscattered electron (BSE) imaging was carried out with an FEI Co. Quanta 200F Environmental Scanning Electron Microscope (Oxford Instruments X-max, Netherlands). Additional compositional analysis was performed with an EDAX Genesis Energy-Dispersive Spectrometer. All EDS spectra were collected at 20 kV using a beam current of 26 nA. Quantitative EDS spectra was subsequently converted into relative concentration data.

3.3 Cement preparation

Cement samples were prepared by thoroughly mixing the glass powder (section 3.1) with E11 PAA (PAA-Mw, ~120,000 & <90 μm, Sigma-Aldrich, Canada) and distilled/de-ionized water on a glass plate (Figure 3.1a). The cements were formulated in a powder : liquid (P:L) ratio of 1:0.74 with 50 wt% additions of PAA; considering that the powder is the glass series and the liquid is the PAA and water mixture, where 1 g of glass powder was mixed with 0.37 g E11 PAA and 0.37 ml water. As can be seen in Figure 3.1b, complete mixing was undertaken within 20-30 s in ambient room temperature (23±1 °C). The sample is then kept in the incubator at 37 ºC and 30 to 80 % relative humidity (depending on the test) for 1 h before placing it into the distilled water and keeping in the oven for 1, 7 and 30 days prior to characterization and/or testing. The cements are now reported with the same nomenclature (Control, LGa-1, and LGa-2) that was assigned to the glasses that they are fabricated from.

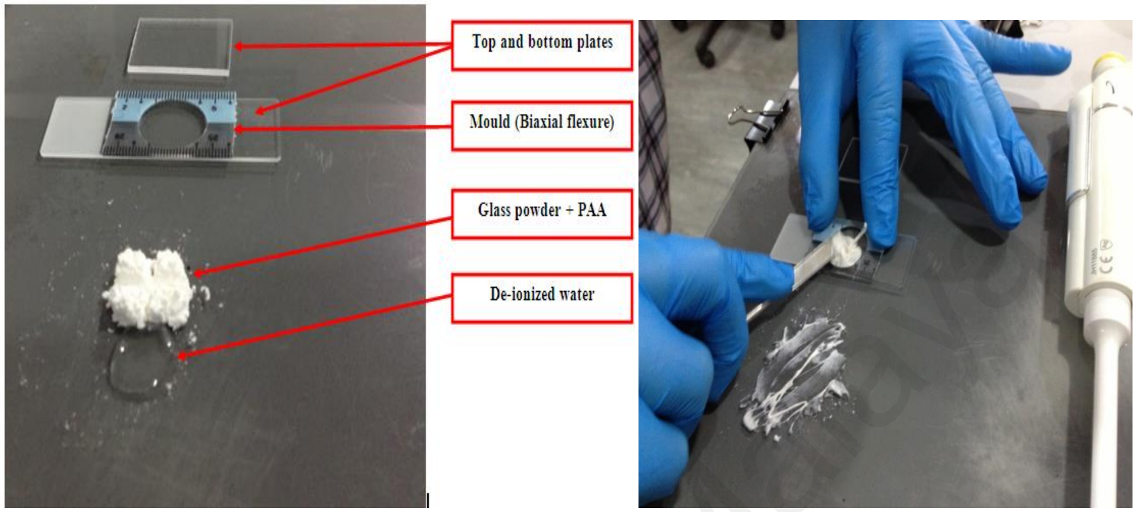

(a) (b)

Figure 3.1: Cement preparation (a) Preparations prior to the cement mixing (b) cement mixing and mould filling

3.4 Rheological properties

3.4.1 Net setting time

The net setting times (T_s) of 3 cement samples for each cement formulation were tested in ambient air (23±1 °C) according to ISO 9917 (Appendix A), and was defined as "the time elapsed between the end of mixing and the time when the needle fails to make a complete circular indentation in the cement" (ISO 9917-1:2007); when viewed using x2 magnification.

3.4.2 Working time

The working time (T_w) was defined as "the period of time from the start of mixing during which it was possible to manipulate the material without having an adverse effect on its properties" (Wren A.W. et al., 2012).

The T_w of 3 cement samples for each cement formulation were measured in ambient air (23±1 °C) using a stop watch according to the method described by Kao et al. (1996). A 28 g indenter with a flat end of 2.0 mm diameter was lowered vertically onto the surface of the cement beginning 1.0 min from the start of mixing at 23 °C. The indenter was allowed to remain for 5 s. This was repeated every 10 s until the needle failed to make a complete circular indentation in the cement when viewed using a low magnification hand lens.

3.5 Cement characterization

3.5.1 Fourier Transform Infrared (FTIR) Spectroscopy

Three cement cylinders shown in Figure 3.2 (6 mm high and 4 mm diameter) were prepared from each glass type for 1, 7 and 30 day FTIR analysis. The analysis required a powder with a mean particle size <90 μm. Hence, a pestle and mortar were used to grind the cement. The spectra were collected 5 times for each cement formulation in ambient air (23±1 °C).

The spectra were collected using an FTIR spectrophotometer-Thermo Scientific-Nicolet iS10 (Thermo Scientific, USA) equipped with a room temperature Deuterated Tri-Glycine Sulfate (DTGS) KBr detector. Analysis was performed in the wave-number ranging from 650 to 4000 cm^{-1} with a spectral resolution of 4 cm^{-1}. Sampling information is presented in Appendix B.

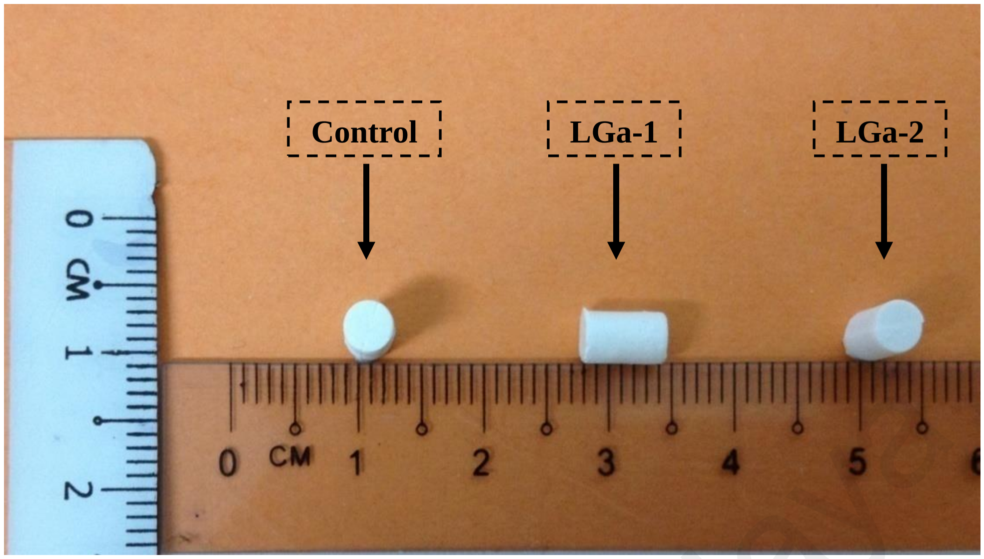

Figure 3.2: Cement samples used for FTIR spectroscopy

3.5.2 Ion release studies

GPC cylinders (6 mm high and 4 mm diameter, where n=3) were prepared from each glass type for the ion release profiles (Figure 3.2). Samples were then submersed in 10 ml of distilled water for 1, 7 and 30 days. The containers were rotated on a hybridization oven (Labnet ProBlot™ 12 Hybridization Oven, BioExpress, USA) at 37 ºC. The ion release profiles of cement samples were measured using the Agilent 4100 (Agilent technologies, Inc., USA) Microwave Plasma–Atomic Emission Spectrometer (MP–AES). MP–AES calibration standards for Ga, Ca, Zn and Si elements were prepared from a stock solution on a gravimetric basis. Three target calibration standards were prepared for each ion with 0.3, 0.5 and 1.0 Part Per Million (PPM) concentrations while distilled water was used as a blank. Samples for Ca, Zn and Ga analysis were diluted in a ratio of 1:10; that is, each 1 ml of concentrated sample was mixed with 10 ml of distilled water while samples for Si analysis were diluted in a ratio of 1:30. A pilot study was conducted to determine the appropriate ratio for dilution of all elements.

3.5.3 Contact angle measurement

The GPC discs shown in Figure 3.3 (1 mm high and 12 mm diameter mould, where n=5) were prepared from each glass type for the contact angle measurements. Each mould was filled with the cement within 1 min of mixing, compressed between PMMA plates and left clamped in the incubator at 37 °C and > 30% relative humidity. Not more than 60 min after the end of mixing, the cement samples were removed from the mold and placed in distilled water at 37 °C for a further 1, 7 and 30 days.

Measurements were taken using an OCA 20 optical contact angle measuring instrument (Data Physics Instruments GmbH, 70794 Filderstadt, Germany). The distilled water (d_w) was used to perform the contact angle analysis. Contact angle data were recorded in ambient air (25±1 °C) using a static sessile drop method 20 s post drop placement; a method described by Moshaverinia et al. (2011). The d_w drops (2 μL) were deposited with a micro-syringe (Data Physics Instruments GmbH, 70794 Filderstadt, Germany) on each sample (Figure 3.4).

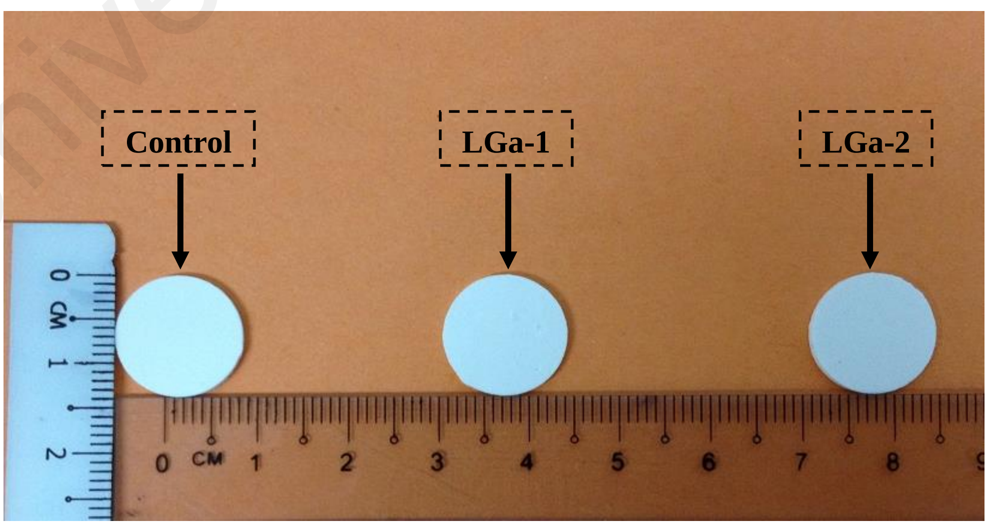

Figure 3.3: GPC disc samples used for contact angle analysis

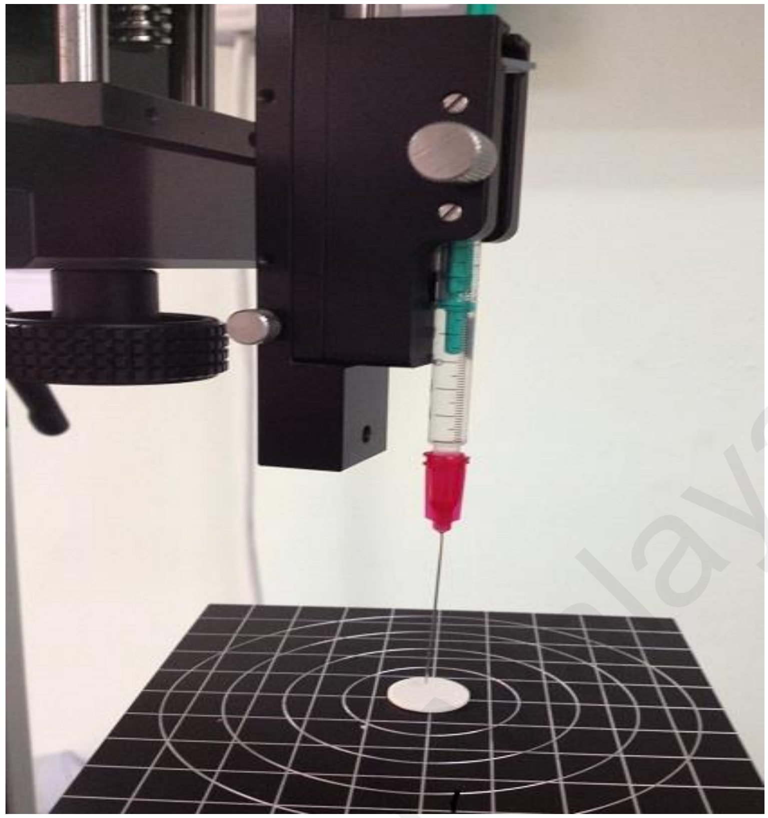

Figure 3.4: The micro syringe used to deposit the d_w drops on the GPC samples

3.5.4 Atomic Force Microscopy (AFM)

Cement discs (15 x 1 mm, where n=1) were prepared for the AFM. Measurements were taken at three different sites on each sample. Samples were tested after 1, 7 and 30 days. AFM was performed using Ambios Q-Scope™ 250/400 Nomad™ Series Atomic Force Microscope (Ambios Technology Inc., Santa Cruz, CA, USA). Intermittent-contact (wave) mode imaging was performed using a silicon nitride cantilever probe (Figure 3.5). A typical scan rate of 1 Hz and a scan size of 10 µm were used at a resolution of 256-512 pixels/line.

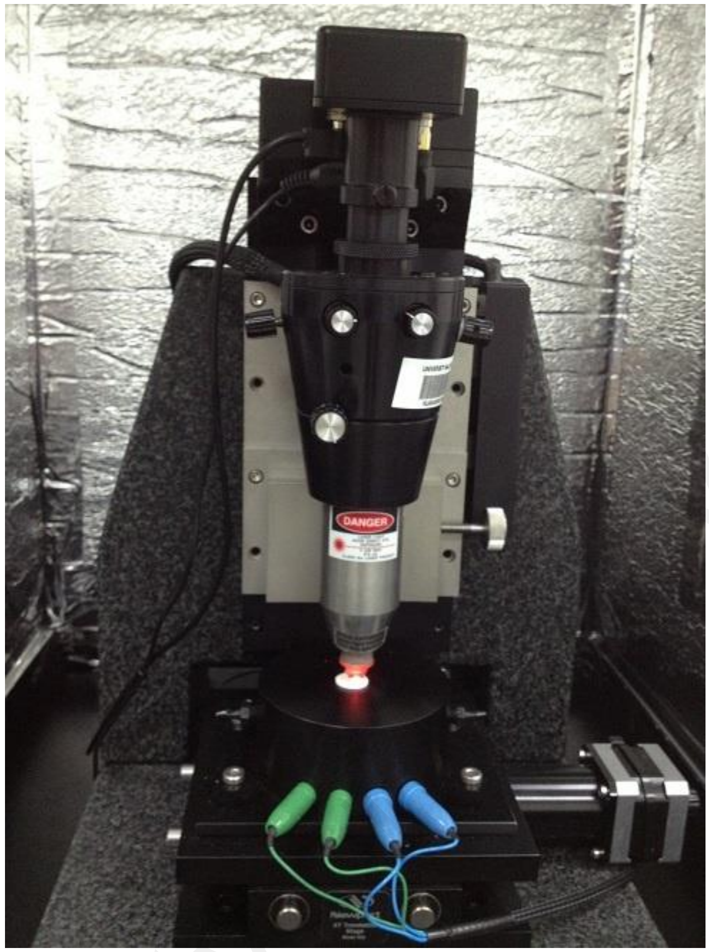

Figure 3.5: Non-contact cantilever probe

3.6 Mechanical properties

3.6.1 Compressive strength test

The compressive strengths (σ_c) of 5 cement samples from each cement formulation were evaluated in ambient air (23±1 °C) according to ISO9917 (Appendix B). Samples were tested after 1, 7 and 30 days. Testing was undertaken on an Instron Universal Testing Machine (Instron Microtester 5848, Instron Corp, USA) using a ±2 kN load cell at a crosshead speed of 1 mm.min^{-1} (Figure 3.6).

(a) (b)

Figure 3.6: (a) Experimental setup (b) Red arrow points toward the sample loaded in instron

3.6.2 Biaxial flexure test

The flexural strengths (σ_f) of 5 cement samples from each cement formulation were evaluated in ambient air (23±1 °C) by a method described by Williams J.A. et al. (2002). 1 mm thick discs were made in PMMA molds, measuring 22.5 mm diameter. Each mould was filled with cement within 1 min of mixing, compressed between PMMA plates and left clamped at 37 °C and > 80% relative humidity. Not more than 60 min after the end of mixing, the cement samples were removed from the mold and placed in distilled water at 37 °C for a further 23 h before testing.

Disc samples were tested after 1, 7 and 30 days. Testing was undertaken on an Instron Universal Testing Machine (Instron Microtester 5848, Instron Corp, USA) using a ±2 kN load cell at a crosshead speed of 1 mm.min^{-1}. The crosshead indentor is a knife edge of 2.5

mm diameter. The fixture type is a 3 point support allowing the load to be applied at the center of the disc. The discs are positioned equidistant around the 15 mm support span diameter, with only 3 mm of unsupported cement on each side of the support span (Figure 3.7). Timoshenko S. and Woinowsky-Kreiger S. (1959) presented a formula for maximum tensile stress (Eq. 3.1) to convert the load at break to biaxial tensile strength.

$$SS(MPa) = \frac{Load\ (N)}{t^2}\left[(1+v)\left\{0.485\ \ln\left(\frac{a}{t}\right) + 0.52\right\} + 0.48\right] \ldots\ldots\ldots\ldots.\ldots\ldots Eq. 3.1$$

Where

v is the Poisson’s ratio,

a is the radius of the support diameter, and

t is the thickness of the specimen in mm.

According to Akinmade A.O. and Nicholson J.W. (1995), the value of v for conventional glass ionomer cements is 0.30. Thus, Eq. 3.1 is reduced to Eq. 3.2:

$$SS(MPa) = \frac{Load\ (N)}{t^2}\left\{0.63\ \ln\left(\frac{a}{t}\right) + 1.156\right\} \ldots\ldots\ldots\ldots\ldots\ldots\ldots\ldots\ldots\ldots\ldots\ldots\ldots\ldots\ldots. Eq. 3.2$$

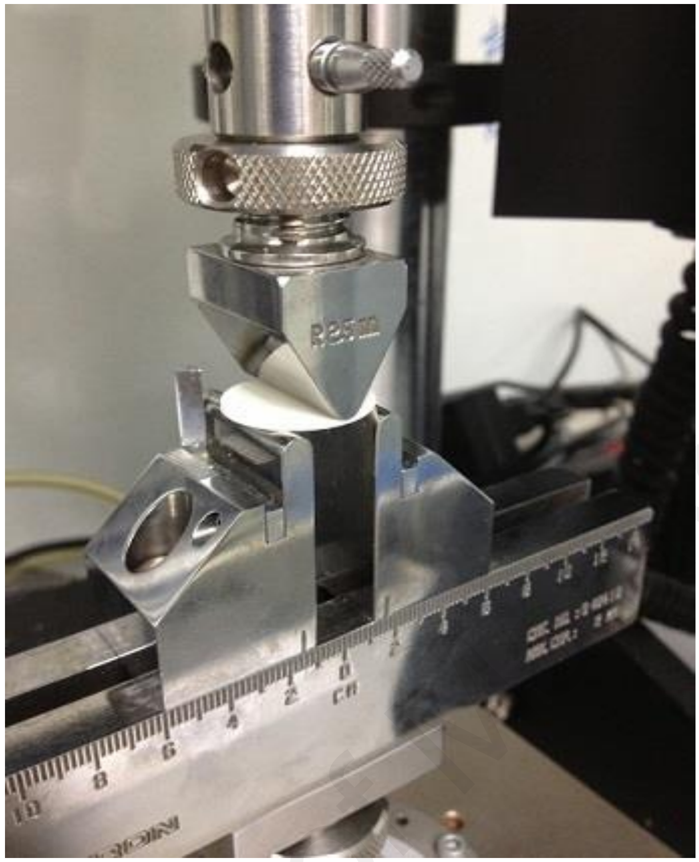

Figure 3.7: A GPC disc positioned on the support span whereas the knife edge crosshead indenter is used to apply the fixture force

3.7 Ex-vivo study

3.7.1 Sample collection and preparation

This study utilized a biological bovine sterna model (Figure 3.8). Sterna were harvested from freshly slaughtered bovines (Slaughterhouse & Meat Products, Shah Alam, Malaysia). All animals were in normal condition with ages ranging between 2 to 3 years. A midline incision in the sternum was made using an oscillating power saw (EFA Meat Processing Power, Maulbronn, Germany). The sternum halves were then collected and stored at -80°C.

Figure 3.8: The bovine sternal model

Prior to specimen preparation, sterna were stored at 0-5 °C for 24 h. The specimens were prepared by detaching the ribs and the surrounding tissues using a universal band saw machine (L-300, Luxo Corporation, NY, USA). Each sternum was utilised to obtain 5-6 specimens by cutting the sternal halves horizontally. Figure 3.9 shows the surface treatment and sample preparation steps. A surgical blade (Ribbel International Limited, KL, Malaysia) was used to remove any tissue remaining on the surface of the bone marrow (Figure 3.9a). The cement was then prepared and applied on the sternal halves using a spatula (Figure 3.9b). Labeled symmetrical halves were than approximated together, and clamped using cable ties (Butterworth Eng Tat Trading Sdn. Bhd., KL, Malaysia) (Figure 3.9c).

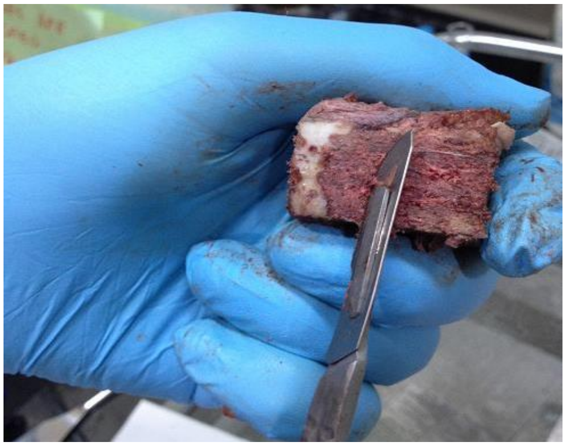

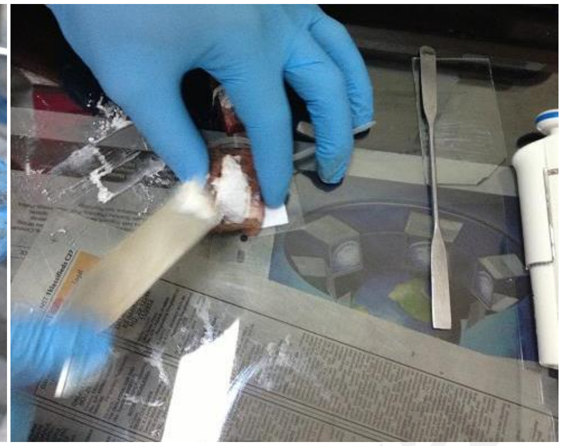

(a) (b)

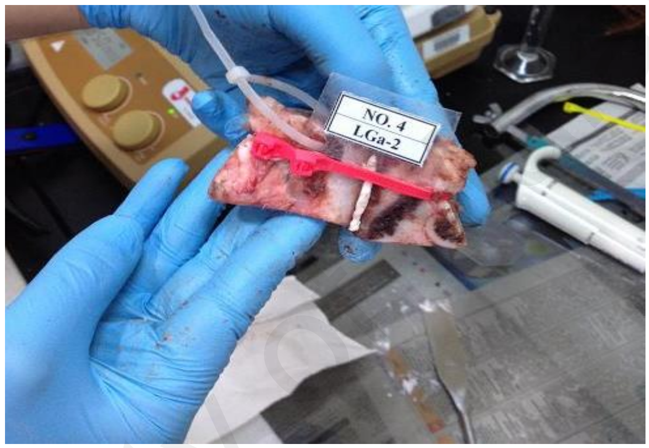

(c)

Figure 3.9: Sample preparation steps (a) surface treatment (b) Cement application (c) approximation, labeling and clamping

Five samples were prepared for each GPC type. Samples were then submersed in a single container of Phosphate Buffered Saline (PBS) dissolved in distilled water according to company instructions (Sigma-Aldrich, KL, Malaysia) with 1% formaldehyde (Mw~30, 37 wt% sol. in water, stab. with 10 – 15% methanol, Acros Organics, KL, Malaysia). PBS was used to mimic the physiological fluid because it is associated with fewer deleterious effects when compared with the distilled water (Steiner M., and Ramp W.K., 1988), while the formaldehyde was used to prevent the growth of bacteria or fungus (Van Haaren E.H., et al., 2008). The container was kept at 37 °C. The same procedure was followed for 1, 7 and 30 days' investigations.

3.7.2 Tensile failure test

A model was designed (Figure 3.10) for tensile failure test of the bovine sterna, where two correspondent holes were drilled into each side of the sternal halves to facilitate the insertion of brake cables.

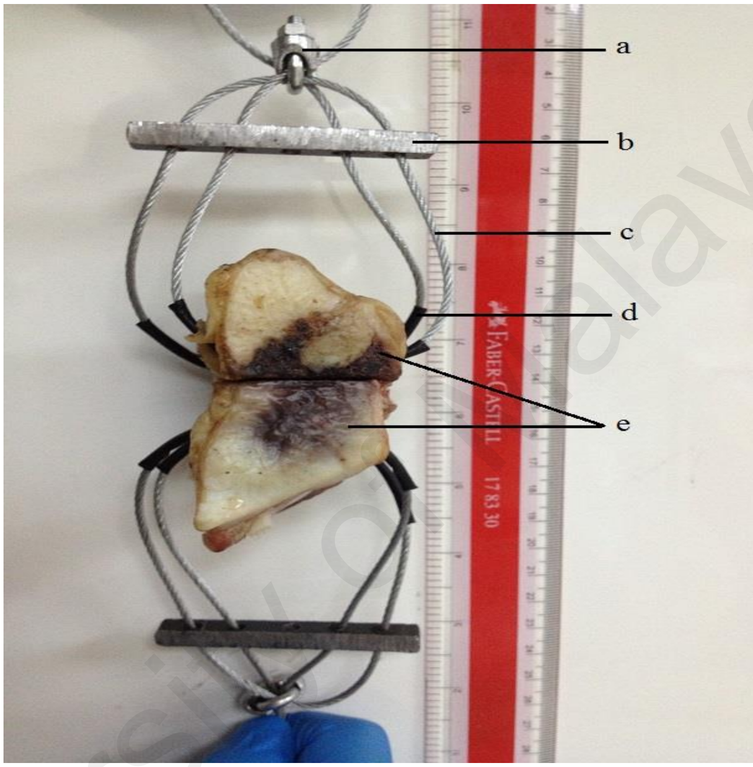

Figure 3.10: The design model for tensile failure test, (a) a nut to fix all wires together (b) metal rod to hold all wires and distribute tension force (c) bicycle's brake cable (d) a sheath to reduce the incidence of cable break through the bone (e) sternal halves

The tensile testing of 5 samples was performed in ambient air (23±1 °C). Samples were tested after 1, 7 and 30 days. Testing was undertaken on an Instron Universal Testing Machine (Instron Microtester 5848, Instron Corp, USA) using a ±2 kN load cell at a crosshead speed of 1 mm.min^{-1}. The nuts (Figure 3.10a) were directly gripped from the Instron jaws as can be seen in Figure 3.11. The tensile strength was calculated using eq. 3.3:

$$\text{Tensile strength (MPa)} = \frac{\text{Load at break}}{\text{original width} * \text{original thickness}} \ldots\ldots\ldots\ldots \text{ Eq. 3.3}$$ (Tranoudis I and Efron N, 2004)

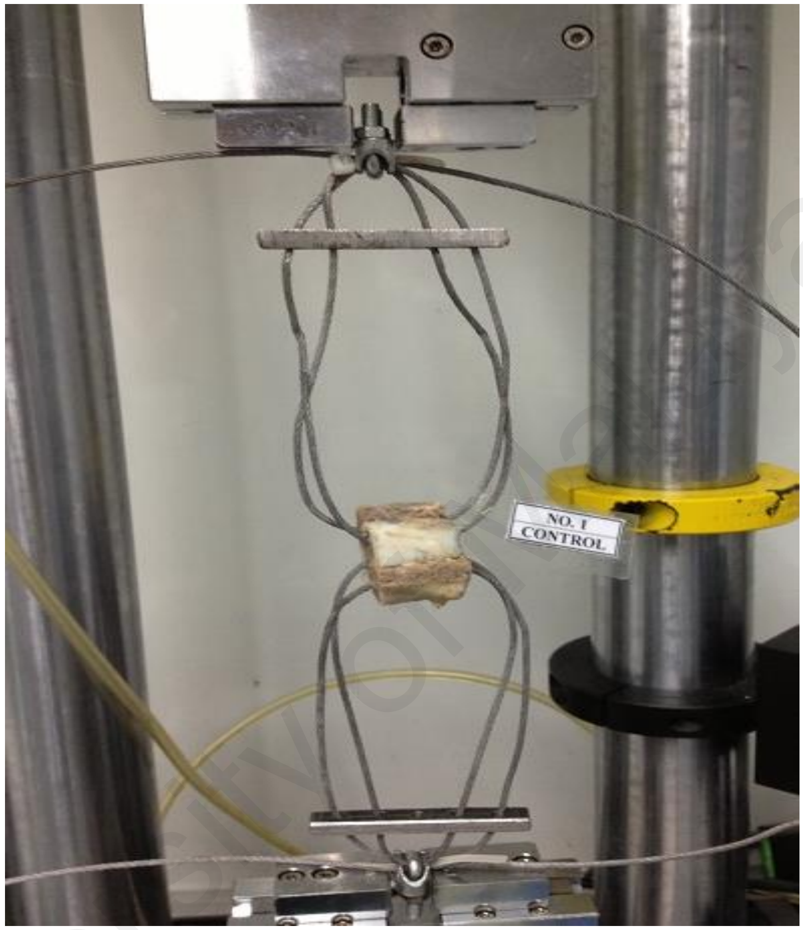

Figure 3.11: Connection of the sternal model to the Instron Jaws prior to the bone tensile test

3.7.3 Scanning electron microscopy & Energy Dispersive X-ray Analysis

Samples tested for the tensile strength were stored at -80°C for 1 h prior to freeze-drying them using the freeze dryer (Lyph-Lock 6L, Labconco Corp.) for 24-48 h. Prior to the SEM-EDS analysis, a universal band saw machine (L-300, Luxo Corporation, NY, USA) was used to prepare the samples for the SEM. Samples were cut vertically so that the adhesion between the cement and bone is seen from the internal side (a cross-sectional view). Samples from the freeze dryer were tested directly for the EDS with no other preparation techniques.

SEM-EDS analysis was undertaken with an FEI Co. Quanta 200F Environmental Scanning Electron Microscope (Oxford Instruments X-max, Netherlands). SEM images were collected at 12.5 kV. All EDS spectra were collected at 20 kV using a beam current of 26 nA. Quantitative EDS spectra were subsequently converted into relative concentration data.

3.8 Statistical analysis

One way analysis of variance (ANOVA) was used to analyze the data. *Post-hoc* Bonferroni test was used to compare the relative means and to report the statistically significant differences when $p < 0.05$. Statistical analysis was performed using SPSS software (IBM SPSS statistics 21, IBM Corp., Armonk, NY, USA).

CHAPTER FOUR

RESULTS & DISCUSSION

4. Results and discussion

4.1 Glass characterization

4.1.1 XRD

XRD was performed to determine if any crystalline phases are present within the starting phases of the glass. Figure 4.1 shows the XRD data. XRD confirmed that all fired glasses were fully amorphous; that no crystalline species are present in either Control, LGa-1 or LGa-2 during glass forming. Results from XRD show that any changes in the properties of the glasses will be related to the inclusion of Ga but not due to any phase changes in the forming glass (Wren A.W. et al., 2012).

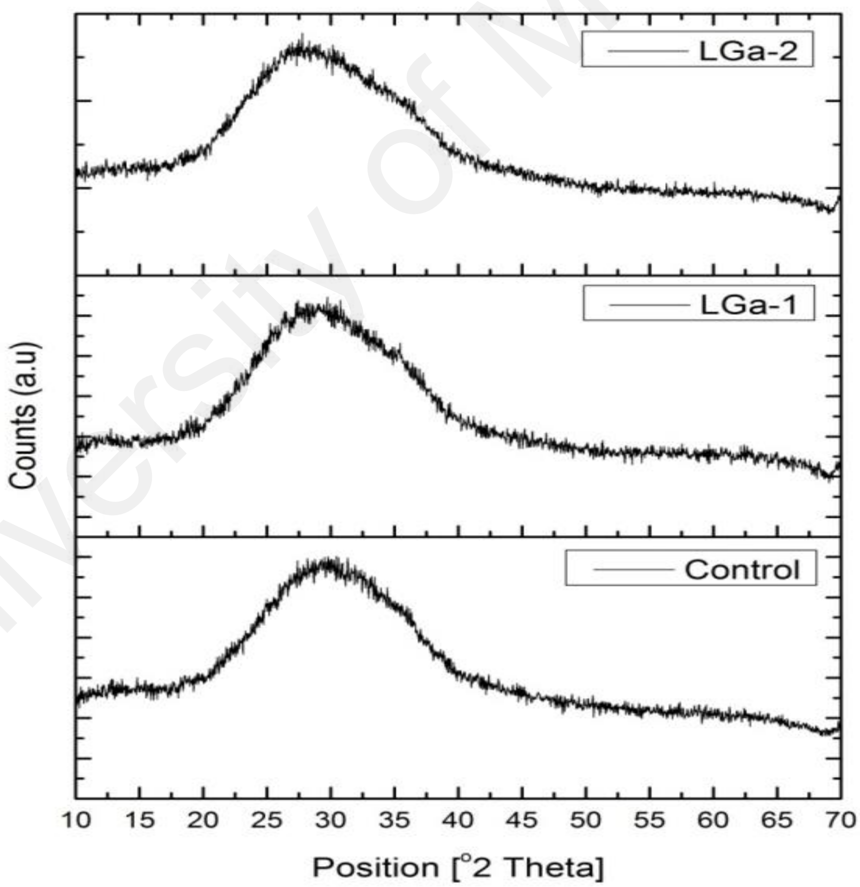

Figure 4.1: XRD patterns of Ga-containing glass series

4.1.2 PSA

Each glass was then subjected to PSA. Figure 4.2 shows the mean particle size for each glass. Control-glass was found to have the highest mean particle diameter of 4.71 μm. A similar value was obtained for the LGa-1 (4.44 μm) while LGa-2 had a mean particle diameter of 3.88 μm. The variation in the particle size is not expected to cause significant changes in the subsequent properties of the glasses since any changes will be resulting from the Ga inclusion. The particle size is important whereas the lesser is the particle size, the quicker is the dissolution resulting in a quicker set. Furthermore, it was found that Ga acts as a network former and a network modifier in the glass series. Acting as a network modifier was found to be important so that the substitution of Ga with Zn does not exhibit any change (Wren A.W. et al., 2012).

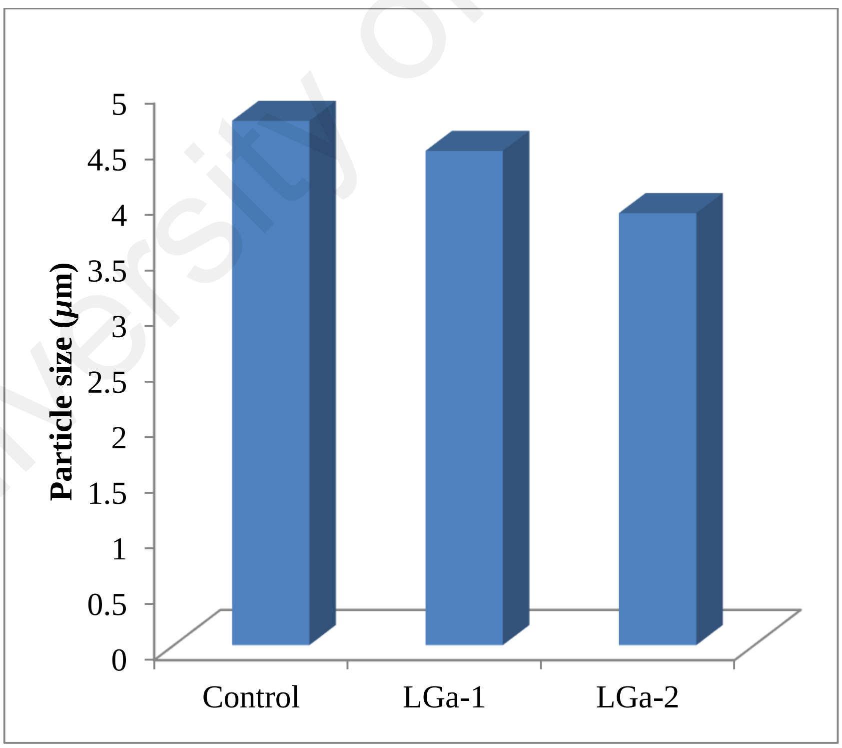

Figure 4.2: PSA results representing the mean particle size

4.1.3 SEM & EDX

Each glass was subjected to SEM and is presented in Figure 4.3. The Control-glass (Figure 4.3a) has larger particle size than LGa-1 (Figure 4.3b) and LGa-2 (Figure 4.3c). Further, Control-glass was found to be more granular than LGa-1 and LGa-2 hence matching with the results from the PSA. Similar results can be seen for LGa-1 and LGa-2 except that the LGa-2 has more particles with smaller particle diameter than LGa-1.

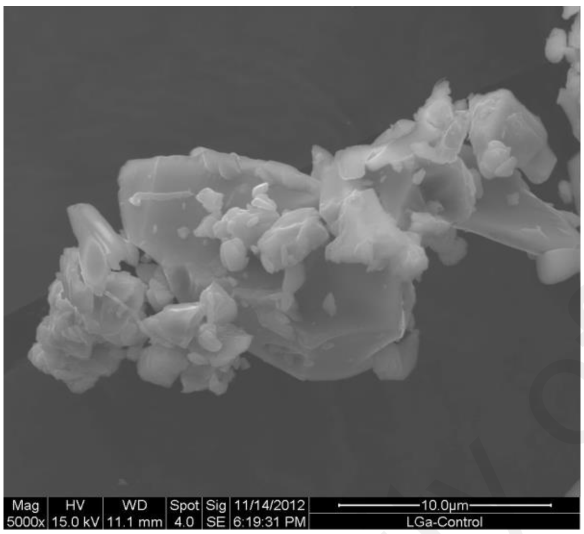

(a)

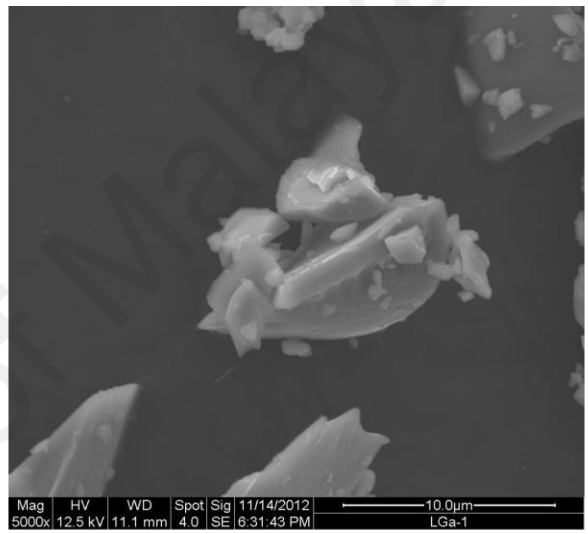

(b)

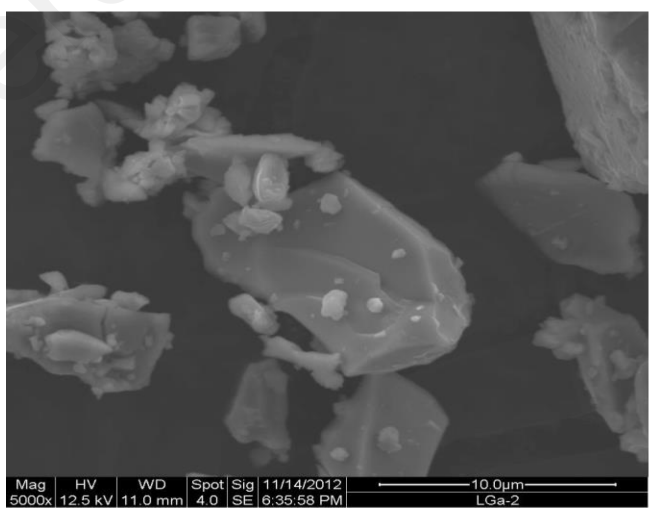

(c)

Figure 4.3: SEM images (a) Control-glass (b) LGa-1 (c) LGa-2

Results from SEM images prove the network connectivity (NC) results presented by Wren et al. (2012), who presented that Ga acts as a network former for LGa-1 and LGa-2 by substituting the Zn.

EDX was carried out to confirm the presence of the ions that were incorporated in the starting glass. Figure 4.4 presents the EDS scan peaks for the Control-glass (Figure 4.4a), LGa-1 (Figure 4.4b) and LGa-2 (Figure 4.4c). Peaks show the composition of each glass and confirm the starting formulation of the glass whereby it was found that the Control glass contains Zn, Si, and Ca. On the other hand, LGa-1 (Figure 4.4a) and LGa-2 (Figure 4.4b) were found to have the same elements but with the addition of Ga.

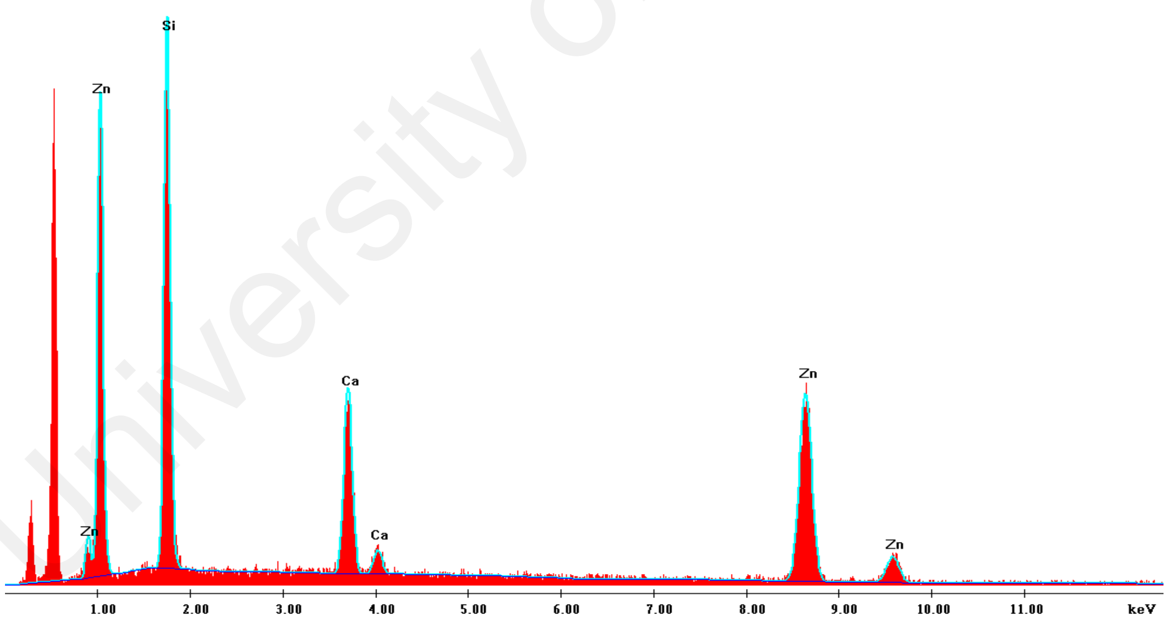

(a)

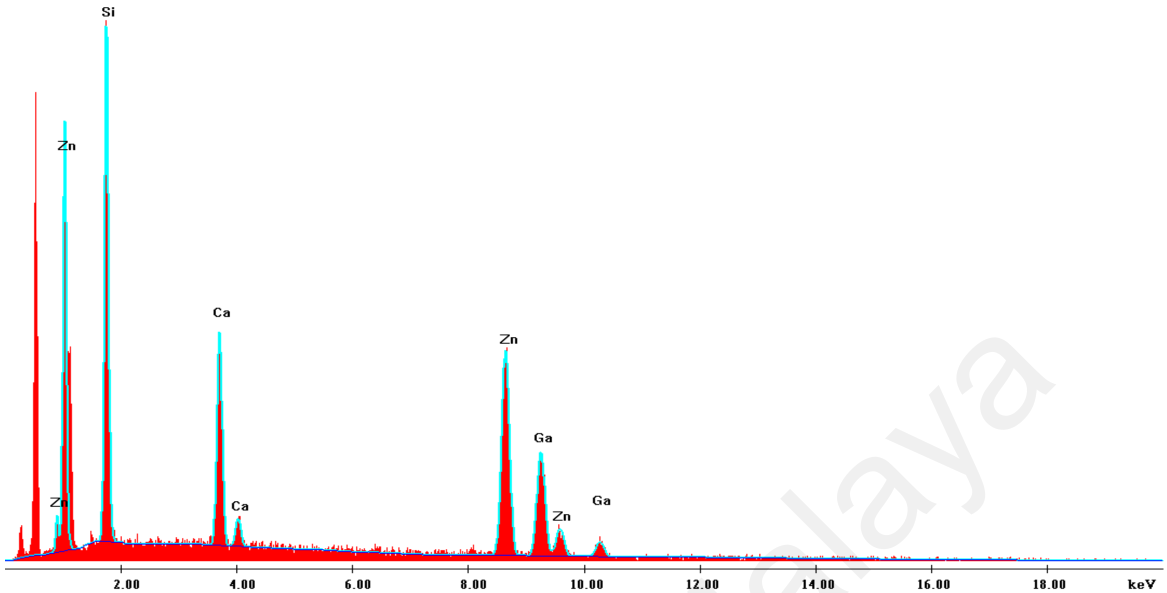

(b)

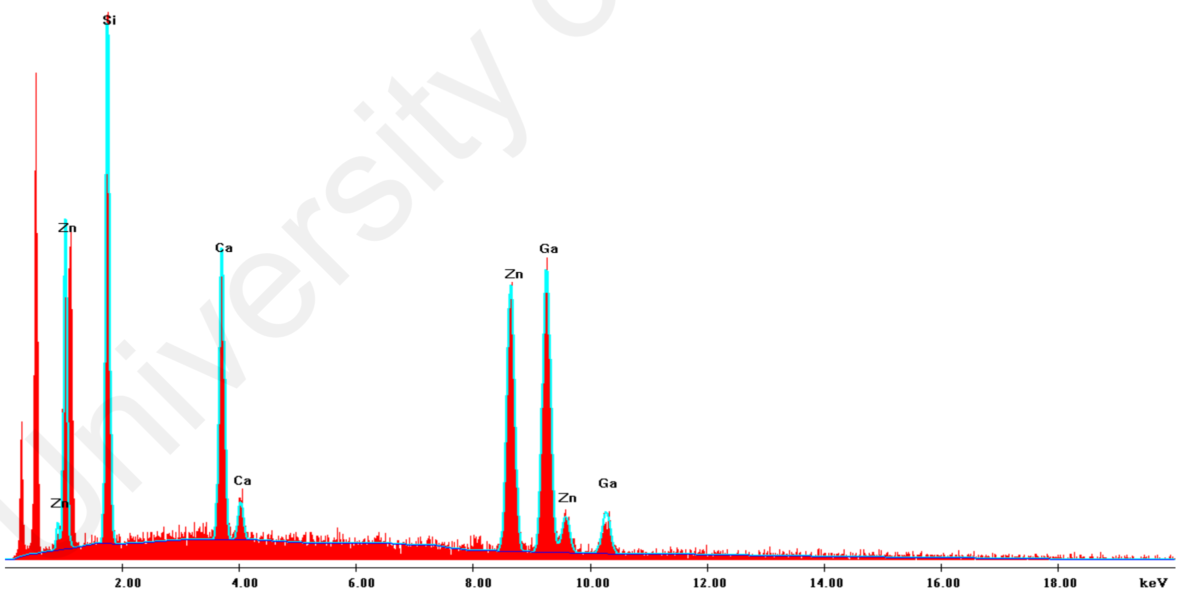

(c)

Figure 4.4: EDX survey (a) Control-glass (b) LGa-1 (c) LGa-2

4.2 Rheological properties

The rheological properties of the cements formulated from these glasses were of significant importance. Those properties were assumed to provide some indications relevant to the role of the Ga^{3+} ions in changing the working and net setting times.

4.2.1 Net setting time

The setting time is the time required by the cement to become in a solid form. According to the ISO standard for dental based cements (Table A.1), a setting time between 1.5 and 6 min is required. During the surgical operation, considering sternotomy, the surgeon needs sufficient time to apply the material on the sternum before setting occurs. However, there is no standard for these cements considering the orthopaedic application but a setting time longer than 6 minutes might result in some complications such as cement movement and inability to control the incision. Therefore, it was important to find the effect of Ga inclusion on the net setting time considering the sternotomy surgical operation. Figure 4.5 presents the net setting times of the cement series. T_s increased from ~ 113 s for Control to 254 s for LGa-2. There was a statistically significant difference ($P < 0.05$) between the three glasses in the series when tested for the T_s. A significant increase in the T_s was also realized with the addition of Ga; increased from ~ 242 to 254 s for LGa-1 and LGa-2 respectively.

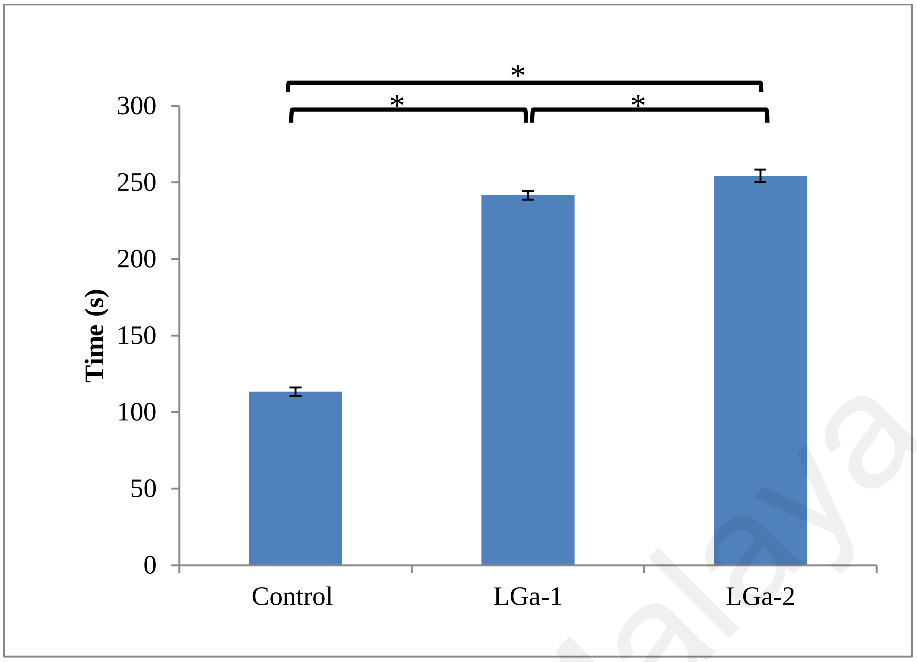

Figure 4.5: Net setting times. Stars and bars show statistical significance ($p < 0.05$).

4.2.2 Working time

The working time is the time through which the material can be manipulated. There is no standard for the normal working time. However, considering the sternotomy application, the working time should be within the range of a few minutes to allow the surgeon to apply the cement on the whole sternum along with the ability to manipulate its content on the sternum. Figure 4.6 presents the working times of the cement series. Similar to the net setting time, the T_w increased, from ~ 75 to 137 s, as the concentration of Ga increased from 0.00 to 0.16 mol%. There was a statistically significant difference ($P < 0.05$) between the three glasses in the series when tested for the T_w. A significant increase in T_w was also realized with the addition of Ga; increasing from ~ 117 to 137 s for LGa-1 and LGa-2 respectively.

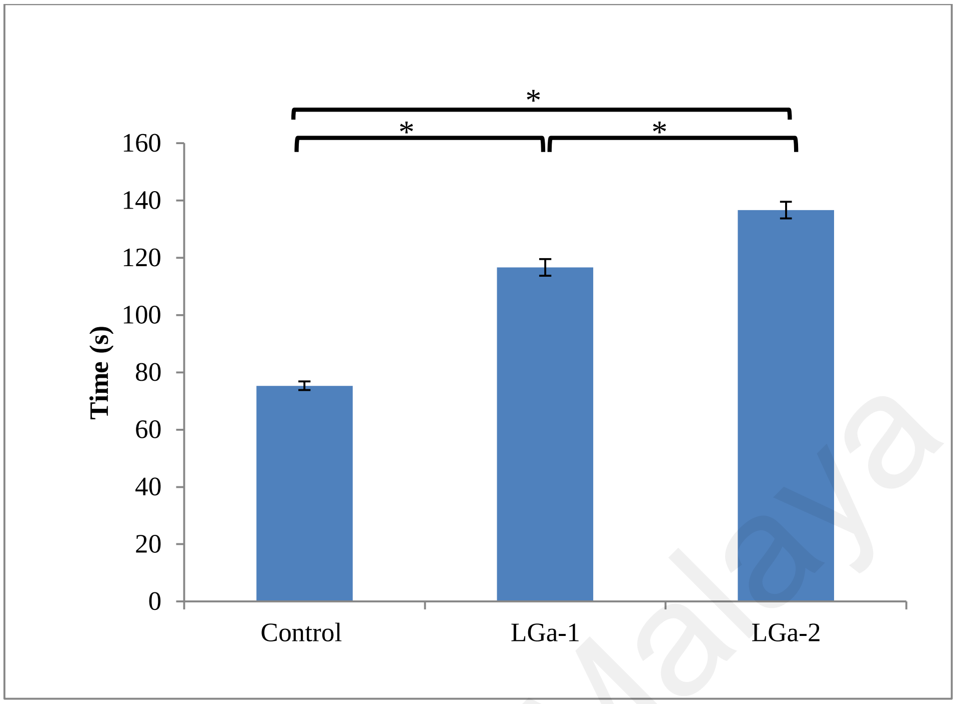

Figure 4.6: Working times. Stars and bars show statistical significance ($p < 0.05$).

Results from the rheological properties indicate that the addition of Ga to the glass phase provides a material with handling properties more suited to sternotomy applications since the T_w (~75 s) and T_s (~113 s) of the Control glass are considered short.

4.3 Cement characterization

4.3.1 FTIR spectroscopy

FTIR was conducted to investigate the reaction kinetics between the glass powder and the PAA. FTIR spectra obtained for the grounded cement powder at 1, 7 and 30 days post cement preparation and storage in distilled water are shown in Figure 4.7a-c respectively. Similar trends were observed for the Control, LGa-1 and LGa-2 cement series through GPC maturation. The broad peak at 3200 to 3300 cm^{-1} was observed for all spectra (Figure 4.7), which is assigned to the O-H stretch of adsorbed water (Driessen M.D. et al., 1998). Figure 4.7a shows that the addition of Ga resulted in a greater water absorption in LGa-1 and LGa-

2, ~85 % Transmission (%t), when compared with the Control glasses, ~95 %t. Figure 4.7b shows that the water absorption increased for the Control (~85 %t) with the cement maturation over 7 days while it remained constant for LGa-1 and LGa-2 (~85 %t). However, an increased intensity (~70 %t) of O-H group was observed for 30 day measurements (Figure 4.7c), implying that all cement formulations increased O-H content when aged. The shoulder peak at ~1700 cm^{-1} (Figure 4.7a) is assigned to the un-reacted carboxyl (COOH) functional group in the PAA (Crisp S. et al., 1974). In the 1 day samples, the Control does not display this peak while both LGa 1 & 2 samples do. Thus the presence of Ga in the 1 day samples inhibits COOH reactions resulting in the presence of un-reacted COOH functional groups. The presence of un-reacted COOH in the 1 day LGa samples (Figure 4.7a) implies that there would also be increased levels of un-reacted COOH in these samples during the mixing and working stages, which would explain the increased wettability of these samples during the working and setting regimes (Wilson A.D., 1974; Powis D.R. et al., 1982). This is not the case for the 7 and 30 days LGa samples, which show an increase in transmission in the 1700 cm^{-1} wavenumber. Thus, the level of un-reacted COOH diminishes irrespective of Ga content, which may indirectly imply an increase in cross-linking in the cements. Although the level of cross-linking can be more directly measured using the 1550 cm^{-1} and 1400 cm^{-1} peaks. Both Zhang et al. (2008) and Rajamathi et al. (2005) assign the 1550 cm^{-1} peak to the asymmetric stretching vibration of the carboxyl COO, which could be assumed to be an asymmetrically bonded COO-*X* molecule, where *X* represents a possible metal cation, due to its asymmetric nature. This was shown to be the case by Matsuya et al. (1999) where they attribute this peak to the asymmetric vibration between the bonded COO^- and Ca^{2+} ions. In an in-depth FTIR study by Maltsev and Shevelkov VF (1972) this peak is assigned to the Ga ions, which most likely is the Ga content of the COO-Ga (metal carboxylate) molecule. Thus, it is safe to assume that this peak highlights the level of cross-linking (bonding) between the dissociated COO- group and metal cations, such as the Ca^{2+}, Ga^{2+} and Zn^{2+}, to form a metal carboxylate and thusly can serve as an indicator for increased or decreased cross-linking in the cements (Crisp S. et al., 1974). The intensity of the ~1550 cm^{-1} peak of the 1 day samples was found to be relatively similar, with the Control and LGa-2 samples having 89 %t while the LGa-1 samples show 90 %t, thus there is effectively no difference in the level of cross-linking between these samples at 1 day. At 7 days, the LGa samples experience relatively no change in %t, while the Control sample experiences a drop in %t with an increase in the peak height, of 3 %, to 86 %t. Thus, there is a slight increase in the level of bonded COO- in these samples. At 30 days, all samples experience a drop in transmission at this wavenumber with the Control dropping to 72 %t and the LGa 1 & 2 samples dropping to 78 %t. Thus, ageing the samples resulted in an increase in the level of reacted COO-. The peak at ~1400 cm^{-1} is assigned to the symmetric metal carboxylate (Cook W.D., 1982; Young A.M. et al., 2000) in much the same manner as the ~1550 cm^{-1} peak is for the asymmetric metal carboxylate ion. In the 1 day samples, the Control, LGa-1 and LGa-2 present similar peak intensities with 91, 93 and 92 %t. After 7 days the only change experienced by this peak is in the LGa-2 samples with a slight decrease in peak height to 94 %t. The real change occurs in the 30 days samples. The Control experiences the largest increase in peak height with an increase to 82 %t, while the LGa 1 & 2 samples experience a drop in transmission to 86 %t. In a similar manner to the 1550 cm^{-1} peak, as the samples ages, the level of symmetric COO and metal ion bonding increases, effectively increasing the level of cross-linking in the cements. The 1070 cm^{-1} peak represents the Si-O-Si bridges (Tsybeskov L. et al., 1994) of the cements and as such its relative increase or decrease in intensity correlates to an increase or decrease in the formation of bridging oxygens. Over the full 30 days, both LGa 1 and 2 samples experience negligible change in the transmission levels of this peak and remain constant at 94 cm^{-1} and 93 cm^{-1} respectively, implying that the number of Si-O-Si remains constant when ages. The Control samples experience fluctuation over the 30 days, ranging from 87 %t, 89 %t and 82 %t for the 1, 7 and 30 day samples, respectively. Thus there is effectively no change in the %t at this wavenumber until the 30 day samples, implying that the level of Si-O-Si bonds increases when aged in water.

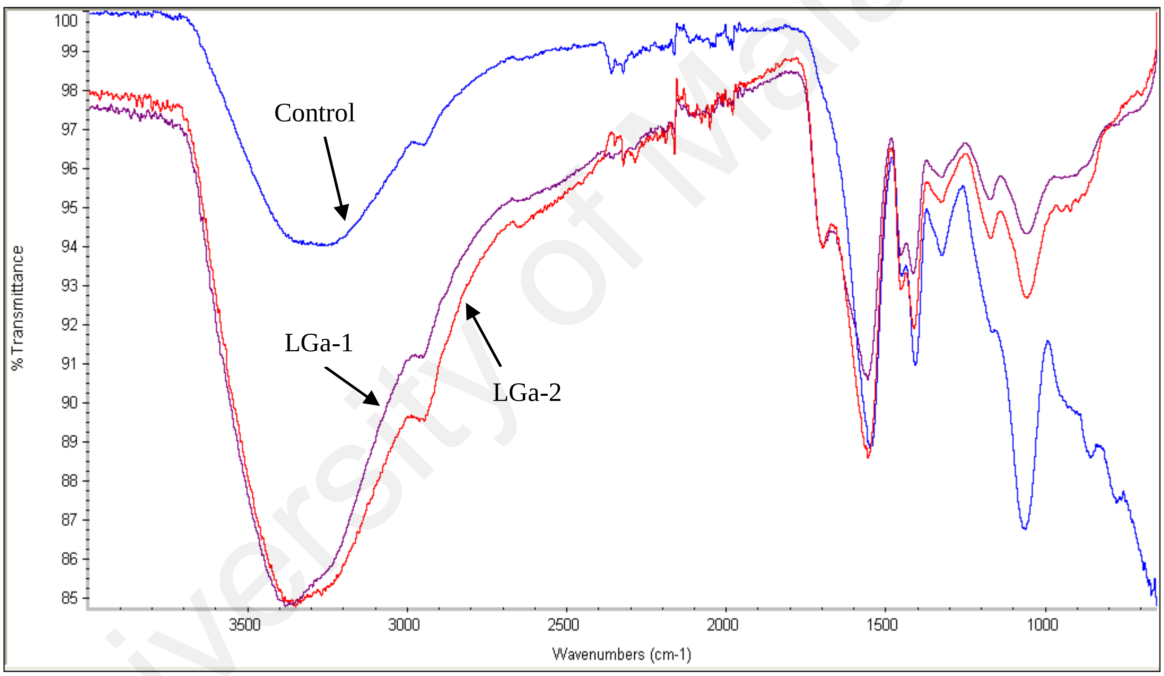

(a)

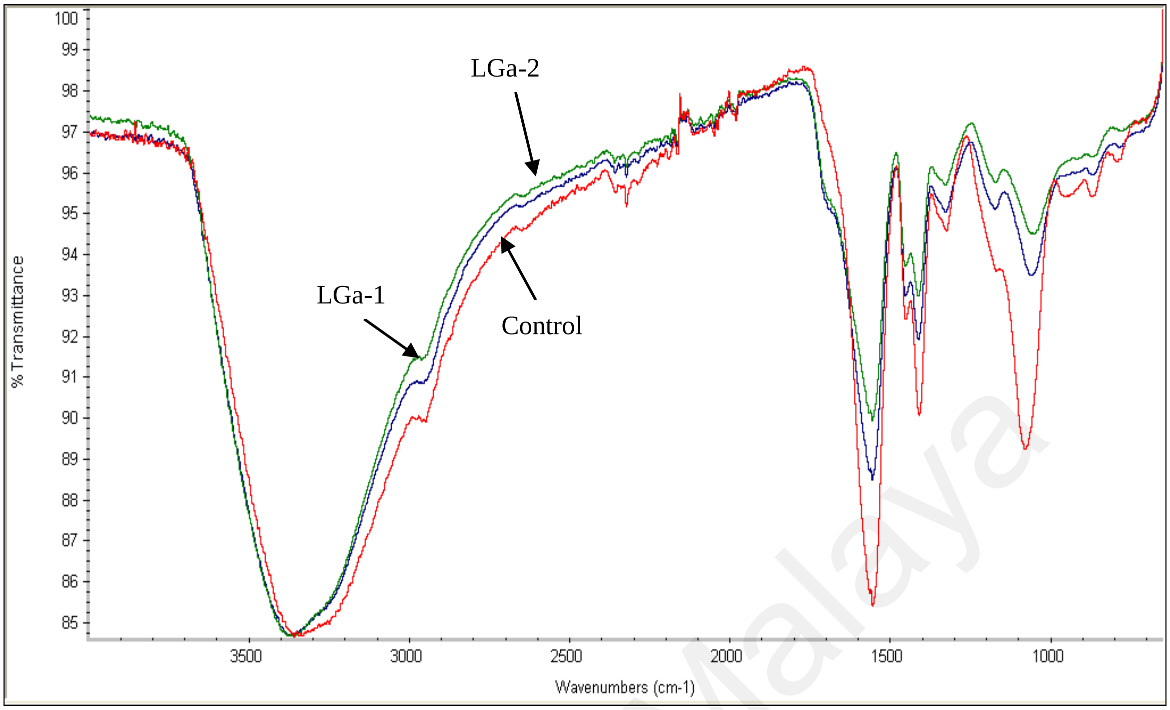

(b)

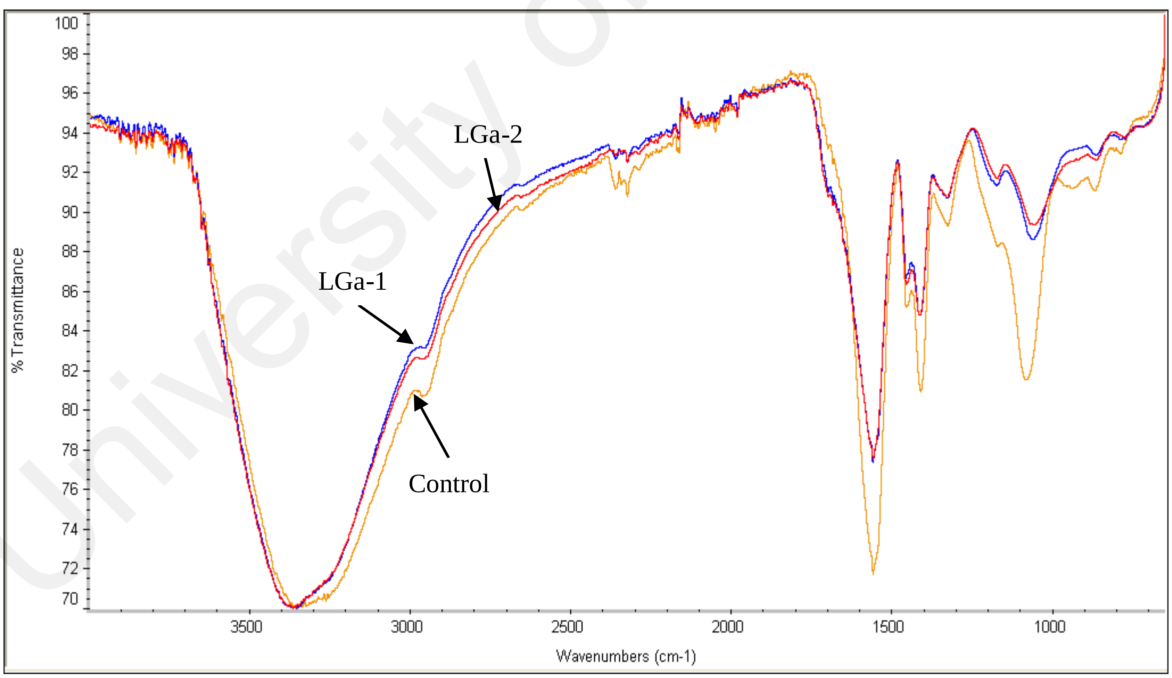

(c)

Figure 4.7: FTIR spectrum of the cement series over (a) 1 day (b) 7 days and (c) 30 days post cement preparation

4.3.2 Ion release studies

Ion release studies were performed in order to evaluate the solubility of the cement series in relation to Ga incorporation into the glass phase. These studies are significant to determine the therapeutic effect that these cements might have upon implantation into the skeleton. Figure 4.8 shows the release profile of Ca^{2+} over 1, 7 and 30 days post cement preparation. Ca^{2+} release was found to increase for 1 and 7 days for all cement series and for 30 days for Control and LGa-1 cements. The maximum release of Ca^{2+} ions was ~5 ppm for LGa-2 at 7 days evaluation. It can be noted that the Ca^{2+} release profile increases with the addition of Ga. However, similar results were obtained for the Control and LGa-1 cements. This is expected due to the low concentration of Ga (0.08 %mol) in the LGa-1 cement in comparison with the 0.16 %mol incorporated for the LGa-2. Figure 4.9 shows the Zn^{2+} release from the cements. Similar results of Ca^{2+}, with higher concentrations, were obtained for Zn^{2+} over 1, 7 and 30 days. Also, similar to the Ca^{2+} release profile, the maximum Zn^{2+} release was obtained for LGa-2 at 7 days evaluation, which peaked at ~10 ppm. Results of Zn^{2+} release (Figure 4.9) showed that the concentration of Zn increases with the addition of Ga in the starting glass, however, the %mol of Zn in the starting glasses decreases from 0.40 to 0.24 %mol. This is expected due to the longer setting reaction resulting from the addition of Ga, hence slower cross-linking after the attack of the PAA on the glass structure. Once the disruption for the glass network occurs, the Zn^{2+} and Ca^{2+} ions will start releasing before the complete cross-linking occurs to set the cement, which was shown by FTIR to occur up to 30 days, hence ingress of the Ca^{2+} and Zn^{2+} ions into the distilled water can be most easily achieved with the LGa-2. Figure 4.10 shows the Si release from the cements. The Si release was found to increase with maturation. Similar results were obtained for the Control and LGa-1 cements over all periods, however, a relatively high release of Si was obtained for the LGa-2 cements over 1, 7 and 30 days, peaking at ~28 ppm. As discussed earlier, the higher concentration of Si release for the LGa-2 is caused by the longer setting reaction and the easier solubility of these ions during the setting reaction. FTIR results proved that the cements have the Si-O-Si bond. The silica bond will be formed during the setting reaction and will be loosely bound at the surface of the glass particles. These silica molecules will then dissolve immersing the cement samples in the distilled water and hence Si ions will move into the solution. This process was found to be fast for the first 7 days of LGa-2 cement, hence facilitating the relatively high concentration obtained for the Si release from LGa-2 cement; while it should be considered that the Si release did not increase significantly for 30 days evaluation for LGa-2 cement. Figure 4.11 shows the Ga^{3+} release from the cements. No Ga^{3+} release was obtained in the Control cement as expected, however, it was found that there was no Ga^{3+} release for LGa-1 over 1 day evaluation. Additionally, very low concentrations of Ga^{3+} release were detected for 7 days (~0.2 ppm) and 30 days (~0.3 ppm) evaluation of LGa-1. Ga^{3+} release from LGa-2 cements presented low concentration (~0.4 ppm) of Ga^{3+} ions after 1 day, but unlike LGa-1, LGa-2, presented relatively high concentrations of Ga^{3+} after 7 days (~3 ppm) and 30 days (~3 ppm). The low concentration of Ga^{3+} release, when compared to other ions, can be due to the reduced mobility of the trivalent (III) ions in the system. Another factor is the low maturation behavior of Ga^{3+} ions. Overall, the low release profile of Ga^{3+} ions (~3 ppm) is sufficient to bind Ga^{3+} to the DNA phosphate, forming a stable complex (Tajmir-Riahi H.A., et al., 1992). This is important in achieving better clinical outcomes that will reduce the post-operative complications as sufficient release of Ga^{3+} ions (~3 ppm) may inhibit the DNA synthesis by modifying its 3D structure, the modulate protein synthesis, and the activity of some enzymes such as DNA polymerases, ATPases, tyrosine-specific protein phosphatise and ribonucleotidereductase (Collery P. et al., 2002). On the other hand, this low concentration of ion release is necessary to avoid the reported toxicity of Ga ions (Moschèn et al., 2001).

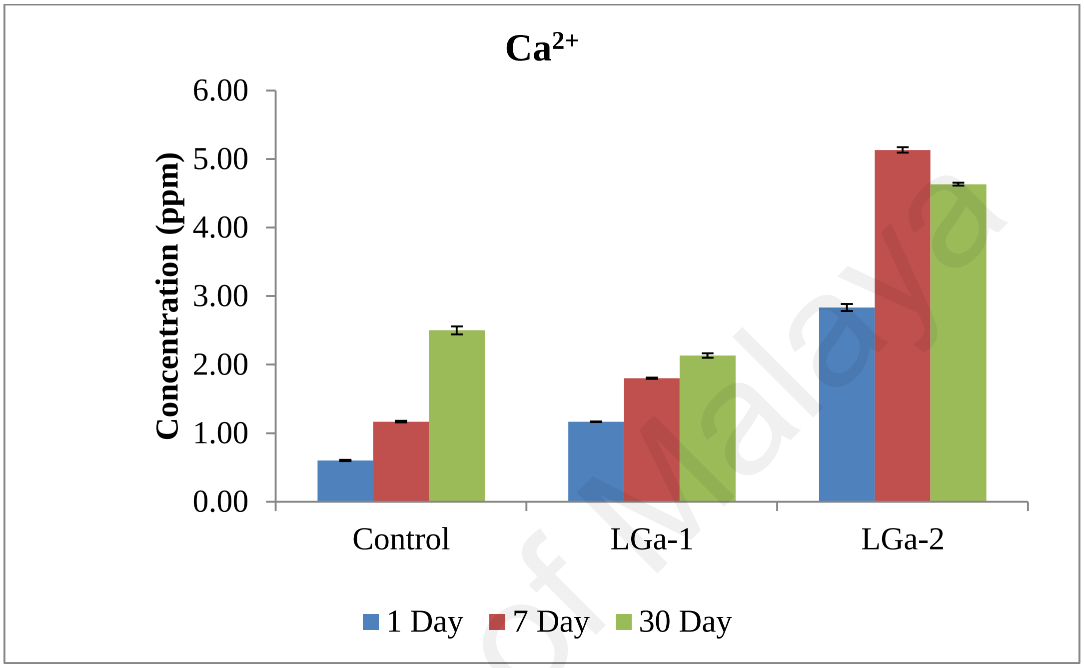

Figure 4.8: Calcium release profiles for cement series over 1, 7 and 30 days

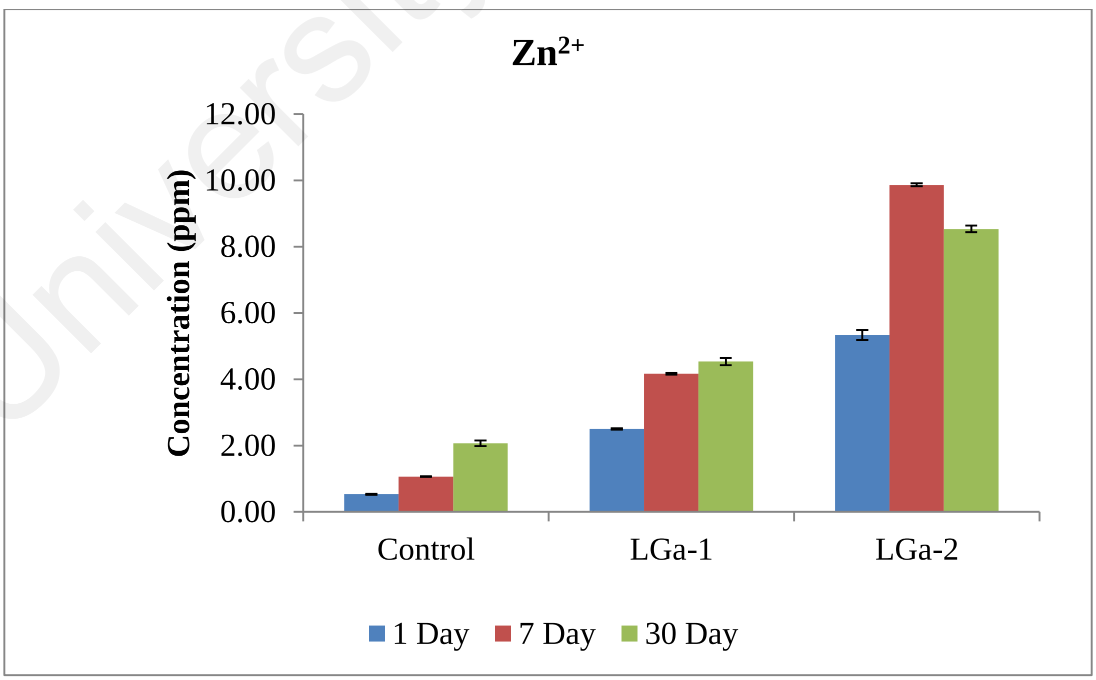

Figure 4.9: Zinc release profiles for cement series over 1, 7 and 30 days

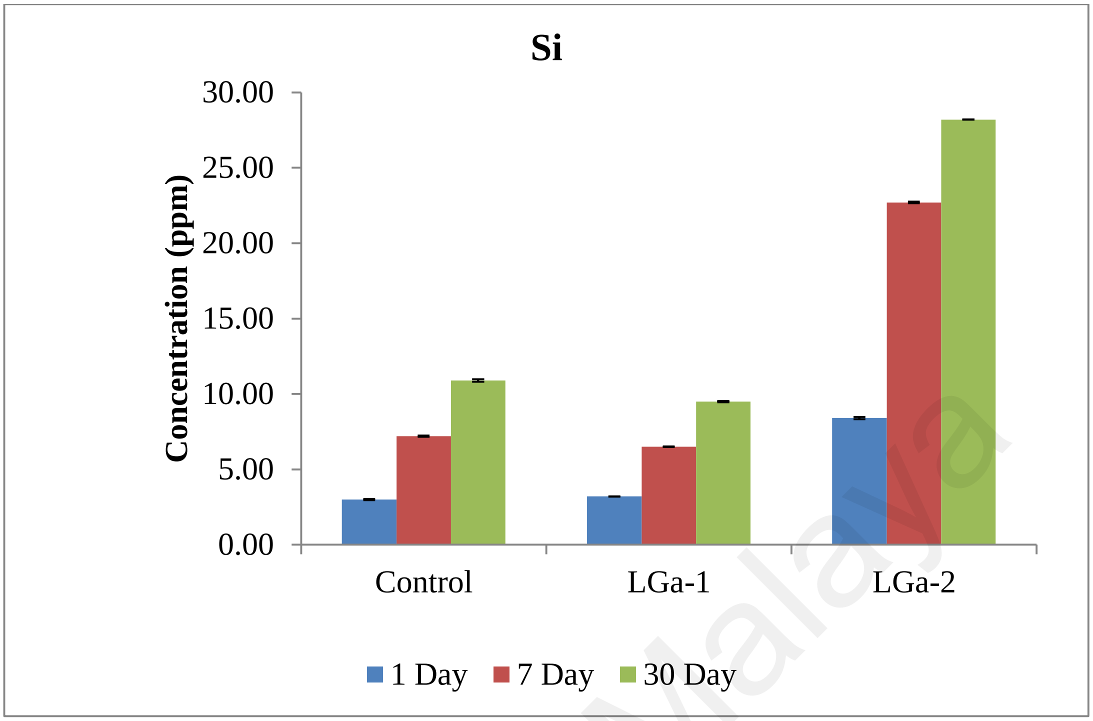

Figure 4.10: Silicon release profiles for cement series over 1, 7 and 30 days

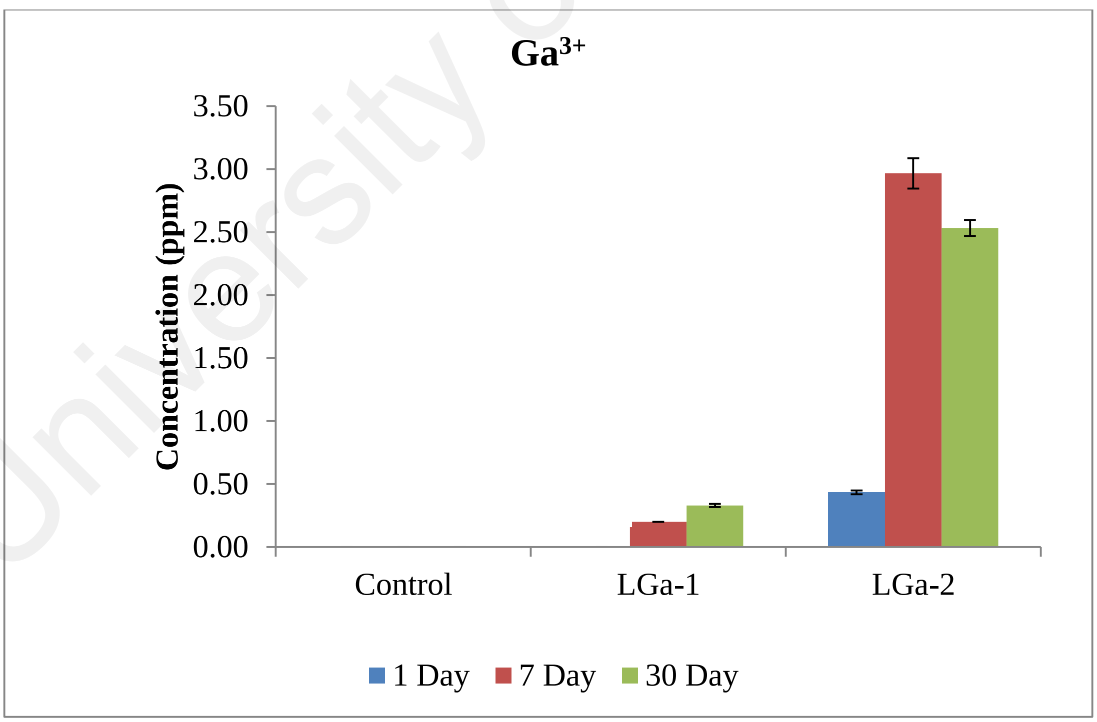

Figure 4.11: Gallium release profiles for cement series over 1, 7 and 30 days

4.3.3 Contact angle measurement

Contact angle measurements were recorded to determine the tendency of the cement surface to absorb water (hydophilicity) in relation to Ga incorporation in the glass precursors, hence evaluating the cement surface chemistry. Figure 4.12 shows the contact angle measurements of the cement formulations tested over 1, 7 and 30 days. The contact angle was found to decrease over 1, 7 and 30 days. It can also be seen that the addition of Ga in the glass composition appears to reduce the contact angle of the cement. The Control glass was found to have the highest contact angle over 1 (~46º), 7 (~37º) and 30 (~40º) days in comparison to LGa-1 and LGa-2, however, there was no statistical significant difference between Control and LGa-1 for 7 days (P= 0.057) and 30 days (P= 1.000). Hence, confirming the results and discussions regarding the quicker set and maturation of the Control glasses when compared to LGa-1 and LGa-2. Results from the contact angle measurements provide few other indications. According to Mittal KL (2006), the wettability of the surface increases with the decrease in contact angle. Contact angles <90º are considered hydrophilic. Further, lower contact angles are associated with both higher roughness and adhesion-ability. In general, all cement samples are hydrophilic. However, hydrophilicity increases with Ga concentration in the glass series.

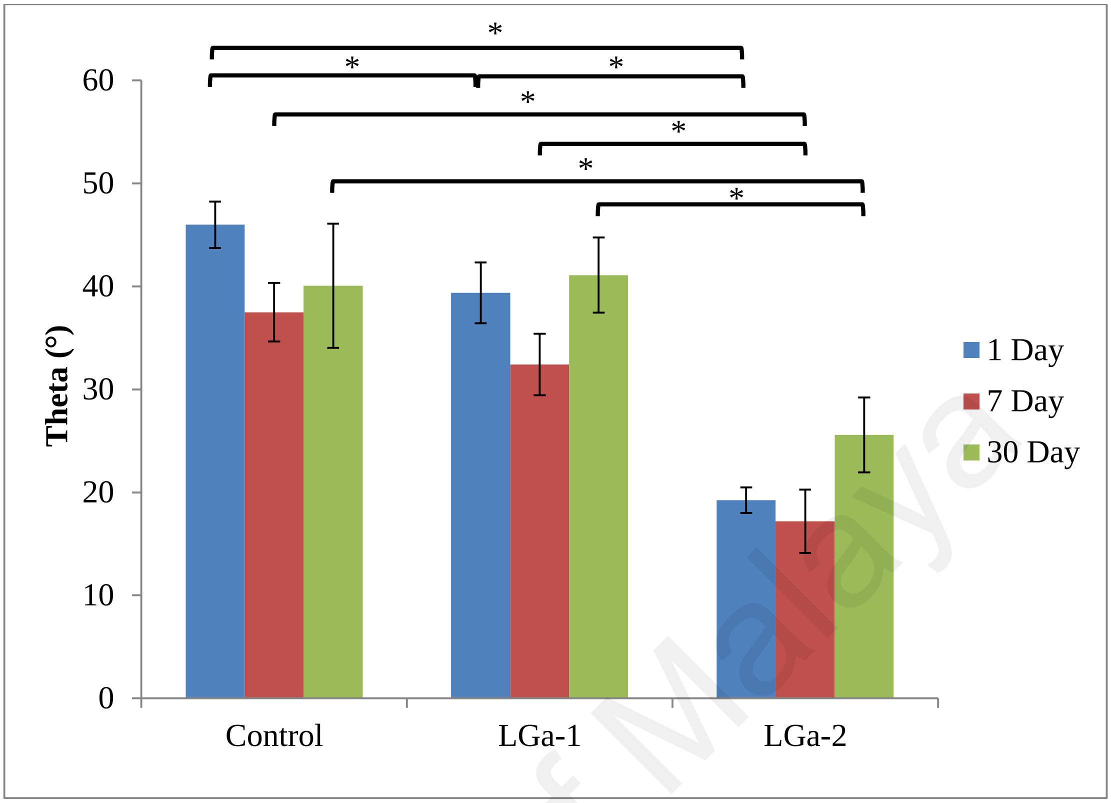

Figure 4.12: Contact angle measurements (d_W) for cement series over 1, 7 and 30 days. Stars and bars show statistical significance ($p < 0.05$).

4.3.4 AFM

AFM was important for evaluating surface morphology and roughness (Ra). Figure 4.13 shows the 3D surface morphology of the cement series over 1, 7 and 30 days. The coloured section refers to the magnitude of the Ra (in nm). Figure 4.14 shows the Ra of the cement series over 1, 7 and 30 days. Figures 4.13a-c show the 1 day surface morphology. It can be seen that the Control cement (Figure 4.13a) is more granular in comparison to LGa-1 and LGa-2 represented by different size holes distributed on the surface. It can also be seen that the step height is dissimilar throughout the surface and hence representing a higher Ra at one end. Figures 4.13b and c show more homogeneous surfaces in comparison to the Control cement. Similar results, with higher Ra can be realized in Figures 4.13d-f for the 7 days surface evaluation. However, the surface morphology of the LGa-2 presented some elevations at some points of the surface. This might be due to the longer maturation time of the cement. Figures 4.13g-i show the 30 days surface morphology. Similar to 1 and 7 days evaluation, results for 30 days show that the Control cement is more homogeneous when compared with 1 and 7 days evaluation, with higher strength at some points on the surface. It can also be seen that the surface morphology for LGa-1 and LGa-2 are similar with low Ra at some points and high Ra at some other points. Interestingly, it was seen that the addition of Ga to the cement series increases Ra according to the values obtained from Figure 4.14. Values are ~47, 180 and 266 nm for Control, LGa-1 and LGa-2 respectively for 1 day measurements. For 7 day measurements, the Ra increased from ~54 nm for Control to ~145 nm for LGa-1 and to ~299 nm for LGa-2. Measurements for 30 days presented similar results, where the Ra data are ~ 109, 321, 235 nm for Control, LGa-1 and LGa-2 respectively. It can be seen from Figure 4.14 that there was no statistical significant difference between the Ra of the Control, LGa-1 and LGa-2 cements, respectively. AFM results show that the increased setting reaction due to the addition of Ga results in increased Ra. This may be due to the network disruption occurring during the increased maturation time of the Ga samples. The behaviour of Ga ions is expected to have a similar structural role to that of the Al so that the Ga ions replaces the Si ions partly, imparting a negative charge on the glass network. Since Ga is a network modifier, it is expected that Ga^{3+} disrupts the connectivity of Si-O-Si network by introducing the NBO species (Wren A.W., et al., 2012), as shown in the FTIR results. These results confirm the results of the contact angle measurements and prove the discussions presented by Mittal KL (2006).

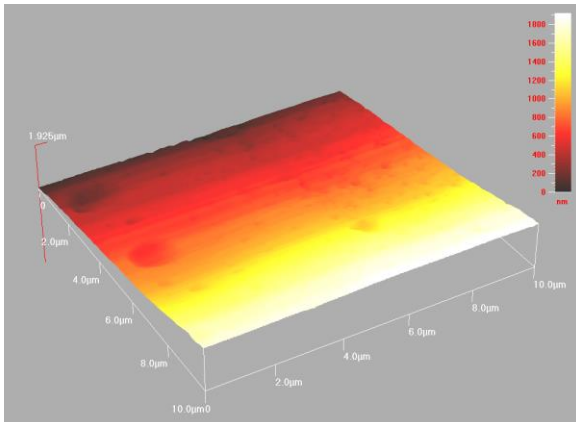
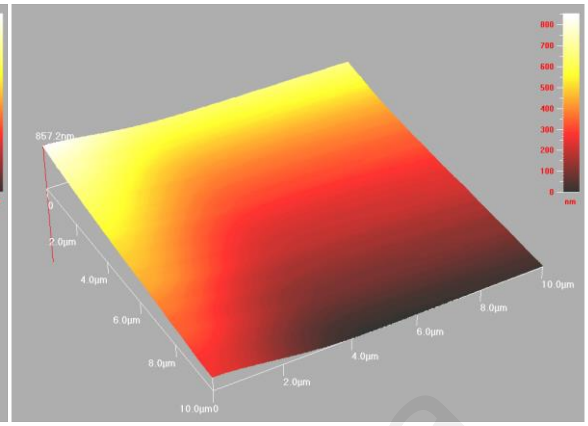

(a) (b)

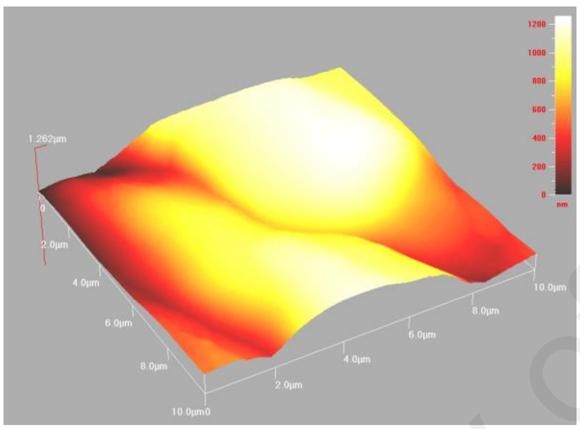
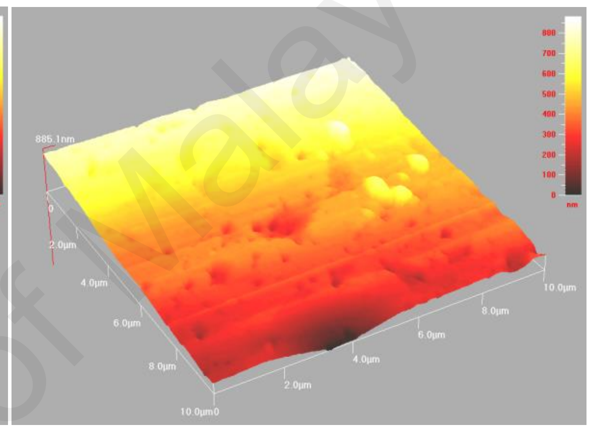

(c) (d)

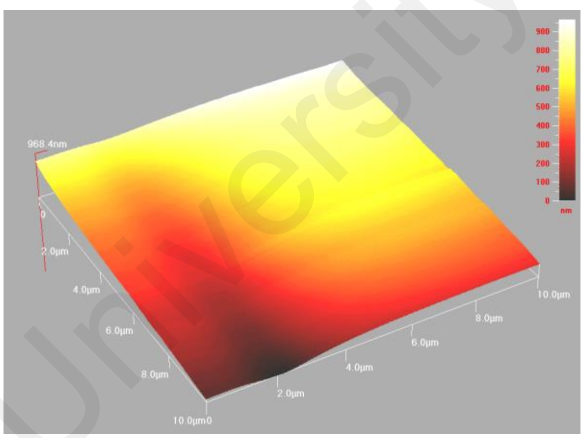
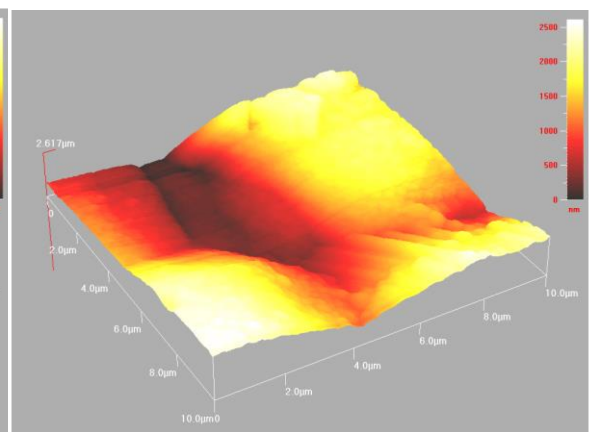

(e) (f)

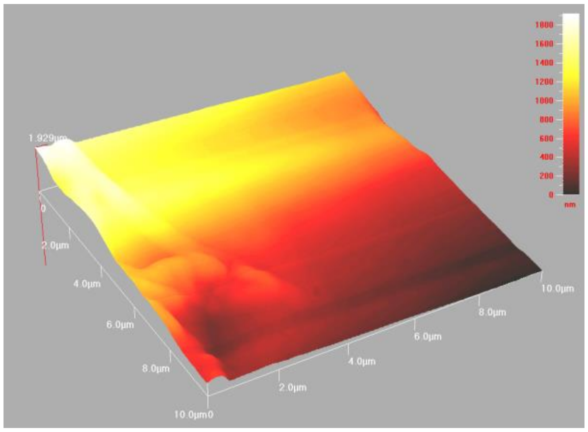
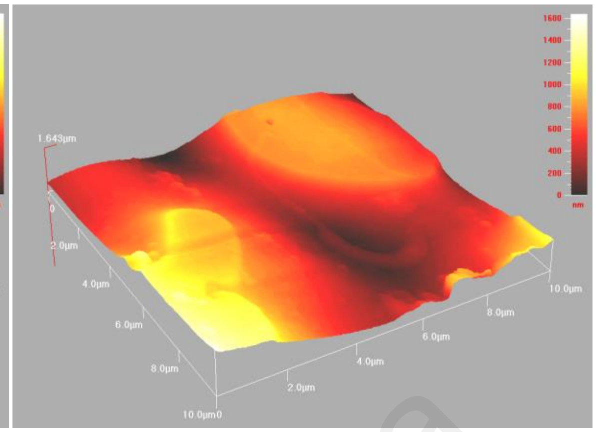

(g) (h)

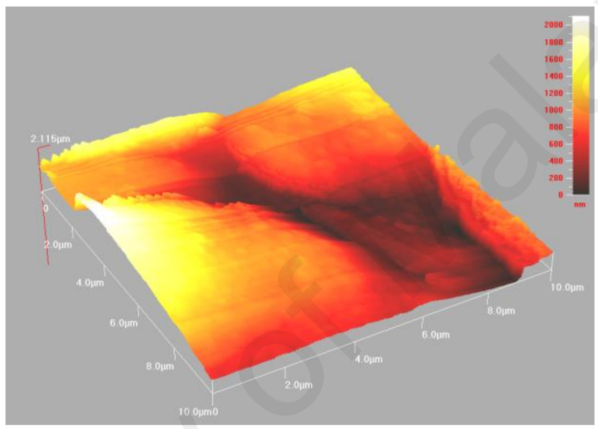

(i)

Figure 4.13: 3D surface morphology of the cement series observing (a) control (b) LGa-1 and (c) LGa-2 for 1 day evaluation; (d) control (e) LGa-1 and (f) LGa-2 for 7 day evaluation and (g) control (h) LGa-1 and (i) LGa-2 for 30 day evaluation

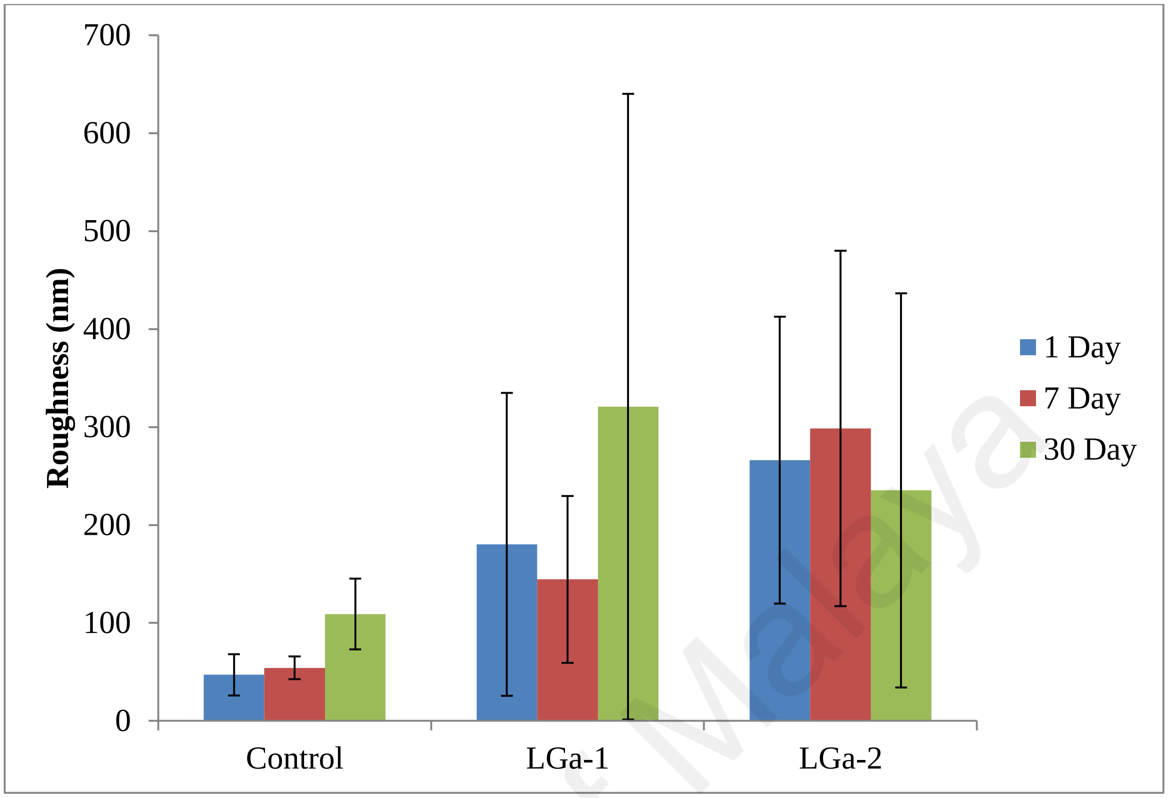

Figure 4.14: Roughness measurements for the cement series over 1, 7 and 30 days. Stars and bars show statistical significance ($p < 0.05$).

4.4 Mechanical properties

4.4.1 Compressive strength

The compressive strength study was done in accordance to ISO 9917 standard for dental based cements. All samples were submersed in distilled water for 1, 7 and 30 days before testing. Figure 4.15 shows the compressive strength results for all cement formulations. In general, similar to the results presented in the literature (Wren A.W., et al., 2012), the Control glass has the highest strength, LGa-1 has the lowest and LGa-2 has higher strength than LGa-1 and lower than, but comparable to, the cement based on the Control glasses. According to FTIR, all the samples have similar levels of water content at 1 day, and identical water contents when aged 7 and 30 days. Thus, the change in the mechanical properties does not seem to be dependent on the water content. It is highly likely that

Control samples experience greater strengths due to the increased level of cross-linking when compared to the LGa 1 and 2 samples, however this does not explain the increased compressive strengths experienced by the LGa-2 samples compared to the LGa-1 samples. Both Ga containing cement formulations experience very similar FTIR traces, with similar levels of cross-linking taking place across all aged samples. However, the increase in the strength for LGa-2 is might be related to the longer setting reaction that facilitates the improved cross-linking and due to the higher mol% of the Ga which is expected to have a similar behaviour to Al ions in the GPCs due to the same valence state and hence increasing the strength. This indicates, that LGa-2 can be used instead of the Control glass due to the comparable strength values.

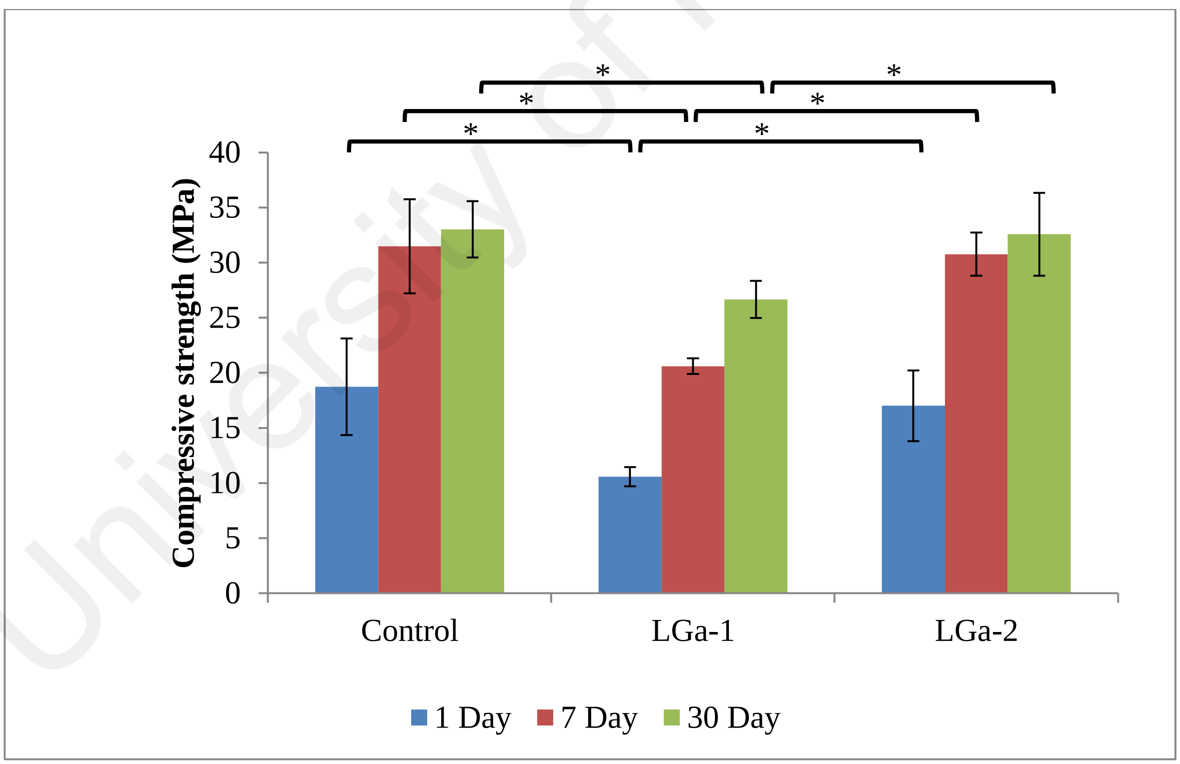

Figure 4.15: Compressive survey results for the cement series over 1, 7 and 30 days. Stars and bars show statistical significance ($p < 0.05$).

4.4.2 Biaxial flexure test

Biaxial flexure test was also performed in order to investigate into the effect of Ga addition on the mechanical properties of GPCs when aged in distilled water for 1, 7, and 30 days. Figure 4.16 shows the biaxial flexural strength results. The σ_f obtained display slight improvements between Control and LGa-2 samples over the 1, 7 and 30 day samples. In accordance with the results presented by Wren et al. (2012), the addition of Ga was found to decrease both σ_c and σ_f, however, there was no statistical significant difference between Control and LGa-2 for 1, 7 and 30 days measurements of σ_c and for 7 days measurement of σ_f. Interestingly, our results indicate that LGa-2 can provide slightly higher (~21, 23, 29 MPa) biaxial flexural strength when compared to Control (~14, 19, and 21 MPa) and LGa-1 (~16, 21, and 22 MPa) glass and a compressive strength comparable to that of the Control glass.

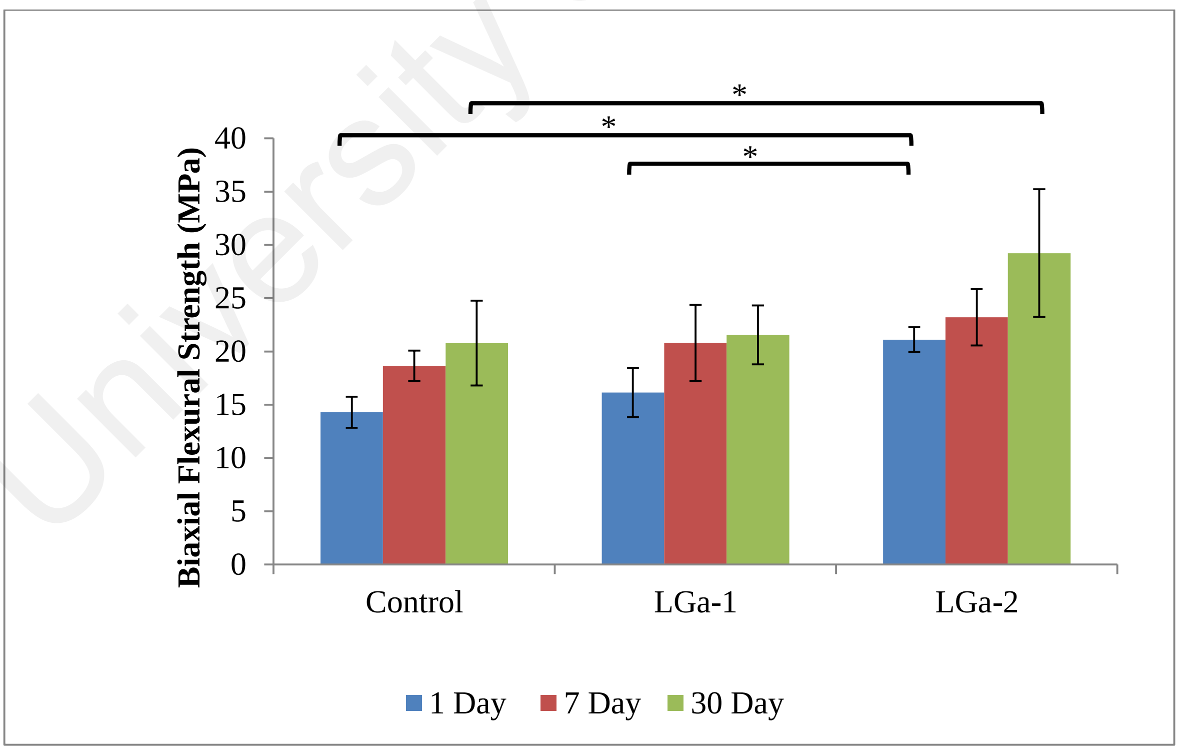

Figure 4.16: Biaxial flexural strength survey results for the cement series over 1, 7 and 30 days. Stars and bars show statistical significance ($p < 0.05$).

4.5 Ex-vivo study

4.5.1 Tensile strength test

The work seeks the development of Ga-containing GPCs for fixation purposes in the skeleton, particularly, in the incidence of sternal closure, post sternotomy surgery. Figure 4.17 shows the *ex-vivo* tensile strength measurements for all cement series over 1, 7 and 30 days. As can be seen, the strength was found to increase after 1 day, however, 30 day measurements showed similar results to the 7 day measurements. Additionally, it can be observed that the strength for LGa-1 decreases significantly while it increases for LGa-2. The strengths for Control cements were ~ 0.4, 0.6 and 0.5 MPa for 1, 7 and 30 day measurements, respectively. For LGa-1, the strengths are ~ 0.2, 0.3 and 0.3 MPa while LGa-2 strength values are ~ 0.3, 0.4, 0.4 MPa respectively, over the same periods. In general, all results were low. There is a statistical significant difference between Control and LGa-1, but there was no significant difference between Control and LGa-2. Hence, matching with the discussions presented in section 4.4.1. It was reported (Alhalawani A. M.F. and Towler M.R., 2013) that the indirect measurements for the forces imposed on the sternum resulted in a force of 260 N during a ~ 5.6 kPa pressure generating cough. It was also presented that forces from 160 N to 400 N and 550 N to 1650 N are imposed on the sternal midline during breathing and coughing, respectively. The Kryptonite cement, supported by wires, was able to resist ~600 N (Alhalawani A. M.F. and Towler M.R., 2013), whereas wires alone showed ~2 mm displacement at ~400 N. Our Ga-GPCs resulted in lower strength values, considering LGa-2, strength values are ~100, 69 and 92 N for 1, 7 and 30 days assessment respectively. However, our study did not consider the use of wires for improved support and higher strength values.

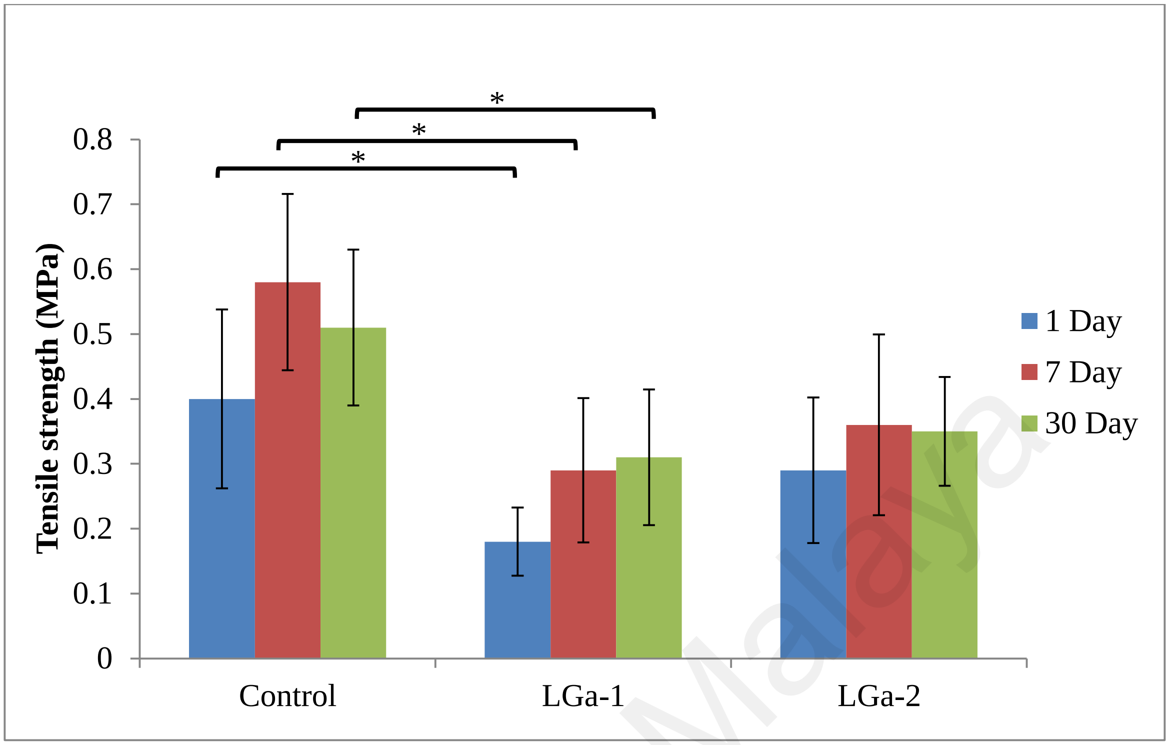

Figure 4.17: *Ex-vivo* tensile strength measurements for the tensile tested bones over 1,7 and 30 days. Stars and bars show statistical significance ($p < 0.05$).

4.5.2 SEM

Further investigations also included evaluating failure mechanism using the SEM. Figure 4.18 shows the SEM images for the cement series over 1, 7 and 30 days. In Figure 4.18, the red arrows point toward the attachment between the cement and the bone marrow while the letters C and B indicate the area of cement and bone, respectively. The cement area can be clearly seen and differentiated from that of the bone by its granular and brighter view. Figures 4.18a-c show the SEM images for the attachment between the bone and Control, LGa-1 and LGa-2 cements respectively over day 1. Figures 4.18d-f show the SEM images for the attachment between the bone and Control, LGa-1 and LGa-2 cements respectively over 7 days. Figures 4.18g-i show the SEM images for the attachment between the bone and the Control, LGa-1 and LGa-2 cements respectively over 30 days.

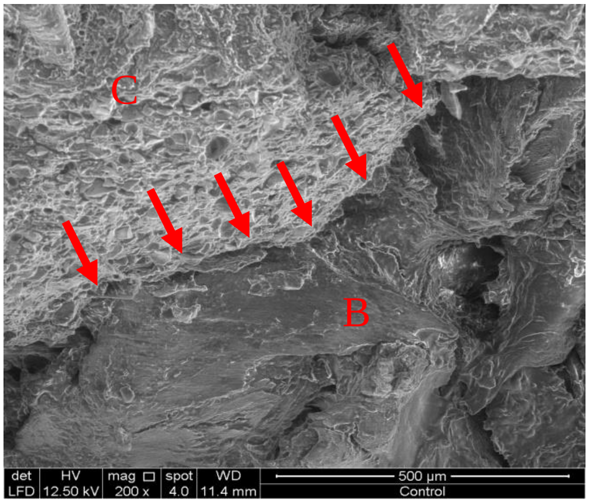
C
B
det HV mag spot WD
LFD 12.50 kV 200 x 4.0 11.4 mm
500 µm
Control
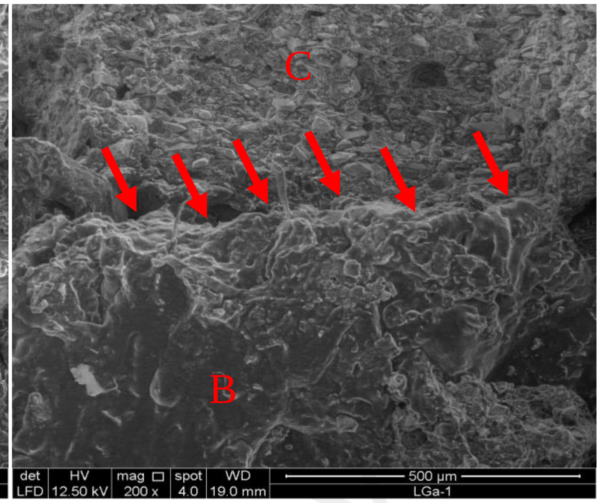
C
B
det HV mag spot WD
LFD 12.50 kV 200 x 4.0 19.0 mm
500 µm
LGa-1

(a) (b)

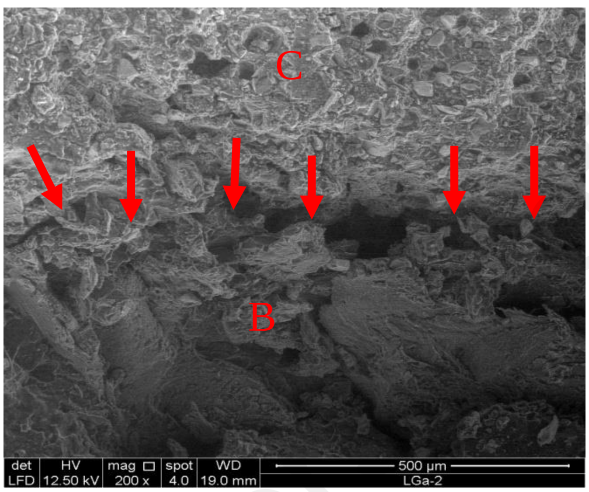
C
B
det HV mag spot WD
LFD 12.50 kV 200 x 4.0 19.0 mm
500 µm
LGa-2
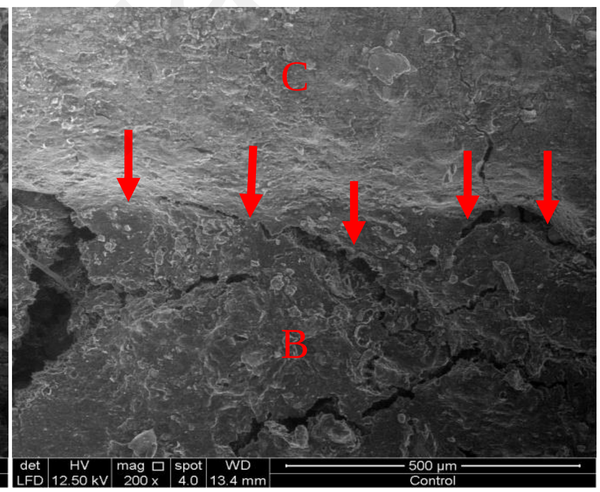
C
B
det HV mag spot WD
LFD 12.50 kV 200 x 4.0 13.4 mm
500 µm
Control

(c) (d)

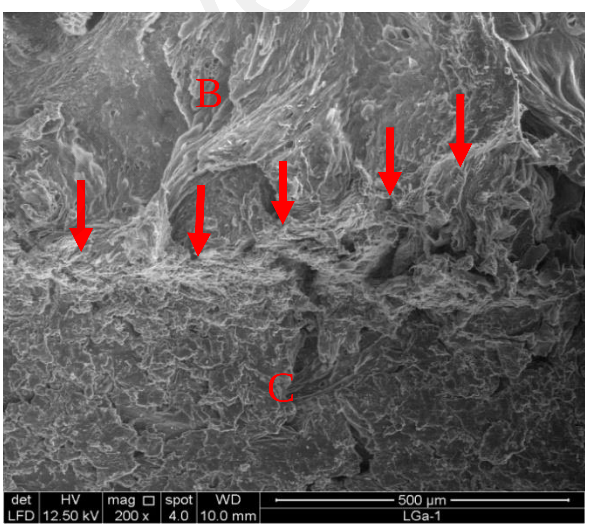
B
C
det HV mag spot WD
LFD 12.50 kV 200 x 4.0 10.0 mm
500 µm
LGa-1
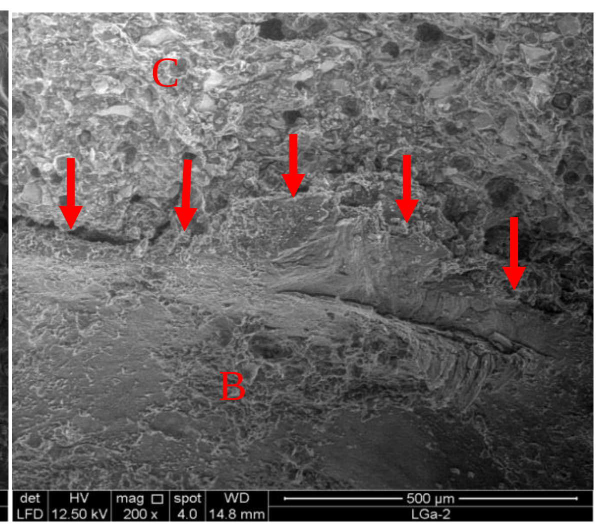
C
B
det HV mag spot WD
LFD 12.50 kV 200 x 4.0 14.8 mm
500 µm
LGa-2

(e) (f)

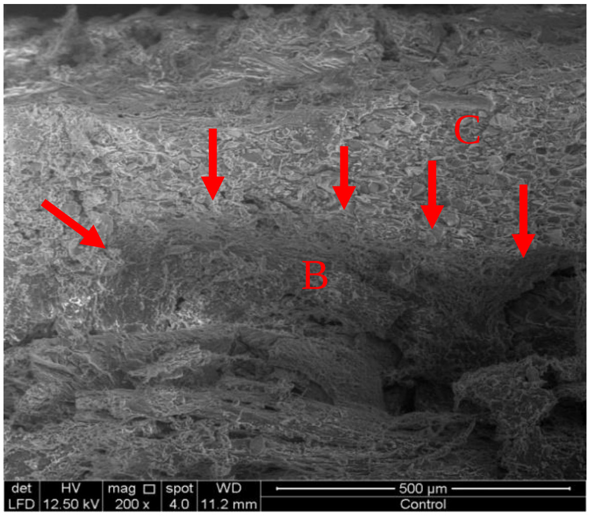

(g)

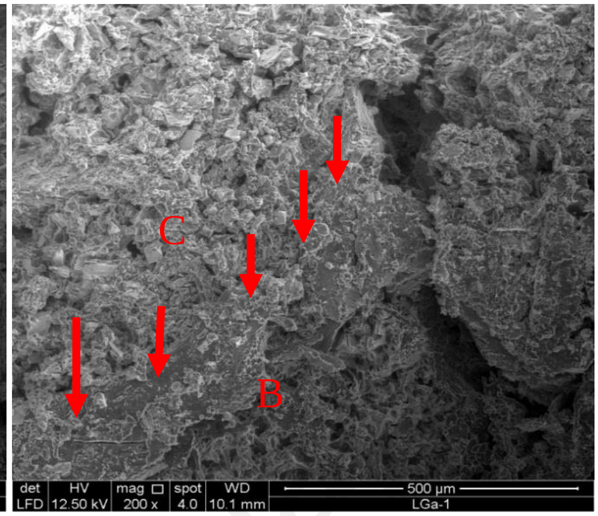

(h)

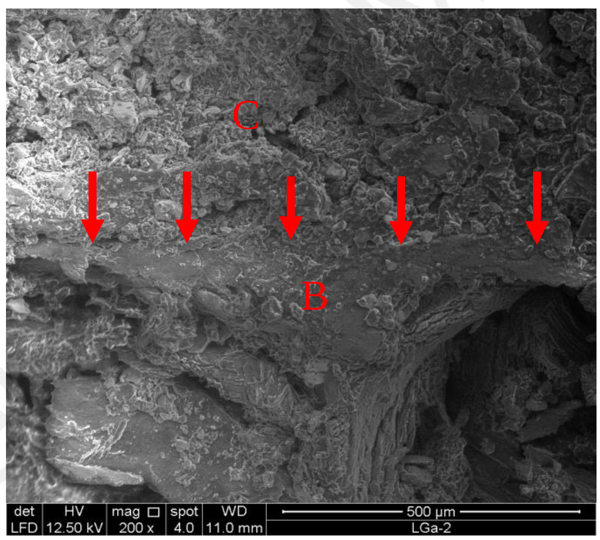

(i)

Figure 4.18: SEM cross-sectional images for the tensile tested bones, observing (a) control (b) LGa-1 and (c) LGa-2 for 1 day evaluation; (d) control (e) LGa-1 and (f) LGa-2 for 7 day evaluation and (g) control (h) LGa-1 and (i) LGa-2 for 30 day evaluation. The red arrows point towards the attachment between the cement and the bone marrow while the letters C and B refer to cement and bone, respectively.

It can be observed that the failure is adhesive in all of the images since the cement is completely attached to the bone in all images. It can be also seen that the attachment improves with cement maturation. This is related to the bone resorption which occurred due to the integration and bonding of some of the ions from the cement such as Ca^{2+} and Zn^{2+} with the similar ions from the bone. However, it must be considered that the integration is not similar to that of the normal living bone. In general, it can be seen that the Ga-containing cements bond completely to the bone observed at all periods, while the 7 and 30 day images show better attachment when compared to day 1.

4.5.3 EDX

EDX was also performed to obtain the wt% of each of the ions incorporated at the starting glass. Table 4.1 shows the wt% of the ions over 1, 7 and 30 days observed from the EDX survey measurement. The Ca^{2+} concentration values are ~17, 10 and 11 % for Control, LGa-1 and LGa-2 respectively over day 1, ~ 22, 20 and 17 % over 7 days and ~ 32, 19 and 17 % over 30 days. It can be seen that the concentration increases with time for all cements except for LGa-1 and LGa-2 at 30 days investigation as expected, however, it was not expected that the Ca^{2+} concentration decreases with the addition of Ga. This might be caused by the adsorption of the bone for some of the Ca^{2+} ions during the setting reaction, especially that Ca^{2+} ions are no longer produced into the bone. The Zn^{2+} concentration values are ~55, 39 and 23 % for Control, LGa-1 and LGa-2 respectively over day 1, ~46, 37 and 24 % over 7 days and ~48, 38 and 25 % over 30 days. Similar concentration values were obtained at all periods while in similar trend to the Ca^{2+} ions, in that the addition of Ga was found to decrease the wt% of Zn^{2+}. It can also be seen that the concentration of Zn^{2+} over all periods for all cements is higher than that of the Ca^{2+}. The Si concentration values were found as ~27, 26 and 37 % for , LGa-1 and LGa-2 respectively over day 1, ~32, 25 and 26 % over 7 days and ~36, 25 and 23 % over 30 days. The Si concentration increased over all periods for the Control glass, remained similar for LGa-1 and decreased over all periods for LGa-2. The results of the Si concentration did not follow the same trend as those of the Ca^{2+} and Zn^{2+}. This confirms our expectations of the adsorption of the bone for the ions Ca^{2+} and Zn^{2+} while the adsorption of the Si is slow due to the strength of the bond Si-O-Si on the surface of the cement. In addition, this also might be related to the lower % of the Si in the normal living tissues when compared to the Zn^{2+} and Ca^{2+}. The Ga^{3+} concentration values were according to the authors' expectations. The Control cement has zero wt% while for the LGa-1 and LGa-2 the concentration of Ga^{3+} increased with the addition of Ga. Ga^{3+} concentrations values were ~0, 25 and 28 % for Control, LGa-1 and LGa-2 respectively over 1 day, ~0, 18, and 39 % over 7 days and 0, 18 and 36 % over 30 days. Results of Ga^{3+} concentration are matching with the results achieved from the ion release study. However, the high concentration of LGa-1 (25%) over 1 day was not expected since there was no ion release from LGa-1 after 1 day. In general, the EDX of the tested bone samples provided an indication of the presence of all incorporated ions over all periods.

Table 4.1: EDX survey results observing the wt% for the Ca, Zn, Si and Ga ions over 1, 7 and 30 days

	Control			**LGa-1**			**LGa-2**		
	1 day	**7 day**	**30 day**	**1 day**	**7 day**	**30 day**	**1 day**	**7 day**	**30 day**
Ca^{2+}	17.1	22.4	32	10.4	19.6	19.2	11.1	17.3	16.7
Zn^{2+}	55.5	45.6	48.2	38.9	37.2	37.7	23.0	23.8	24.5
Si	27.4	32.0	36.1	25.7	25.1	24.8	37.4	25.8	22.9
Ga^{3+}	0.0	0.0	0.0	25.1	18.2	18.3	28.4	39.3	35.9

4.6 Limitation of the study

- During the FTIR experiment, it was not possible to identify a band below 650 cm^{-1} due to the limited wavelength band of the instrument ranging between 650 and 4000 cm^{-1}. Further research is required since Ga^{3+} particles might absorb the IR at lower wavelengths around 450 cm^{-1} and there is no research into the IR absorption for the stretching vibration between Ga^{3+} and the PAA.
- Results from ion release studies facilitated the discussion that LGa-2 will contribute to a significant reduction in the post-operative complications, post sternotomy. However, further anti-bacterial and cell culture studies are required to prove this expectation.
- Our *ex-vivo* study does not consider osteoporosis, bleeding and bone resorption; complications regularly encountered during sternotomy fixation and repair. Additionally, the normal bone resorption after application of Ga-cements in the *in-vivo* study or the surgical procedure is expected to provide better attachment and higher strength between the cement and the bone.
- The tensile tests were performed on small samples with an average cross-sectional-area of 350 mm^2. However, the application of Ga-cements on the complete sternum would be expected to provide higher strength due to the bond that will be formed across the whole sternum. In the same context, due to the small sample size, authors performed several pilot studies to find the best way to perform the tensile failure test. The Authors found it difficult to test the samples by attaching the sternal ribs to the Instron jaws and hence this is considered as one of the main reasons for the low strengths achieved. The forces imposed by the sternal ribs distribute across the area while in our case, the force is exerted on a small cross-sectional area of the sternum.

- The surgical procedure does not consider the use of Formaldehyde which was used on the sterna studies here in order to avoid the growth of bacteria or fungus. As discussed earlier, the use of Formaldehyde with PBS is recommended to save the bone grafts but no research was found on the effect of Formaldehyde on the bioactive glasses. Hence, the *in-vivo* or the surgical procedure will eliminate any effects on the strength due to the use of this chemical.

CHAPTER FIVE

CONCLUSION

5. Conclusion

5.1 Conclusion

The importance of this study arises from the lack of an ideal device/material, whether currently available or under test, that can address all the concerns that arise from sternal closure post-sternotomy. The ideal sternal closure should ensure stability, reduced rate of post-operative complications, and a short hospitalization period, alongside cost-effectiveness. The purpose of such a device is to reduce the post-operative complications such as the sternal infections and withstand the maximum physiological forces imposed on the sternum.

In this study, we have developed a novel glass polyalkenoate cement for fixation and stabilization of the rib cage post sternotomy. LGa-2 has been shown to be one of the most appropriate cements for sternotomy application. XRD analysis showed that the addition of Ga did not cause phase changes in the starting glass proved by the fully amorphous structure of all fired glasses. The results show that having 0.16 mol% of Ga (LGa-2) in the glass series has prolonged the setting and working times. This will be an advantage to the surgeon, as it will give the surgeon sufficient time to apply the cement, while the kinetic reactions are not affected. LGa-2 cements were found to facilitate greater ion release of Ca^{2+}, Zn^{2+}, Si and Ga^{3+} ions. Ga ion is known to be an anti-inflammatory and anti-bacterial ion, which will result in reduced sternal infections, post sternotomy. The release profiles of known therapeutic ions also indicated that the Ga-GPCs may contribute to bone absorption and regeneration, post sternotomy. Further, our experiments showed that all tested cement formulations are hydrophilic. However, hydrophilicity increases with Ga concentration in the glass series. This implied that LGa-2 will result in higher adhesion-ability for the sternotomy. Additionally, results from the AFM analysis showed that the addition of Ga to the glass series increases the Ra which was expected due to the increased maturation time of the Ga-based cements. The presence of Ga has a positive effect on the compressive strength of the samples with strengths increasing over 10 MPa in the 1 day samples compared to the Control glass. However, storage in water had relatively little effect in comparison to the Control, which continued up to the 30 day samples. The addition of Ga had relatively little effect on the biaxial flexural strength. The mechanical properties of LGa-2 were found comparable to the Control glasses for both, the biaxial flexural and compressive strengths. This indicates that the developed Ga-based cements can replace the Control glasses with improved anti-bacterial activity and thus reduced sternal infections, post sternotomy. Similarly to the mechanical properties, tensile testing of the bovine sterna proved that the LGa-s samples are comparable to the Control samples.

The limitations of our study included the use of non-living sterna in which chemotherapeutic effects, bleeding and bone regeneration could not be investigated. The tensile test was performed on a small sample size; a full human sternum is expected to provide better results. Also the effect of formaldehyde, which is a toxic acid, on the bioactive glasses was not considered. Recommendations for the future work suggest the utilization of cadaver sternums for *ex-vivo* study and followed by an *in-vivo* study. These will overcome the major limitations of our study.

Supplementary

Appendix A: Determination of net setting time (ISO 9917-1:2007)

A.1 Apparatus

A.1.1 Cabinet, capable of being maintained at a temperature of (37 ± 1) °C and a relative humidity of at least 90 %.

A.1.2 Indentor, of mass (400 ± 5) g, with a needle having a flat end of diameter (1,0 ± 0,1) mm which is plane and perpendicular to the long axis of the needle.

A.1.3 Metal mould, similar to that shown in Figure A.1. Dimensions in millimeters, with ± 0,15 tolerance on dimensions.

A.1.4 Metal block, of minimum dimensions 8 mm × 75 mm × 100 mm positioned within the cabinet and maintained at (37 ± 1) °C.

A.1.5 Aluminium foil.

A.1.6 Timer, accurate to 1 s.

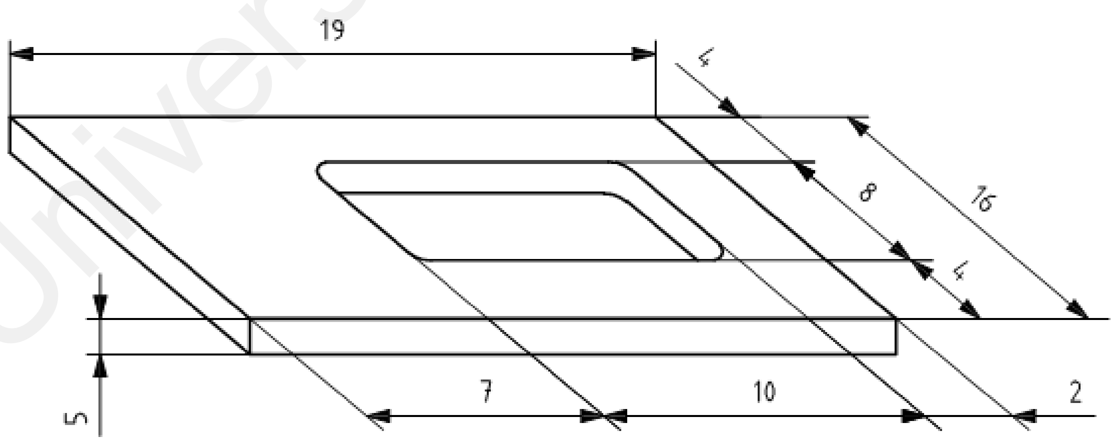

NOTE: Internal corners may be square or rounded.

Figure A.1: Mould for preparation of specimens for determination of net setting time

A.2 Procedure

Place the mould (A.1.3), conditioned to (23 ± 1) °C, on the aluminium foil (A.1.5) and fill to a level surface with mixed cement.

Sixty seconds after the end of mixing, place the assembly, comprising mould, foil and cement specimen, on the block (A.1.4), in the cabinet (A.1.1). Ensure good contact between the mould and foil, and between the foil and block.

Ninety seconds after the end of mixing, carefully lower the indentor (A.1.2) vertically on to the surface of the cement and allow it to remain there for 5 s. Carry out a trial run to determine the approximate setting time, repeating the indentations at 30 s intervals until the needle fails to make a complete circular indentation in the cement, when viewed using × 2 magnification. Clean the needle, if necessary, between indentations. Repeat the process, starting the indentation at 30 s before the approximate setting time thus determined, making indentations at 10 s intervals.

Record the net setting time as the time elapsed between the end of mixing and the time when the needle fails to make a complete circular indentation in the cement. Repeat the test two more times.

A.3 Treatment of results

Record the results of the three tests. Each result shall fall within the range specified in Table A.1.

Table A.1: Requirements for dental cements (ISO 9917-1:2007)

Chemical type	**Application**	**Net setting Time (Min)**		**Minimum Compressive Strength (MPa)**
		min.	**max.**	
Glass polyalkenoate	Base/lining	1,5	6	50
Glass polyalkenoate	Restoration	1,5	6	100

Appendix B: FTIR sampling information

Number of background scans: 32 (Background scans were taken because the instrument is single beam splitter and to avoid the transmittance errors due to the water vapor and CO_2 in the ambient air; absorbers of IR radiation).

Number of sample scans: 32

Resolution: 4000

Sample gain: 8

Detector: DTGS KBr

Beamsplitter: KBr

Source: IR

Appendix C: Determination of compressive strength (ISO 9917-1:2007)

C.1 Apparatus

C.1.1 Cabinet, maintained at a temperature of (37 ± 1) °C and a relative humidity of at least 30 %.

C.1.2 Split mould and plates, as shown in Figure C.1. The mould shall have internal dimensions (6,0 ± 0,1) mm high and (4,0 ± 0,1) mm diameter. The mould and plates shall be made of stainless steel or a material which will not be affected by the cement. When testing polyacid-based cements, face the plates with acetate sheets to prevent adhesion.

C.1.3 Screw clamps, as shown in Figure C.1.

C.1.4 Screw micrometer or equivalent measuring instrument, having graduations of 2 µm or smaller.

C.1.5 Mechanical tester, capable of being operated at a cross-head speed of (0,75 ± 0,30) mm/min or at a loading rate of (50 ± 16) N/min.

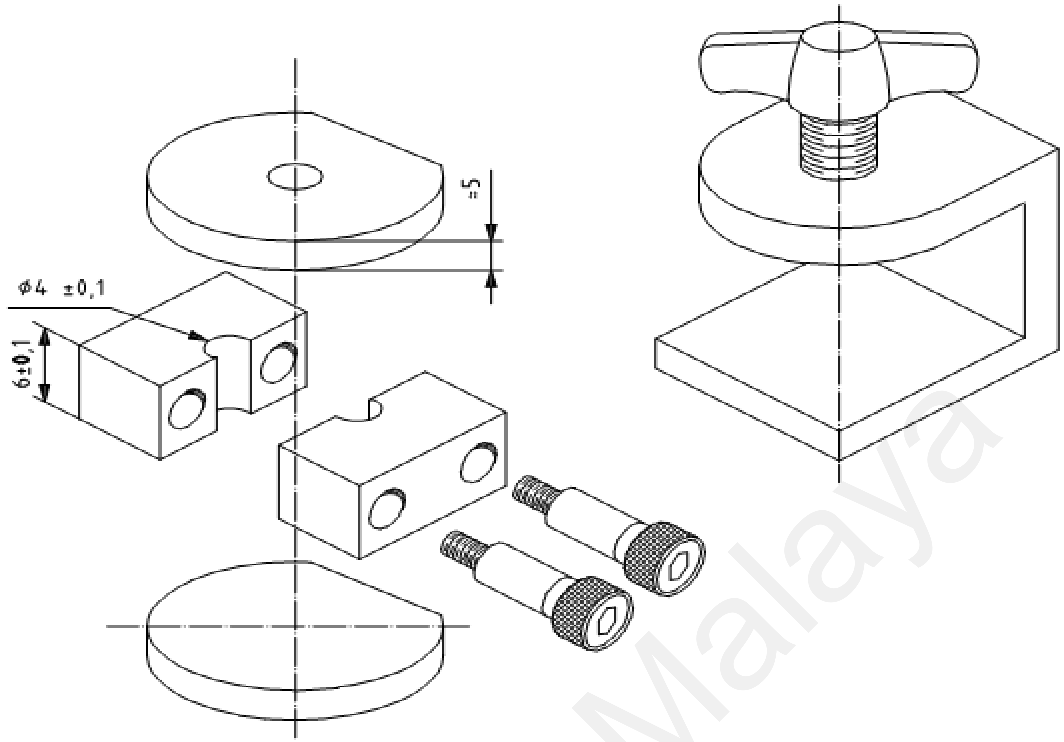

Figure C.1: Mould and clamp for preparation of specimens for compressive strength test

C.2 Preparation of test specimens

Condition the split mould and plates (C.1.2) and screw clamp (C.1.3) at (23 ± 1) °C. Within 60 s of the end of mixing, pack the cement, prepared in accordance with the manufacturer's instructions, to a slight excess in the split mould.

In order to consolidate the cement and avoid trapping air, convey the largest convenient portions of mixed cement to the mould and apply to one side using a suitable instrument. Fill the mould to excess in this manner and then place on the bottom plate with some pressure.

Remove any bulk extruded cement, place the top metal plate in position on the mould and squeeze together. Put the mould and plates in the screw clamp and tighten. No later than 120 s after the end of mixing, transfer the whole assembly to the cabinet (C.1.1).

One hour after the end of mixing, remove the plates and grind the ends of the specimen flat and at right angles to its long axis. An acceptable method for doing this is to use wet 400 grade silicon carbide paper, but in any event the abrasive shall be no coarser.

Remove the specimen from the mould immediately after surfacing and check visually, without magnification, for air-voids or chipped edges. Discard any such defective specimens.

NOTE To facilitate the removal of the hardened cement specimen, the internal surface of the mould may be evenly coated, prior to filling, with a 3 % solution of micro-crystalline or paraffin wax in petroleum ether. Excess ether is allowed to evaporate before the mould can be used. Alternatively, a thin film of silicone grease or PTFE dry-film lubricant may be used.

Prepare five such specimens and, immediately after the preparation of each, immerse it in water, grade 3 as defined in ISO 3696:1987, at (37 ± 1) °C for (23 ± 0,5) h.

Calculate the diameter of each specimen by taking the mean of two measurements at right angles to each other, made to an accuracy of 0,01 mm using e.g. a screw micrometer (see C.1.4).

C.3 Procedure

Twenty-four hours after the end of mixing, place each specimen with the flat ends between the platens of the mechanical tester (C.1.5) and apply a compressive load along the long axis of the specimen. Apply a sheet of damp filter paper (e.g. Whatman No. 1) to both top and bottom platens of the test machine in the area which will contact the specimens. Use a fresh piece of paper for each test.

Record the maximum force applied when the specimen fractures and calculate the compressive strength, C, in megapascals, using the equation C.1:

$$C = 4p/\pi d^2 \quad \text{Eq. C.1}$$

Where

p is the maximum force applied, in newtons;

d is the measured diameter of the specimen, in millimetres.

C.4 Treatment of results

If at least four of the five results are above the minimum strength specified in Table A.1, the material shall pass the test. If three or more of the five results obtained are below the minimum strength specified in Table A.1, the material shall fail the test.

If only three specimens satisfy the minimum strength requirement in Table A.1, prepare and test a further five specimens. To pass the test, at least eight of the total of ten results shall be above the minimum strength value specified in Table A.1.

Appendix D: Publications

1. Alhalawani, A., M. F., & Towler, M. R. (2013). A review of sternal closure techniques. *J Biomater Appl*., 28: 483-497.
2. Alhalawani, A., M. F., Curran, D. J., Pingguan-Murphy, B., Boyd, D., & Towler, M. R. (2013). A Novel Glass Polyalkenoate Cement for Fixation and Stabilisation of the Ribcage, Post Sternotomy Surgery: An ex-Vivo Study. *J. Funct. Biomater.*, 4: 329-357.

Bibliography

Ailakis, J. (2011). Gentamicin. Retrieved from: http://www.kemh.health.wa.gov.au/services/nccu/guidelines/drug_protocols/Gentamicin.pdf

Akinmade, A. O., & Nicholson, J. W. (1995). Poisson's ratio of glass-polyalkenoate ('glass-ionomer') cements determined by an ultrasonic pulse method. *Journal of materials science: Materials in Medicine*, 6, 483-485.

Alhalawani, A., M. F., & Towler, M. R. (2013). A review of sternal closure techniques. *J Biomater Appl*., DOI: 10.1177/0885328213495426.

Ana, I. D., Matsuya, S., Ohta, M., & Ishikawa, K. (2003). Effects of added bioactive glass on the setting and mechanical properties of resin-modified glass ionomer cement. *Biomaterials*, 24, 3061–3067.

Badellino, M., Cavarocchi, N. C., Kolff, J., Alpern, J. B. & McClurken, J. B. (1988). Sternotomy closure with Parham bands. *J Cardiac Surg*, 3, 235– 236.

Barthelemy, A. (2006). Post-sternotomy mediastinitis. In D. Mathieu (eds.), *Handbook on Hyperbaric Medicine* (pp. 567–576). New York, NY: Springer.

Baskett, R. J., MacDougall, C.E., & Ross, D.B. (1999). Is mediastinitis a preventable complication? A 10-year review. *Ann Thorac Surg*, 67, 462–5.

Bernstein, L.R. (1998). Mechanisms of Therapeutic Activity for Gallium. *Pharmacological Reviews*, 50, 665-682.

Bertolini, M. J., Zaghete, M. A., Gimenes, R., & Padovani, G. C. (2008). Determination of the properties of an experimental glass polyalkenoate cement prepared from niobium silicate powder containing fluoride. *Dental materials*, 24, 124–128.

Blanche, C., & Shaux, A. (1988). The use of absorbable microfibrillation collagen to control sternal bone marrow bleeding. *Int Surg*, 73, 42–3.

Boestan, I. N. & Sarvasti, D. (2005). Choosing a prosthetic heart valve. *Folia Medica Indonesiana*, 41, 169-181.

Boyd, D., Clarkin, O. M., Wren, A. W. & Towler, M. R. (2008). Zinc-based glass polyalkenoate cements with improved setting times and mechanical properties. *Acta Biomaterialia*, 4, 425–431.

Boyd, D., & Towler, M. R. (2006). The Effect of Strontium on the Rheology and Mechanical Properties of Zinc Based Glass Polyalkenoate Cements. *European Cells and Materials*, 11, 26.

Boyd, D., Li, H., Tanner, D. A., Towler, M. R. & Wall, J. G. (2006). The antibacterial effects of zinc ion migration from zinc-based glass polyalkenoate cements. *J Mater Sci Mater Med*, 17, 489-494.

Brook, I. M. & Hatton, P. V. (1998). Glass-ionomers: bioactive implant materials. *Biomaterials*, 19, 565-571.

Brook, I. M., Craig, G. T., Hatton, P. V. & Jonck, L. M. (1992). Bone cell interactions with a granular glass-ionomer bone substitute material: in vivo and in vitro culture models. *Biomaterials*, 13, 721–725.

Cahalin, L. P., LaPier, T. K. & Shaw D. K. (2011). Sternal Precautions: Is It Time for Change? Precautions versus Restrictions – A Review of Literature and Recommendations for Revision. *Cardiopulmonary Physical Therapy Journal*, 22, 5-15.

Casha, A. R., Ashraf, S. S., Kay, P. H. & Cooper, G. J. (1999a). Routine sternal closure using interlocking multitwisted wires. *Eur J Cardiothorac Surg*, 16, 353-355.

Casha, A. R., Gauci, M., Yang, L., Saleh, M., Kay, P. H. & Cooper, G. J. (2001). Fatigue testing median sternotomy closures. *Eur J Cardiothorac Surg.*, 19, 249-253.

Casha, A. R., Yang, L. & Cooper, G. J. (1999b). Measurement of chest wall forces on coughing with the use of human cadavers. *J Thorac Cardiovasc Surg*, 118, 1157-1158.

Casha, A. R., Yang, L., Kay, P. H., Saleh, M. & Cooper, G. J. (1999c). A biomechanical study of median sternotomy closure techniques. *Eur J Cardiothorac Surg.*, 15, 365-369.

Chawengkijwanich, C. & Hayata, Y. (2008). Development of TiO2 powder-coated food packaging film and its ability to inactivate Escherichia coli in vitro and in actual tests. *Int. J. Food Microbiol.*, 123, 288-292.

Cheng, W., Cameron, D. E., Warden, K. E., Fonger, J. D. & Gott V. L. (1993). Biomechanical study of sternal closure techniques, *Ann Thoruc Surg*, 55, 737-740.

Chitambar, C. R. (2010). Medical applications and toxicities of gallium compounds. *Int J Environ Res Public Health*, 7, 337-361.

Chou, S. S., Sena, M. J. & Wong, M. S. (2011). Use of SternaLock Plating System in Acute Treatment of Unstable Traumatic Sternal Fractures. *Ann Thorac Surg*, 91, 597–599.

Choukairi, F., Ring, J., Thekkudan, J. & Enoch, S. (2011). Management of sternal wound dehiscence, *Wounds*, 7, 99-105.

Cicilioni, O. J., Stieg, F. H. & Papanicolaou, G. (2005). Sternal Wound Reconstruction with Transverse Plate Fixation. *Plast Reconstr Surg*, 115, 1297-1303.

Clarke, B. (2008). Normal Bone Anatomy and Physiology. *Clin J Am Soc Nephrol*, 3, 131–139.

Cohen, D. J., & Griffin, L. V. (2002). A biomechanical comparison of three Sternotomy closure techniques. *Ann Thorac Surg*, 73, 563–568.

Collery, P., Keppler, B., Madoulet, C. & Desoize, B. (2002). Gallium in cancer treatment. *Crit Rev Oncol Hematol*, 42, 283–296.

Cook, W. D. (1982). Dental polyelectrolyte cements. I. Chemistry of the early stages of the setting reaction. *Biomaterials*, 3, 232-236.

Coughlan, A., Boyd, D., Douglas, C. & Towler M. (2008). Antibacterial coatings for medical devices based on glass polyalkenoate cement chemistry. *J Mater Sci Mater Med*, 19, 3555-3060.

Cox, M. A. J. (2009). *Local mechanical properties of tissue engineered heart valves* (Doctoral thesis, Universiteitsdrukkerij Technische Universiteit Eindhoven, Netherlands). Retrieved from http://alexandria.tue.nl/extra2/200911307.pdf

Crisp, S., Pringuer, M. A., Wardleworth, D. & Wilson, A. D. (1974). Reaction in glass ionomer cements: II. An infrared spectroscopic study. *J Dent Res*, 53, 1414-1419.

Curran, D. J., Fleming, T. J., Towler, M. R. & Hampshire, S. (2011). Mechanical parameters of strontium doped hydroxyapatite sintered using microwave and conventional methods. *J Mech Behav Biomed Mater*, 4, 2063-2073.

Dalton, M. L., Connally, S. R. & Sealy, W. C. (1992). Julian's reintroduction of Milton's operation. *Ann Thorac Surg*, 53, 532–533.

Dasika, U. K., Trumble, D. R. & Magovern, J. A. (2003). Lower sternal reinforcement improves the stability of sternal closure. *Annals of Thoracic Surgery*, 75, 1618-1621.

Decoteau, D., Flannery, D., Hart, A. & Zec, H. (2006). *Comparison of Cancellous and Cortical Bone Screws for Sternal Application* (Undergraduate thesis, Worcester Polytechnic Institute, Worcester, Massachusetts, USA). Retrieved from http://www.wpi.edu/Pubs/E-project/Available/E-project-042606-150133/unrestricted/FINAL_REPORT_MQP.pdf

Diefenbeck, M., Muckley, T. & Hofmann, G. O. (2006). Prophylaxis and treatment of implant-related infections by local application of antibiotics. *Injury*, 37, 95-104.

Dieselman, J. C. (2011). *Comparison of Alternative Rigid Sternal Fixation Techniques* (Master thesis, Worcester polytechnic institute, Worcester, Massachusetts, USA). Retrieved from http://www.wpi.edu/Pubs/ETD/Available/etd-011212-115454/unrestricted/jdieselman_sternal_fixation.pdf

DiMaio, F. R., (2002). The science of bone cement: A historical review, *Orthopedics*, 25, 1399-1407.

Doctors Research Group, Inc., (2009). Kryptonite bone void filler- biocompatibility and osseointegration, Southbury, CT.

Dogan, O. F., Oznur, A. & Demircin, M. (2004). A New Technical Approach for Sternal Closure with Suture Anchors (Dogan Technique). *Heart Surg Forum*, 7, 328-332.

Driessen, M. D., Miller, T. M. & Grassian, V. H. (1998). Photocatalytic oxidation of trichloroethylene on zinc oxide: characterization of surface-bound and gas-phase products and intermediates with FT-IR spectroscopy. *J Mol Catal A: Chemical*, 131, 149-156.

Driscoll, C., Green, J., Beatty, C., McCaffrey. T. & Marrs, C. (1998). In vitro characteristics of a Glass lonomer Cement. *Skull Base Surgery*, 8, 175-180.

Dugdale, D. C., (2012). Osteomyelitis, *PubMed health*, Retrieved from http://www.ncbi.nlm.nih.gov/pubmedhealth/PMH0001473/

Elahi, M. M., Mitra, A., Mir, H., Nott, R. & Spears, J. (2004). Composite Plate and Wire Fixation for Complicated Sternal Closure. *Ann Plast Surg*, 53, 217-221.

Exley, C. (1999). A molecular mechanism of aluminium-induced Alzheimer’s disease? *J Inorg Biochem*, 76, 133–140.

Fawzy, H., Osei-Tutu, K., Errett, L., Latter, D., Bonneau, D., Musgrave, M. & Mahoney J. (2011). Sternal plate fixation for sternal wound reconstruction: initial experience (Retrospective study). *J Cardiothorac Surg*, 6, 63.

Fedak, P. W., Kolb, E., Borsato, G., Frohlich, D. E., Kasatkin, A., Narine, K., Akkarapaka, N. & King, K. M. (2010). Kryptonite Bone Cement Prevents Pathologic Sternal Displacement. *The Society of Thoracic Surgeons*, 90, 979-985.

Ford, M., Brunelli, J., Song, D., Costello, P., Dunn, R. M. & Billiar, K. (2011). Design of a Screw-Plate System to Minimize Loosening in Sternal Fixation. *Bioengineering Conference (NEBEC), 2011 IEEE 37th Annual Northeast, 1-3 April 2011*,1 – 2.

Friberg, Ö., Dahlin, L. G., Kallmann, J., Kihlstro, E., Soderquist, B. & Svedjeholm, R. (2009). Collagen-gentamicin implant for prevention of sternal wound infection; long-term follow-up of effectiveness. *Interact Cardiovasc Thorac Surg*, 9, 454-458.

Friberg, Ö., Dahlin, L. G., Levin, L. A., Magnusson, A., Granfeldt, H., Källman, J. & Svedjeholm, R. (2006a). Cost effectiveness of local collagen-gentamicin as prophylaxis for sternal wound infections in different risk groups. *Scand Cardiovasc J*, 40, 117–25

Friberg, Ö., Dahlin, L. G., Söderquist, B., Källman, J. & Svedjeholm R. (2006b). Influence of more than six sternal fixation wires on the incidence of deep sternal wound infection. *Thorac Cardio-vasc Surg*, 54, 468 –473.

Gandy, K. L. & Moulton, M. J. (2008). Sternal plating to prevent malunion of transverse sternotomy in lung transplantation. *Ann Thorac Surg*, 86, 1384 –1385.

Geyer, G. & Helms, J. (1997). Ionomer-based cement as a bone substitute in reconstructive middle ear surgery. *HNO*, 45, 442–447.

Geyer, G., Dazert, S. & Helms, J. (1997). Performance of ionomeric cement (Ionocem®) in the reconstruction of the posterior meatal wall after curative middle-ear surgery. *J Laryngol Otol*, 3, 1130-1136.

Goenka, S., Balu, R. & Kumar, T. S. (2011). *Effects of nanocrystalline calcium deficient hydroxyapatite (nCDHA) incorporation in glass ionomer cements (GIC)* (Undergraduate thesis, Visvesvaraya national institute of technology, Nagpur, India). Retrieved from http://www.tms.org/Students/Winners/2012_Goenka.pdf

Grapow, M. T. R., Melly, L. F., Eckstein, F. S. & Reuthebuch, O. T. (2012). A new cable-tie based sternal closure system: description of the device, technique of implantation and first clinical evaluation. *J Cardiothorac Surg*, 7, 59.

Grevious, M. A. (2009). *Chest Reconstruction: Sternal Dehiscence Reconstruction*. Retrieved from http://emedicine.medscape.com/article/1278627-overview

Guida, A., Towler, M. R. & Wall, J. G. (2003). Preliminary work on the antibacterial effect of strontium in glass ionomer cements. *J Mater Sci Lett*, 22, 1401–1403.

Gunja, N., Pai, S., McMahon, N., Dupak, E., Lalikos, J., Dunn, R., Francalancia, N., Pins G. & Bil1iar, K. (2004). A Biomechanical Study of a Rigid Plating System for Sternal Fixation. In *Bioengineering Conference, 2004. Proceedings of the IEEE 30th Annual Northeast, 17-18 April 2004,* 156- 157.

Guo, G.-W. & Liang, Y.-X. (2001). Aluminum-induced apoptosis in cultured astrocytes and its effect on calcium homeostasis. *Brain Res*, 888, 221–226.

Harjula, A. & Jarvinen, A. (1983). Postoperative median Sternotomy dehiscence. *Scand J Thorac Cardiovasc Surg*, 19, 277–81.

Hatcher, B., (2011). A Cadaveric, Biomechanical Analysis of Sternal Fixation Systems, *Biomet Microfixation.* Retrieved from http://www.biometmicrofixation.com/downloads/Sternal-Cadaveric.pdf

Hatton, P. V., Hurrell-Gillingham, K. & Brook, I. M. (2006). Biocompatibility of glass-ionomer bone cements. *J dent*, 34, 598–601.

Huh, J., Bakaeen, F., Chu, D. & Wall, M. J. (2008). Transverse sternal plating in secondary sternal reconstruction. *J Thorac Cardiovasc Surg*, 136, 1476-1480.

Hurrell-Gillingham, K., Reaney, I. M., Brook, I. & Hatton, P. V. (2006). In vitro biocompatibility of a novel Fe_2O_3 based glass ionomer cement. *J dent*, 34, 533–538.

International Organization for Standardization, ISO 9917-1:2007. Dentistry – Water-based cements – Part 1: Powder/liquid acid-base cements, Geneva: ISO.

Jolly, S., Flom, B. & Dyke, C. (2012). Cabled Butterfly Closure: A Novel Technique for Sternal Closure. *Ann Thorac Surg*, 94, 1359–1361.

Jonck, L. M., Grobbelaar, C. J. & Strating, H. (1989). Biological evaluation of glass-ionomer cement (Ketac-0) as an interface material in total joint replacement. A screening test. *Clinical Materials*, 4, 201–224.

Jonck, L. M. & Grobbelaar, C. J. (1990). Ionos bone cement (glass-ionomer): an experimental and clinical evaluation in joint replacement. *Clinical Materials*, 6, 323–359.

Jonck, L. M., Grobbelaar, C. J. (1992). A glass ionomer for reconstructive surgery. Ionogran—an ionomeric micro implant. A biological evaluation. *Clinical Materials*, 9, 85–103.

Julian, O. C., Lopez-Belio, M., Dye, W. S., Javid, H. & Grove, W. J. (1957). The median sternal incision in intracardiac surgery with extracorporeal circulation; a general evaluation of its use in heart surgery. *Surgery*, 42, 753–761.

Kalush, S. L. & Bonchek, L. I. (1976). Peristernal closure of median Sternotomy using stainless steel bands. *Ann Thorac Surg*, 21, 172–173

Keaveny, T. M., Morgan, E. F. & Yeh, O. C. (2002). Bone mechanics. In Kutz M., *standard handbook of biomedical engineering and design*. NY, USA: McGraw-Hill Professional.

Kenny, S. M. & Buggy, M. (2003). Bone cements and fillers: A review, *J Mater Sci Mater Med*, 14, 923-938.

Khaled, Z. (2009). *Development of a new generation of bone cements using nanotechnology* (Doctoral dissertation, the University of Western Ontario, London, Ontario, Canada). Retrieved from http://www.nt.ntnu.no/users/skoge/prost/proceedings/aiche-2008/data/papers/P134944.pdf

Kim, B., Kim, D., Cho, D. & Cho, S. (2003). Bactericidal effect of TiO2 photocatalyst on selected food-borne pathogenic bacteria. *Chemosphere*, 52, 277-281.

Kjaergard, H. K. & Trumbull, H. R. (2000). Bleeding from the sternal marrow can be stopped using vivostat patient-derived fibrin sealant. *Ann Thorac Surg*, 69, 1173–1175.

Knobloch, L. A. Kerby, R. E., Seghi, R., Berlin, J. S. & Lee, J. S. (2000). Fracture toughness of resin based luting cements. *J Prosthet Dent*, 83, 204-209.

Kohanski, M. A., Dwyer, D. J. & Collins, J. J. (2010). How antibiotics kill bacteria: from targets to networks. *Nat Rev Microbiol*, 8, 423-435.

Korff, A., Jalowy, T., Mueller, M., Fuertjes, T., Dohmen, G., Radermacher, K. & Follmann. A. (2011). Evaluation of a synergistic handheld instrument for resternotomy controlled by an integrated optical sensor. *Conf Proc IEEE Eng Med Biol Soc.*, 7368-7371.

Lee, T. Y., Estrera, A. L., Safi, H. J. & Khalil, K. G. (2007). Total Sternal Reconstruction Using a Titanium Plate-Supported Methyl Methacrylate Sandwich. *Ann Thorac Surg*, 84, 664-666.

Levin, L. S., Miller, A. S., Gajjar, A. H., Bremer, K. D., Spann, J., Milano, C. A. & Erdmann, D. (2010). An Innovative Approach for Sternal Closure. *Ann Thorac Surg*, 89, 1995-1999.

Lobenhoffer, P., Gerich, T., Witte, F. & Tscherne, H. (2002). Use of injectable calcium phosphate bone cement in the treatment of tibial pateau fractures: a prospective study of twenty-six cases with twenty-month mean follow-up, *J Orthop Trauma*, 16, 143–149.

Lohbauer, U. (2010). Dental Glass Ionomer Cements as Permanent Filling Materials? — Properties, Limitations and Future Trends. *Materials*, 3, 76-96.

López Almodóvar, L. F., Bustos, G., Lima, P., Cañas, A., Paredes, I., Buendía, J. A. (2008). Transverse Plate Fixation of Sternum: A New Sternal-Sparing Technique. *Ann Thorac Surg*, 86, 1016-1017.

Losanoff, J. E., Basson, M. D., Gruber, S. A., Huff, H. & Hsieh, F. H. (2007). Single Wire Versus Double Wire Loops for Median Sternotomy Closure: Experimental Biomechanical Study Using a Human Cadaveric Model. *Ann Thorac Surg*, 84, 1288–1293.

Losanoff, J. E., Collier, A. D., Wagner-Mann, C. C., Richman, B. W., Huff, H., Hsieh, F. H., Diaz-Arias, A. & Jones, J. W. (2004). Biomechanical Comparison of Median Sternotomy Closures. *Ann Thorac Surg*, 77, 203–209.

Mair, H., Kaczmarek, I., Oberhoffer, M., Groetzner, J., Daebritz, S. & Reichart, B. (2005). Surgical Nu-Knit hemostat for bleeding control of fragile sternum. *J Thorac Cardiovasc Surg*, 130, 605–606.

Maltsev, A. A. & Shevelkov, V. F. (1972). Infrared absorption spectra of aluminum, gallium and indium suboxidevapors. Some regularities in frequencies of oscillations of suboxides of elements of the III group and evaluation of molecular constants of B2O. Kolebatel'nyye Spektry v Neorganicheskoy Khimii, Izd-vo Nauka, Moscow, pp. 89-92.

Marieb, E. N. & Hoehn, K. (2013). *Human anatomy and physiology* (9th ed.). London, England: Pearson, 2013.

Marco, R. F. Di, Lee, M. W., Bekoe, S., Grant, K. J., Woelfel, G. F. & Pellegrini, R. V. (1989). Interlocking Figure-of-8 Closure of the Sternum. *Ann Thorac Surg*, 47, 927-929.

Matros, E., Aranki, S.F. & Bayer ,L.R. (2010). Reduction in incidence of deep sternal wound infections: Random or real?. *J Thorac Cardiovasc Surg*, 139, 680 – 685.

Matsuya, S., Matsuya, Y. & Ohta, M. (1999). Structure of bioactive glass and its application to glass ionomer cement. *Dent Mater J*, 18, 155-166.

Mavros, M. N., Mitsikostas, P. K., Alexiou, V. G., Peppas, G. & Falagas, M. E. (2012). Gentamicin collagen sponges for the prevention of sternal wound infection: A meta-analysis of randomized controlled trials. *J Thorac Cardiovasc Surg*, 144, 1235-1240.

McGregor, W. E., Payne, M., Trumble, D. R., Farkas, K. M. & Magovern, J. A. (2003). Improvement of sternal closure stability with rein-forced steel wires. *Ann Thorac Surg*, 76, 1631– 1634.

McGregor, W. E., Trumble, D. R. & Magovern, J. A. (1999). Mechanical analysis of midline sternotomy wound closure. *J Thorac Cardiovasc Surg*, 117, 1144-1149.

Mittal, KL. (2006). *Contact angle, wettability and adhesion* (4^{th} ed.). NY, USA: CRC.

Mittapalli, M. R. (1979). Primary osteomyelitis of sternum, *Thorax*, 34, 680-681.

Mitra, A., Elah, M. M., Tariq, G. M., Powel, R. & Spears, J. (2004). Composite plate and wire fixation for complicated sternal closure. *Ann Plast Surg*, 53, 217–221.

Moschèn, Schweizer, K., Wagner, C. A., Geis-Gerstorfer, J. & Lang, F. (2001). Effects of gallium and mercury ions on transport systems. *J Dent Res*, 80, 1753-1757.

Moshaverinia, A., Chee, W. W., Brantley, W. A. & Schricker, S. R. (2011). Surface properties and bond strength measurements of N-VinylCarprolactam (NVC)-containing glass-ionomer cements. *J Prosthet Dent*, 105, 185-193.

Mossad, S. B., Serkey, J. M., Longworth, D. L., Cosgrove, D. M. & Gordon, S. M. (1997). Coagulase-Negative Staphylococcal Sternal Wound Infections After Open Heart Operations. *Ann Thorac Surg*, 63, 395-401.

Muehrcke, D. D., Barberi, P. & Shimp, W. M. (2007). Calcium Phosphate Cements to Control Bleeding in Osteoporotic Sternums. *Ann Thorac Surg*, 84, 259–261

Muehrcke, D. D., Shimp, W. M. & Aponte-Lopez, R. (2009). Calcium Phosphate Cements Improve Bone Density When Used in Osteoporotic Sternums, *Ann Thorac Surg*, 88, 1658–1661.

Murray, K. D. & Pasque, M. K. (1997). Routine Sternal Closure Using Six Overlapping Figure-of-8 Wires. *Ann Thorac Surg*, 64, 1852–1854.

Nagaraja Upadhya, P. & Kishore, G. (2005). Glass Ionomer Cement – The Different Generations. *Trends Biomater Artif Organs*, 18, 158:165.

Nazarian, A. (2008). *Relative interaction of material and structure in normal and pathologic bone* (Doctoral dissertation, ETH Zürich University, Switzerland). Retrieved from http://e-collection.library.ethz.ch/eserv/eth:30811/eth-30811-01.pdf

Norman W., (1999). Subdivisions of the Thoracic Cavity. Retrieved from http://home.comcast.net/~wnor/thoraxlesson3.htm

Ohara, G. H., Kojima, K. E., Rossi, J. C., Telles, M., Soares, T.V.C., Salomao, C. & Sanda, M. (1995). Experimental study of the biocompatibility of castor bean polyurethane resin intraosseous and intrarticularly implanted in rabbits, *Acta ortop bras*, 3, 62-68.

Ortega, R., Suda, A. & Devès, G. (2003). Nuclear microprobe imaging of gallium nitrate in cancer cells. *Nuclear Instruments and Methods in Physics Research Section B: Beam Inter Mater Atoms*, 210, 364-367.

Ozaki, W., Buchman, S. & Iannettoni, M. (1998). Biomechanical study of sternal closure using rigid fixation techniques in human cadavers. *Ann Thorac Surg*, 65, 1660-1665.

Pai, S. (2005). *In vivo characterization of respiratory forces on the sternal midline following median sternotomy* (Master thesis, Worcester polytechnic institute, Worcester, Massachusetts, USA). Retrieved from http://www.wpi.edu/Pubs/ETD/Available/etd-083005-145245/unrestricted/SPai.pdf

Pai, S., Dunn, R. M., Babbitt, R., Strom, H. M., Lalikos, J. F., Pins, G. D., Billiar & K. L. (2008). Characterization of forces on the sternal midline following median sternotomy in a porcine model. *J Biomech Eng*, 130, 051004.

Pairolero, P. C. & Arnold, P. G. (1984). Management of recalcitrant median sternotomy wounds. *J Thorac Cardiovasc Surg*, 88, 357–64.

Pham, H. N., McDowell, T. & Wikins, E. (1995). Photocatalytically-mediated disinfection of water using TiO2 as a catalyst and spore-forming Bacillus pumilus as a model. *J Environ Sci Health A*, 30, 627-636.

Placek, L., Wren, A. W., Coughlan, A. & Towler, M. R. (2012). Gallium Containing Glass Polyalkenoate Bone Cements: Glass Characterization and Physical Properties, *Bioengineering Conference (NEBEC), 2012 38th Annual Northeast, 16-18 March 2012, Philadelphia, PA, USA*. 225- 226.

Plass, A., Grünenfelder, J., Reuthebuch, O., Vachenauer, R., Gauer, J. M., Zünd, G. & Genoni, M. (2007). New Transverse Plate Fixation System for Complicated Sternal Wound Infection After Median Sternotomy. *Ann Thorac Surg*, 83, 1210–1212.

Polizzi, S., Pira, E., Ferrara, M., Bugiani, M., Papaleo, A., Albera, R. & Palmi, S. (2002). Neurotoxic effects of aluminium among foundry workers and Alzheimer's disease. *Neurotoxicology*, 23, 761–774.

Porter, K., Roplekar, R., & Mohanna, P. (2012). A five year audit study on deep sternal wound infections and associated dehiscence post median Sternotomy: an analysis of patient outcome, risk factors and a proposed management strategy. *Inter J Surg*, 10, 1–52.

Powis, D. R., Follerås, T., Merson, S. A. & Wilson, A. D. (1982). Improved adhesion of a glass ionomer cement to dentin and enamel. *J Dent Res*, 61, 1416-1422.

Provenzano, M. J., Murphy, K. & Riley, L. H. (2004). Bone Cements: Review of Their Physiochemical and Biochemical Properties in Percutaneous Vertebroplasty, *AJNR Am J Neuroradiol*, 25, 1286–1290.

Rajamathi, J. T., Britto, S. & Rajamathi, M. (2005). Synthesis and anion exchange reactions of a layered copper–zinc hydroxy double salt, $Cu_{1.6}Zn_{0.4}(OH)_3(OAc).H_2O$. *J Chem. Sci*, 117, 629–633.

Raman, J., Song, D. H., Bolotin, G. & Jeevanandam, V. (2006). Sternal closure with titanium plate fixation – a paradigm shift in preventing mediastinitis. *Interact Cardiovasc Thorac Surg*, 5, 336-339.

Ravishankar, R. V. & Jamuna, B. A. (2011). Nanoparticles and their potential application as antimicrobials. *Science against Microbial Pathogens: Communicating Current Research and Technological Advances*, 1, 197-209.

Reser, D., Rodriguez Cetina Biefer, H., Plass, A., Ruef, C., Seifert, B., Bettex, D., Biaggi P., Falk, V. & Salzberg, S. P. (2012). Incidence of Sternal Wound Infection After Reexploration in the Intensive Care Unit and the Use of Local Gentamycin. *Ann Thorac Surg*, 94, 2033-2037.

Reusche, E., Pilz, P., Oberascher, G., Linder, B., Egensperger, R., Gloeckner, K., Trinka, E. & Iglseder B. (2001). Subacute fatal aluminum encephalopathy after reconstructive otoneurosurgery: a case report. *Hum Pathol*, 32, 1136-1140.

Sabel, M. & Stummer, W. (2004). The use of local agents: Surgicel and surgifoam. *Eur Spine J,* 13, 97–101.

Saha, S. & Pal, S. (1984). Mechanical properties of bone cement: A review. *J Biomed Mater Res*, 18, 435-462.

Sambrook, P. (2001). Bone Structure and Function in Normal and Disease States. In Sambrook, P., Schrieber, L. & Taylor, T. *The Musculoskeletal System: Basic science and clinical conditions*. pp. 68-84. London, United Kingdom: Harcourt publishers.

Schildhauer, T. A., Bauer, T. W., Josten, C. & Muhr, J. (2000). Open reduction and augmentation of internal fixation with an injectable skeletal cement for the treatment of complex calcaneal fractures. *J Orthop Trauma*, 14, 309–317.

Schimmer, C., Reents, W., Berneder, S., Eigel, P., Sezer, O., Scheld, H., …. Leyh, R. (2008). Prevention of Sternal Dehiscence and Infection in High-Risk Patients: A Prospective Randomized Multicenter Trial. *Ann Thorac Surg*, 86, 1897–1904.

Schimmer, C., Ozkur, M., Sinha, B., Hain, J., Gorski. A., Hager, B. & Leyh, R. (2012). Gentamicin-collagen sponge reduces sternal wound complications after heart surgery: A controlled, prospectively randomized, double-blind study. *J Thorac Cardiovasc Surg*, 143, 194-200.

Scholl, L., Chang, E., Reitz, B. & Chang, J. (2004). Sternal Osteomyelitis: Use of Vacuum-Assisted Closure Device as an Adjunct to Definitive Closure with Sternotomy and muscle Flap reconstruction, *J Card Surg*, 19, 453-461.

Schulz, A., Faschingbauer, M. & Jurgens, C. (2005). Sternal non-union——development of a novel fixation device. *Injury Extra*, 36, 569—572.

Sherman, R., Chapman, W. C., Hannon, G., Block, J. E. (2001). Control of bone bleeding at the sternum and iliac crest donor sites using a collagen-based composite combined with autolo-gous plasma: results of a randomized controlled trial. *Ortho-pedics*, 24, 137–41.

Shifrin, D. A., Sohn, S. M., Stouffer, C. W., Hooker, R. L. & Renucci, J. D. (2008). Sternal salvage with rigid fixation in the setting of a massive mediastinal aortic pseudoaneurysm: a case report and review of the literature. *J Plast Reconstr Aes*, 61, 17-20.

Shih, C-C., Shih, C-M., Su, Y-Y. & Lin, S-J. (2004). Potential risk of sternal wires. *Eur J Cardiothorac Surg*, 25, 812–818.

Shih, C-M., Su, Y-Y., Lin, S-J. & Shih, C-C. (2005). Failure analysis of explanted sternal wires. *Biomaterials*, 26, 2053–2059.

Song, D. H., Lohman, R. F., Renucci, J. D., Jeevanandam, V. & Raman, J. (2004). Primary sternal plating in high-risk patients prevents mediastinitis. *Eur J Cardiothorac Surg*, 26, 367–72.

Song, D. H., Wu. L.C., Lohman, R. F., Gottlieb, L. J. & Franczyk, M. (2003). Vacuum assisted closure for the treatment of sternal wounds: The bridges between debridement and definitive closure. *Plast Reconstr Surg*, 111, 92-97.

Spotnitz, W. D. (2008). Invited commentary. *Ann Thorac Surg*, 85, 293.

Stark, P., & Jaramillo, D. (1986). CT of the Sternum, *AJR*, 147: 72-77.

Steiner, M., & Ramp, W. K. (1988). Short-term storage of freshly harvested bone, *J. Oral Maxillofac. Surg.*, 46: 868–871.

Tajmir-Riahi, H. A., Naoui, M. & Ahmad, R. (1992). *A comparative study of calf-thymus DNA binding trivalent Al, Ga, Cr and Fe ions in aqueous solution. In: Metal ions in biology and medicine* (pp. 98-101). Paris, France: John Libbey Eurotext.

Takahashi, Y., Imazato, S., Kaneshiro, A. V., Ebisu, S., Frencken, J. E. & Tay, F. R. (2006). Antibacterial effects and physical properties of glass-ionomer cements containing chlorhexidine for the ART approach. *Dent Mater*, 22, 647-652.

Tavilla, G., van Son, J. A.M., Verhagen, Ad F., Lacquet, L. K. (1991). Modified Robicsek Technique for Complicated Sternal Closure. *Ann Thorac Surg*, 52, 1179-1180.

Timmes, J. J., Wolvek, S., Fernando, M., Bas, M. & Rocko, J. (1973). A New Method of Sternal Approximation. *Ann Thorac Surg*, 15, 544-546.

Timoshenko, S. & Woinowsky-Kreiger, S. (1959). *Symmetrical bending of circular plates. Theory of plates and shells* (2nd Ed.). pp. 106-107. New York, USA: McGraw-Hill.

Tranoudis, I. & Efron, N. (2004). Tensile properties of soft contact lens materials. *Cont. Lens Anterior Eye*, 27, 177-191.

Trumble, D. R., McGregor, W. E. & Magovern, J. A. (2002). Validation of a bone analog model for studies of sternal closure. *Ann Thorac Surg*, 74, 739-744.

Tsybeskov, L., Vandyshev, J. V. & Fauchet, P. M. (1994). Blue emission in porous silicon: Oxygen-related photoluminescence. *Phys Rev B Condens Matter*, 49, 7821-7824.

Valappil, S., Ready, D., Abou Neel, E., Pickup, D., Chrzanowski, W., O'Dell, L., Knowles, J. (2008). Antimicrobial Gallium-doped Phosphate-based Glasses. *Adv Func Mater*, 18, 732-741.

Van Haaren, E.H., van der Zwaard, B.C., van der Veen, A.J., Heyligers, I.C., Wuisman, P.I., Smit, T.H. Effect of long-term preservation on the mechanical properties of cortical bone in goats. (2008). *Acta. Orthopaedica.*, 79: 708–716.

Voss, B., Bauernschmitt, R., Will, A., Krane, M., Kross, R., Brockmann, G., Libera, P. & Lange, R. (2008). Sternal reconstruction with titanium plates in complicated sternal dehiscence. *Eur J Cardiothorac Surg*, 34, 139-145.

Wakayama, I., Song, K.-J., Nerurkar, V. R., Yoshida, S. & Garruto, R. M. (1997). Slow dendritic transport of dissociated mouse hippocampal neurons exposed to aluminum. *Brain Res*, 748, 237–240.

Wangsgard, C. G., Cohen, D. J. & Griffin, L. V. (2008). Fatigue Testing of Three Peristernal Median Sternotomy Closure Techniques. *J Cardiothorac Surg*, 3, 52.

Warrell, R. P., Alcock, N. W. & Bockman, R. S. (1987). Gallium nitrate inhibits accelerated bone turnover in patients with bone metastases. *J Clin Oncol*, 5, 292-298.

Warrell, R. P. & Bockman, R. S. (1989). In: important advances in oncology 1989 (DeVita, V. T., Hellman, S. & Rosenberg, S.A. ed.s), pp. 205-220, J.B. Lippincott, Philadelphia.

Warrell, R. P., Bockman, R. S., Coonley, C. J., Isaacs, M. & Staszewski, H. (1984). Gallium nitrate inhibits calcium resorption from bone and is effective treatment for cancer-related hypercalcemia. *J Clin Invest*, 73, 1487-1490.

Williams, J. A., Billington, R. W. & Pearson, G. J. (2002). The effect of the disc support system on biaxial tensile strength of a glass ionomer cement. *Dent Mater*, 18, 376-379.

Wilson, A. D. (1974). Alumino-silicate polyacrylic acid and related cements. *Brit Poly J*, 6, 165–179.

Wren, A. W., Boyd, D., Thornton, R., Cooney, J. C. & Towler, M. R. (2009). Antibacterial properties of a tri-sodium citrate modified glass polyalkenoate cement. *J Biomed Mater Res B Appl Biomater*, 90, 700-709.

Wren, A. W., Coughlan, A., Placek, L. & Towler, M. R. (2012). Gallium containing glass polyalkenoate anti-cancerous bone cements: glass characterization and physical properties. *J Mater Sci: Mater Med*, 23, 1823-1833.

Wren, A. W., Cummins, N. M., Coughlan, A. & Towler, M. R. (2010). The effect of adding organic polymers on the handling properties, strengths and bioactivity of a Ca–Sr–Zn–Si glass polyalkenoate cement. *J Mater Sci*, 45, 3554–3562.

Wren, A. W., Cummins, N. M., Laffir, F. R., Hudson, S. P. & Towler, M. R. (2011). The bioactivity and ion release of titanium-containing glass polyalkenoate cements for medical applications. *J Mater Sci: Mater Med*, 22, 19–28.

Wren, A. W., Kidari, A., Cummins, N. M. & Towler M. R. (2010). A spectroscopic investigation into the setting and mechanical properties of titanium containing glass polyalkenoate cements. *J Mater Sci: Mater Med*, 21, 2355–2364.

Wren, A. W., Laffir, F. R., Kidari, A. & Towler, M. R. (2011). The structural role of titanium in Ca–Sr–Zn–Si/Ti glasses for medical applications. *J Non-Cryst Solids*, 357, 1021–1026.

Young, A. An ideal adhesive for bone repair : Injectable, rapidly crosslinkable, biodegradable poly(esters) containing reactive calcium phosphate fillers. Retrieved from https://iris.ucl.ac.uk/iris/browse/researchActivity/6059

Young, A. M., Sherpa, A., Pearson, G., Schottlander, B. & Waters, D.N. (2000). Use of Raman spectroscopy in the characterisation of the acid-base reaction in glass-ionomer cements. *Biomaterials*, 21, 1971-1979.

Zeitani, J., Penta de Peppo, A., Bianco, A., Nanni, F., Scafuri, A., Bertoldo, F., …. Chiariello, L. (2008). Performance of a novel sternal synthesis device after median and faulty sternotomy: mechanical test and early clinical experience. *Ann Thorac Surg*, 85, 287-93.

Zhang, Y., Zhu, F., Zhang, J. & Xia L. (2008). Converting layered zinc acetate nanobelts to one-dimensional structured ZnO nanoparticle aggregates and their photocatalytic activity. *Nanoscale Res Lett*, 3, 201–204.

Zurbrugg, H. R., Freestone, T., Bauer, M. & Hetzer, R. (2000). Reinforcing the Conventional Sternal Closure. *Ann Thorac Surg*, 69, 1957-1958.